+:corresponding author (nlewisres@ucsd.edu).

8.4Authors' contributions

H.M.B and N.E.L. conceptualized the work. H.M.B. wrote the paper and generated the figures. All authors carefully reviewed, discussed and edited the paper.

8.2Competing Interests

The authors declare no competing interests.

Declaration of interests

The authors declare that they have no known competing financial interests or personal relationships that could have appeared to influence the work reported in this paper.

1. PMID 22068332: This article demonstrates that proteome allocation strategies minimize machinery costs by high expression of proteins with conserved functions and lower expression of proteins involved in context-specific and multicellular processes such as cell signaling and communication.

2. PMID 32859923: This article quantifies relative ATP levels in relation to genome-wide machinery abundance across three conditions, highlighting the metabolic flexibility of bioenergetic pathways, distinguishing between machinery- or substrate-limited reactions, and identifying relationships between bioenergetics and growth.

3. PMID 25745177: This article uses a model of gene expression to show the variable contributions of macromolecular abundance, synthesis rates, and degradation rates on differential protein expression in non-steady-state conditions.

4. PMID 33173034: This article uses a model of gene expression that accounts for resource loading to demonstrate that, in engineered mammalian circuits, transcriptional resources limit protein abundance.

5. PMID 26575626: This article quantifies the energetic costs of various steps of gene expression, showing that protein translation consumes a considerable fraction of the energy consumed during gene expression, and it also argues that the bioenergy budget scales (across prokaryotes to eukaryotes) with cell size when accounting for the total lifetime of the cell.

6. PMID 31519914: This article provides a unique example of mammalian cell-decision making that optimizes for non-growth phenotypes (in this case, motility) by choosing migratory paths that will be less energetically costly.

7. PMID 27951527: This article introduces the concept of a gene-specific, tissue-independent PTR that indicates that coupling between transcript and protein processes is affected by gene-intrinsic features.

8. PMID 31896772: This article creates a mammalian genome-scale model that couples metabolism with the secretory pathway, demonstrating that trade-offs occur between cell growth and protein secretion.

9. PMID 30638811: This article identifies Pareto fronts from single-cell measurements in tissue, showing that cells have varying extents of specialization according to their spatial location, resulting in division of labor that optimizes tissue-level function.

10. PMID 29398113: This article shows how cell communication via growth factor signaling works in combination with constraints to maintain tissue compositional homeostasis.

11. PMID 35421362: This article demonstrates how cells employ combinatorial strategies to efficiently communicate by only expressing a small number of ligands.

12. PMID 10878248: This article adapts supply-demand analysis from economics to metabolism, showing that reaction flux and metabolite concentration are independently controlled to maintain homeostatic concentrations of metabolites across contexts.

13. PMID 22308336: This article presents a theory for how specialization is favored by evolution due to context-specificity and synergistic effects.

14. PMID 14550310: This article shows that humans regulate diet to intake balanced macronutrient ratios and prioritize protein when a balanced diet is not possible.

Resource Allocation in Mammalian Systems

Hratch M. Baghdassarian[1,2], **Nathan E. Lewis**[2,3,+]

[1]Bioinformatics and Systems Biology Graduate Program, University of California, San Diego, La Jolla, CA, 92093, USA

[2]Department of Pediatrics, University of California, San Diego, La Jolla, CA, 92093, USA

[3]Department of Bioengineering, University of California, San Diego, La Jolla, CA, 92093, USA

Abstract

Cells execute biological functions to support phenotypes such as growth, migration, and secretion. Complementarily, each function of a cell has resource costs that constrain phenotype. Resource allocation by a cell allows it to manage these costs and optimize their phenotypes. In fact, the management of resource constraints (e.g., nutrient availability, bioenergetic capacity, and macromolecular machinery production) shape activity and ultimately impact phenotype. In mammalian systems, quantification of resource allocation provides important insights into higher-order multicellular functions; it shapes intercellular interactions and relays environmental cues for tissues to coordinate individual cells to overcome resource constraints and achieve population-level behavior. Furthermore, these constraints, objectives, and phenotypes are context-dependent, with cells adapting their behavior according to their microenvironment, resulting in distinct steady-states. This review will highlight the biological insights gained from probing resource allocation in mammalian cells and tissues.

Keywords

resource allocation; multicellularity; systems biology; trade-offs; optimality

1. Introduction

Resource allocation governs economies and biology alike. Each biological function has an associated **resource cost** while also conferring a **fitness** benefit by contributing to a cellular **objective**, such as growth (Appendix A). Cells **optimize** for these objectives under the constraints of their **resource budget**. The accumulation of resource allocation decisions to fulfill cell objectives results in observed cell phenotypes. As such, resource constraints limit cells' activity and, consequently, their range of possible phenotypes(Shoval et al., 2012). In this sense, resource allocation can be viewed as a cost-benefit(Dekel and Alon, 2005) or supply-demand(Hofmeyr and Cornish-Bowden, 2000) analysis (Fig. 1). Despite the complexity of mammalian cells, resource allocation is a fundamental principle underlying decision-making. From an evolutionary perspective, organisms that best apply resource allocation strategies will have higher fitness. As such, the consideration of resource allocation illuminates *how* and *why* cells respond to their environment. Specifically, resource costs limit *how* a cell can achieve its objective by constraining the possible mechanisms the

cell can use. Fitness illuminates *why* the cell chooses one specific mechanism over other possibilities.

Decision-making depends strongly on **cellular context**(Shakiba et al., 2021). To make decisions, a cell perceives extracellular cues(Jerby-Arnon and Regev, 2022) such as nutrient availability and communication signals(Armingol et al., 2022a), and processes this information based on its intracellular state (e.g., cell type, genomic variants, epigenetic state). Consequently, the extracellular cues act as signals that a cell can use to assess its resource budget and shape its objectives. Intracellularly, the relayed information of resource availability and objectives in a given context determine pathway activity(Hofmeyr and Cornish-Bowden, 2000). Finally, context can change with time(Gerashchenko et al., 2021; Ghosh et al., 2022; Rooyackers et al., 1996), space(Ben-Moshe and Itzkovitz, 2019; Kleinridders et al., 2018), and disease(Gazestani et al., 2019; Smillie et al., 2019), dynamically shaping cellular objectives that cause trade-offs and transitional costs that further constrain the cell.

Mammalian cells do not act in isolation, but rather in multicellular systems to achieve higher-order functions(Almet et al., 2021; Armingol et al., 2021; Toda et al., 2019). Constraints, contexts, and phenotypes are ubiquitous across biological scales. Thus, the insights into resource allocation may be generalized to tissues and even the whole-organism (Appendix C). With multicellularity, cells become specialized to limit the burden of trade-offs. Additionally, decision-making accounts for coordination and competition from other cells, leading to synergistic effects(Rueffler et al., 2012).

In this Review, we discuss how resource allocation impacts mammalian cell decisions and multicellularity. We begin with two questions at the cellular scale (Fig. 2a):

1. How do metabolic resources (nutrients, machinery, and bioenergetics) constrain the cell?

2. How do cells allocate resources to coordinate activity across molecular processes?

Building on these concepts to understand multicellularity (Fig. 2b), we ask:

3. How do trade-offs imposed by resource constraints affect cellular decision-making, leading to cell specialization?

4. How do specialized cells with distinct tasks coordinate within multicellular systems to achieve higher-order functions?

Here we highlight the role of resource allocation, which is one valuable concept among many to understand biological mechanisms. Our aim is to demonstrate the broad utility and unique insights provided by resource allocation across various areas of biology. Resource allocation provides a unique perspective to uncover fundamental principles that can be applicable across diverse systems. We structure our discussion by first introducing an overarching principle and subsequently illustrating them with wide-ranging examples from various systems in both health and disease. While optimality is not always the driving force, or not yet fleshed out in mammalian systems, such a perspective has been invaluable to the

study of prokaryotes and lower eukaryotes in support of mammalian systems, which we also highlight here.

Throughout these discussions, we explore the plasticity of resource allocation as it changes across contexts. We also briefly highlight powerful systems biology methods that now help address such questions (Appendix B, Table 1). Quantifying and modeling resource allocation provides insights into how cells regulate gene expression, intracellular pathway activity, cell-cell interactions, and ultimately phenotypes. Associated technological and computational innovations are providing high-throughput measurements and analysis tools to decipher how resource allocation, as a governing design principle, shapes the complex processes underlying mammalian phenotypes.

2 Main

2.1 Cellular Resources Constrain Phenotype

The availability of nutrients, **machinery**, and bioenergy define the cellular resource budget, and consumption of these resources defines the resource costs of biological activity (Fig. 1). How does the cell manage its resource budget and how do these constraints affect phenotype?

2.1.1 Nutrients: resources informing allocation

Supplies and signals.: Extracellular nutrients contribute to the total resource budget as substrates for machinery synthesis and bioenergetic pathways (Appendix A, Appendix D). For example, amino acids can be incorporated as building blocks for proteins, whereas glucose and glutamine can be catabolized for energy or nucleotide synthesis (e.g., for oligonucleotides)(Fan et al., 2013; Hosios et al., 2016). However, in managing resource allocation, nutrients play a particularly important role as extracellular cues. Their presence informs the cells of which metabolic pathways may be utilized and ultimately which objectives may be achieved, guiding allocation across the metabolic network. In this sense, through regulatory programs(Efeyan et al., 2015), nutrients will induce activation of specific metabolic pathways and express the associated machinery that catalyze those pathways.

Signals of scarcity.: Nutrient allocation has evolved to cope with nutrient scarcity(Efeyan et al., 2015). Mammalian cells have many strategies to handle nutrient scarcity; the global metabolic network is robust to nutrient inputs, capable of utilizing distinct nutrient-pathway combinations to meet cellular demands(Bennett et al., 2020; Edelman and Gally, 2001; Jeong et al., 2000). For example, cells will shift glucose usage from energy metabolism to *de novo* serine synthesis when serine is scarce(Chaneton et al., 2012) and use fatty acid oxidation to generate energy when glucose is scarce(Cantó et al., 2010). Additionally, cells may degrade intracellular components through autophagy and divert the resultant substrates to the most necessary pathways(Efeyan et al., 2015). Finally, cells may scavenge for more complex extracellular resources, such as proteins and lysophospholipids, to catabolize through mechanisms such as macropinocytosis(Zhu and Thompson, 2019). These resources are often produced by other cells in a multicellular system.

Multicellularity decreases the likelihood of individual cells facing nutrient scarcity. This is because mammalian cells have multiple subcompartments and specialized cell types that improve nutrient storage and delivery systems to create nutrient-rich microenvironments (Chantranupong et al., 2015; Palm and Thompson, 2017). Storage is a multicellular example of the **hedging** strategies discussed later, diverting resources away from current objectives in anticipation of future context-dependent fluctuations in nutrient levels(Fischer et al., 2011).

Allocation in abundance.: Resource allocation in nutrient-rich environments becomes a decision-making problem. Cell activity still comes at a resource cost. Thus, the cell must choose which nutrients to shuttle to which metabolic pathways to most efficiently achieve its objective (Appendix D). Sometimes, it will even disregard available extracellular nutrients, such as non-essential amino acids, choosing instead to produce them intracellularly(Palm and Thompson, 2017).

Since cell activity evolved under nutrient scarcity, mammalian cells must tightly control nutrient uptake to prevent irregular phenotypes such as uncontrolled growth (see Appendix C for consequences of overabundance). Unlike prokaryotes, which typically uptake nutrients upon sensing them, mammalian cells tend to couple nutrient sensors with signaling proteins such as growth factors for an additional layer of regulation (Fig. 3c)(Palm and Thompson, 2017; Rathmell et al., 2000). This additional regulatory layer serves a dual purpose of allowing cells and tissues across the organism to coordinate via combined nutrient- and signaling-protein-circuits, maintaining steady-state circulating nutrient levels and mobilizing nutrient stores when necessary(Itoh et al., 2003; Zisman et al., 2000). Thus, nutrient scarcity tends to be a local and context-specific constraint in multicellular systems, such as in wound-healing and poorly vascularized regions(Zhu and Thompson, 2019). The cell's microenvironment (e.g., nutrient concentration, interactions with other cell types, and presence of other extracellular nutrients) affect metabolic activity. Thus, it is important to appropriately account for a cell's microenvironment when studying resource allocation, which may not always be accurately represented *in vitro*. For example, *in vivo* early-activated CD8+ T-cells utilize glucose differently than those under the super-physiological conditions of cell culture(Ma et al., 2019), shifting flux from aerobic glycolysis to oxidative phosphorylation to create a larger bioenergy budget.

Distribution drives function.: Ultimately, nutrient availability and allocation affect cell phenotypes, such as growth(Chen et al., 2019; Son et al., 2015; Zhu and Thompson, 2019) and secretion(da Silva Novaes et al., 2019), as well as organismal phenotypes, such as development(Hu and Yu, 2017) and immunity. In immunity, nutrient availability affects cell fate, function, and composition. For example, under both amino acid and glucose deprivation, mTORC1 activation and CD4+ T-regulatory cell proliferation decreases(Long et al., 2021). Additionally, effector T-cells rely on both glucose(Cham et al., 2008; Cham and Gajewski, 2005) and glutamine(Carr et al., 2010) for cytokine secretion whereas invariant Natural Killer T cell cytotoxicity is independent of these nutrients(Khurana et al., 2021). In early development, glucose is shuttled to anabolic pathways that trigger synthesis of key machinery controlling blastocyst formation, with cells using other carbon sources such as pyruvate and lactate to generate bioenergy. In the absence of glucose prior

to compaction, zygotes do not invest biosynthetic resources into expressing the glucose transporter SLC2A3, resulting in reduced cell growth and degenerated morulae(Pantaleon et al., 2008).

We note that there is an interplay between the three resource classes: nutrients, machinery, and bioenergetics. So far, this is largely presented as nutrients used to synthesize the cell's machinery, and machinery and metabolic substrates together dictating the bioenergetic pathways that the cell utilizes. However, this crosstalk is not unidirectional, with each resource class depending on the others (Fig. 1a). Building machinery requires energy(Lynch and Marinov, 2015), and without the right machinery, nutrients can't be used effectively. Transporters, for example, are machinery that deliver extracellular nutrients to the cell. In CD8+ T-cells, knocking-out amino acid transporters limits nutrient intake, altering the ratio of terminal effector to memory precursor subpopulations(Huang et al., 2021).

2.1.2 Machinery: resources actuating allocation—As actuators of biological function, the machinery budget contributes to pathway activity and cell phenotype. The machinery component of the resource budget depends on two factors: machinery activity and machinery abundance (Appendix E). Higher activity increases the amount of substrate a single unit of machinery is able to convert into a product. There are innumerable examples in which altered catalytic efficiency, e.g. via point mutations, has disrupted homeostasis and led to disease states (reviewed here(Stefl et al., 2013)). On the other hand, higher abundance increases the proportion of machinery to its substrate. This is evident for individual machinery. For example, CARKL expression levels change depending on activation signals to alter energy metabolism and ultimately dictate macrophage fate.(Haschemi et al., 2012) Similarly, pyruvate kinase isoforms interact based on expression levels to affect nucleotide metabolism and dictate proliferation(Lunt et al., 2015). Abundance is also coordinated across multiple components. CRISPR screens have tested thousands of genes and found that machinery groups by shared effects across multiple phenotypes;(Funk et al., 2022) meanwhile, the abundance of hundreds of secretory pathway machinery together coordinate a cell's capacity for secreting specific proteins(Kuo et al., 2021). Unlike the cell's nutrient budget, which is largely limited by extracellular availability, machinery abundance is constrained by the resource costs of synthesis. Beyond diverting nutrients to anabolism, cells must invest bioenergy and biosynthetic machinery for gene expression.

Machinery Pose Non-negligible Auto-catalytic Costs.: The machinery facilitating anabolism and gene expression are auto-catalytic, meaning they contribute to their own synthesis. As a result, machinery synthesis costs include the use of biosynthetic machinery(Reuveni et al., 2017). For example, in eukaryotes, individual pre-mRNAs compete for the shared pool of splicing machinery to be properly processed(Munding et al., 2013). Since ribosomal genes represent a substantial mass fraction of the proteome, global splicing efficiency is associated with ribosomal expression. Given that ribosome expression increases with growth rate to accommodate increasing biomass production demand, and that nutrient signaling via TOR influences ribosome gene expression, these observations couple cell growth with nutrient and machinery constraints of macromolecular synthesis (Appendix

A). In fact, under nutrient scarcity, reducing splicing efficiency through intron-mediated regulation improves cell survival by decreasing ribosomal expression(Parenteau et al., 2019).

Various gene expression modeling approaches account for this concept of **resource loading** (Appendix E) to study the limiting biosynthetic machinery (Frei et al., 2020; Jones et al., 2020; Qin et al., 2023; Rondelez, 2012). Studies in prokaryotes have quantified costs of translation and ribosome biogenesis, showing them as major constraints on gene synthesis. In mammalian cells, rough estimates for HeLa cells show that all ribosomes must be constantly active to maintain global protein levels(Yewdell, 2001). However, quantification of exogenous gene circuit costs suggests transcriptional machinery loading as a substantial component of resource burden. Frei et al. demonstrate in different human cell lines that a combination of both transcriptional and translational resources can limit gene expression(Frei et al., 2020). This is in line with a study in yeast that found the relative impact of transcriptional and translational costs change across nutrient-limiting conditions, pointing to the crosstalk between machinery and nutrients(Kafri et al., 2016). In exploring the contribution of various intrinsic gene features, a separate study on mammalian cell lines found that those related to transcriptional resources have a larger effect on resource loading(Di Blasi et al., 2023). This is supported by two studies that introduced exogeneous circuits to mammalian cell lines, wherein one studied how RNA polymerase is limiting depending on the competing genes' promoter strength(Qin et al., 2023), and another considered all gene expression resources to identify the Mediator complex(Allen and Taatjes, 2015) as the primary limiting resource(Jones et al., 2020). Overall, these results suggest that, in mammalian cells, transcriptional machinery also impose non-negligible resource limitations on gene expression.

Machinery Biosynthesis has Substantial Energetic Costs.: The energetic costs of machinery synthesis can be quantified across genomic, transcriptional, and translational processes as a function of gene features. Protein synthesis costs are highly sensitive to the energy budget(Buttgereit and Brand, 1995) and are a large resource burden: ribosomal translation alone represents 30% (BioNumbers(Milo and Phillips, 2015) ID 110441) of a mammalian cell's energy budget. Also, net protein synthesis costs represent more than 70% (BioNumbers(Milo and Phillips, 2015) ID 111918) of a generic cell's energy budget (due to the higher contribution of amino acid synthesis relative to polymerization(Lynch and Marinov, 2015)). Lane and Martin argue that protein synthesis costs represent such a substantial portion of the total cellular energy budget that they prevent the evolution of eukaryotic genome complexity without mitochondria(Lane and Martin, 2010). In contrast, Lynch and Marinov contend that, considering the cell's total lifetime, the energy budget scales with cell volume to more than compensate for increased costs of genome complexity, regardless of the presence of mitochondria(Lynch and Marinov, 2015).

Strategies to Minimize Machinery Costs.: Due to these costs, cells employ various strategies to efficiently generate the machinery budget. For example, protein degradation is costly (Appendix A, Appendix D) because proteasomal degradation consumes ATP(Peth et al., 2013) and sequesters proteases. From a resource allocation perspective, this aligns

with the fact that short-lived proteins have low abundance(Cambridge et al., 2011)[,(Li et al., 2021),(Schwanhäusser et al., 2011)], representing just 5%(Li et al., 2021) of the human proteome. By only dedicating degradation resources to lowly expressed proteins, the cell reduces the cost of tuning protein abundance in modes beyond translational control. In contrast to proteasomal degradation, protein turnover via autophagy recovers more energy and nutrient resources than it consumes and represents a large fraction of total protein degradation in mammalian cells(Marchingo and Cantrell, 2022; Singh and Cuervo, 2011).

Short-lived proteins also constitute only a small portion of complexes(Li et al., 2021), supporting the notion that cells conserve protein degradation resources by minimizing their use in more abundant proteins. An alternative strategy proposed to reduce costs in complexes is proportional synthesis. Observed in both prokaryotes(G.-W. Li et al., 2014) and eukaryotes(Taggart and Li, 2018), cells express complex subunits in proportion to their stoichiometries by tuning synthesis rates, avoiding excess resource expenditure on synthesis. Additionally, degradation would be required to achieve proper stoichiometries and clear misfolded proteins resulting from excess expression. Furthermore, there are spatio-temporal variations in complexes' stoichiometries, many of which are regulated beyond transcription(Ori et al., 2016). Together with proportional synthesis, this suggests context-specific tuning of translation rates to minimize synthesis costs.

These various strategies demonstrate that cells work to optimize machinery expression levels by minimizing synthesis costs while maximizing the associated fitness benefits(Dekel and Alon, 2005). This cost-benefit trade-off in gene expression was characterized in a high-throughput manner in eukaryotes, testing the impact of 81 genes' expression levels on growth rate. Crucially, 83% of genes demonstrated distinct fitness curves correlating with differential gene expression(Keren et al., 2016). Thus, minimizing machinery costs has proven to be an accurate optimality principle to predict and understand metabolic activity(Noor et al., 2016, 2014) (Appendix B), such as in relationships between energy metabolism and growth (Appendix A).

2.1.3 Bioenergy: resources fueling allocation—Energy metabolism (e.g., glycolysis and oxidative phosphorylation) uses machinery to transfer the energy stored in extracellular nutrients to its main intermediate currency, ATP, and long-term nutrient stores. This energy budget is spent to fuel a multitude of tasks(Bennett et al., 2020; Rolfe and Brown, 1997; Yang et al., 2021) that prompts the cell to organize its activities accordingly. Several methods identify the energetic cost of executing function at varying resolutions, broadly by measuring or estimating the metabolic flux associated with bioenergy generation or consumption(Ghosh et al., 2022; Schmidt et al., 2021); these include estimates from measures such as the oxygen consumption rate and ATP equivalents, i.e. mechanistic delineation of the number of ATP molecules consumed, each of which yield ~50 kJ/mol (BioNumbers(Milo and Phillips, 2015) ID 100775, 100776) of energy from hydrolysis.

As discussed previously, a large fraction of the energy budget is spent on gene expression and protein translation(Lynch and Marinov, 2015). The remainder of the energy budget is available for other tasks. For example, migrating cells consume energy to displace the extracellular matrix(Mosier et al., 2021; van Helvert et al., 2018). The

energetic cost of motility changes with physical features of the matrix such as stiffness and spatial confinement. As such, cells minimize these migratory costs by choosing context-specific migratory mechanisms(Li et al., 2019) and migrating through paths that require lower energy expenditure(Zanotelli et al., 2019). Neurons also demonstrate energy allocation. They consume energy for functions distributed across maintenance and activity, including neurotransmitter uptake and release by synaptic vesicles and action potential generation(Attwell and Laughlin, 2001; Du et al., 2008; Pulido and Ryan, 2021). Consequently, the brain has a high rate of energetic expenditure(Wang et al., 2010), accounting for 20% of the total energy costs of the human body (BioNumbers(Milo and Phillips, 2015) ID: 103264, 110878), and must use its energy budget efficiently. At the cell-scale, neurons employ combinatorial strategies to express sets of ion channels with specific kinetics that minimize energetic costs while meeting functional requirements (e.g., spiking rate)(Alle et al., 2009; Hasenstaub et al., 2010). At the tissue-scale, energetic constraints limit the total number(Herculano-Houzel, 2011) and active fraction(Lennie, 2003) of neurons in the brain. As such, the brain analogously employs combinatorial strategies to efficiently encode information into sets of neurons in such a manner that limits the number of active neurons, and thus energy demands(Levy and Baxter, 1996),(Attwell and Laughlin, 2001).

While whole-cell modeling has demonstrated that the total energy budget is nearly equivalent to the total energy cost of a synthetic minimal cell(Thornburg et al., 2022), it has also demonstrated excess production of energetic intermediates in *Mycoplasma genitalium*(Karr et al., 2012). Whole-cell modeling approaches (Appendix B, Table 1) are yet to be translated to mammalian cells, but such insights could prove invaluable to understanding energy resource allocation. An excess budget indicates either a deprioritization of evolutionary optimality for the energy budget over other objectives, cell hedging for future energy demands, or incomplete accounting of energy consumption.

2.2   Molecular Processes Coordinate Resources

Mechanistically, resource constraints are tied to the activity of molecular processes such as gene synthesis, metabolism, and molecular communication. These processes can be coupled to each other using systems approaches (Appendix B, Table 1), providing quantitative details regarding how resources are used. Resource constraints that affect the activity of one process propagate to others and eventually affect phenotype (Fig. 1c).

2.2.1   Gene Expression: Coordinating mRNA with Protein—To understand the global relationship between mRNA and protein expression levels, proteomics is often compared with transcriptomics using correlative metrics(Buccitelli and Selbach, 2020; Vogel and Marcotte, 2012). Comparing per cell absolute protein copy numbers to transcripts-per-million mRNA levels in multiple human tissue cell lines identified an average Pearson correlation of 0.6(Edfors et al., 2016). Importantly, a gene-specific, tissue-independent protein-to-RNA (PTR)(Edfors et al., 2016; Wilhelm et al., 2014) ratio increases the correlation; similar results were also shown in single-cells, with remaining variability largely explained by other context-specific effects such as the microenvironment(Popovic et al., 2018). This indicates a gene-specific effect on resource loading, wherein intrinsic

features yield a competitive advantage for shared translational resources. For example, sequence length is a positive indicator of the variation in the PTR ratio, consistent with longer genes having a larger resource cost. Furthermore, the PTR ratio increases with transcriptional abundance(Csárdi et al., 2015; Wang et al., 2019), signifying cooperation between transcription and translation in generating highly abundant proteins. Gene-specific competitive advantages also coordinate across processes within transcription. For example, mammalian cells use "economies of scale", wherein splicing efficiency increases with transcription rate to prioritize production of strongly transcribed genes(Ding and Elowitz, 2019). Distinct intrinsic gene features related to either transcriptional or translational resources may also interact, resulting in a large combinatorial space in which these features can influence resource allocation(Di Blasi et al., 2023).

The role of gene-intrinsic features makes it apparent that abundance alone does not sufficiently explain mRNA to protein coupling. It follows that such features inform gene expression rates; broadly, there are four rates to consider: transcription, translation, mRNA decay, and protein degradation. The gene-specific combinations of these rates give rise to global steady-state levels of mRNA and protein in a context-dependent manner, especially with dynamic responses requiring rapid adaptation(Jovanovic et al., 2015; Rabani et al., 2011). Resource allocation limits the existing rate combinations, with certain combinations resulting in synthesis costs that outweigh the gene's contribution to the cell objective. Specifically, there is an evolutionary lack of genes with high transcription rates and low translation rates, despite these rates being mechanistically feasible. This is driven by a "precision-economy trade-off" between stochastic protein abundance (precision) and resource costs of synthesis (economy), with high transcription and low translation not providing an advantage in either(Hausser et al., 2019).

The four synthesis rates are commonly modeled using a simplified set of ordinary differential equations (Table 1). Derivation of these rates requires absolute quantification–the number of molecules per cell(Liu et al., 2016). Notably, these rates have a larger contribution to changes in the absolute level of a protein than to its relative level(Jovanovic et al., 2015). This makes sense from a resource allocation perspective since there is high inequality in the distribution of absolute protein abundances, with a small number of proteins constituting the majority of the total proteome by mass and copy number(Harper and Bennett, 2016; Li et al., 2021; Wang et al., 2019),(Hukelmann et al., 2016). Thus, highly abundant proteins will sequester a disproportionate fraction of cellular resources, independent of the fact that they tend to have an intrinsic competitive advantage in using cellular resources.

Translational efficiency also impacts gene-specific PTRs(Gingold and Pilpel, 2011). Gene-specific sequences regulate translational efficiency to prevent ribosomal jamming and excess translational machinery costs(Tuller et al., 2010). Genes with high translational efficiency also have high mRNA abundance, enabling them to outcompete their lower efficiency counterparts for ribosomes by both concentration and affinity. Furthermore, these genes are functionally enriched for macromolecular synthesis and energy metabolism(Al-Bassam et al., 2018), indicating the cell is optimizing for the production of its machinery and bioenergy

resource budgets. From a resource loading perspective, ribosome machinery saturation imposes an upper bound on the dynamic range of protein abundance.

2.2.2 Actuation: Coordinating Protein with Metabolism—Metabolism links gene expression to cell phenotype(Basan, 2018; Hofmeyr and Cornish-Bowden, 2000). Metabolic inputs, outputs, and intermediates are incorporated into all the resource classes and molecular processes discussed, forming the basis upon which cell activity occurs(Karr et al., 2012). There are innumerable examples of how metabolic activity affects cell phenotype. For example, shifts from purine to serine synthesis promote cell motility(Kiweler et al., 2022; Soflaee et al., 2022), mitochondrial metabolism modulates stem cell fate(Carey et al., 2015; Schell et al., 2017; Vannini et al., 2016), and many pathways affect growth(Zhu and Thompson, 2019).

Gene expression produces the machinery that catalyzes metabolism. As mentioned previously, machinery activity and abundance together determine the flux that an enzyme-catalyzed biochemical reaction can carry (Appendix E)(Davidi and Milo, 2017; Nilsson et al., 2017). Assuming Michaelis-Menten kinetics, the maximum flux that a reaction can carry is the product of the catalytic rate constant and the enzyme concentration. There are several considerations *in vivo* that may prevent a cell from realizing these maximum rates, which tend to be reported under *in vitro*, nonphysiological conditions. First, the maximum rate assumes that the enzyme is fully saturated. However, cells try to minimize intermediate metabolite concentrations for homeostatic maintenance and quick adaptation to new contexts(Schuster et al., 1991). Yet, enzymes are more efficient at high (saturating) substrate concentrations. Thus, efficient enzyme usage must be balanced against minimizing metabolic intermediates(Tepper et al., 2013) and rapid substrate consumption. More generally, there is a trade-off between control over reaction fluxes and metabolic intermediate concentrations(Hofmeyr and Cornish-Bowden, 2000). Second, reaction thermodynamics affects reaction kinetics via the mass-action ratio due to such variables as intracellular pH and metabolite concentrations(Beard and Qian, 2007). The extent of backwards flux due to thermodynamics requires a higher machinery investment to maintain the same reaction rate (Appendix B)(Noor et al., 2014). Finally, regulatory effects such as allostery and post-translational modifications can alter kinetics to alter reaction rates.

Thus, the observed reaction rate will change with variables such metabolite concentration in a context-dependent manner. Combining proteomic measurements of enzyme abundance with metabolic modeling estimates of fluxomics to estimate *in vivo* observed catalytic rate constants demonstrated that the maximum value identified across multiple growth conditions agrees with the *in vitro* catalytic rate constants. Such studies decompose discrepancies between experimental and theoretical values into the underlying saturating, thermodynamic, and regulatory factors (Appendix E)(Davidi et al., 2016; Noor et al., 2016). The extent to which a reaction is active, the "capacity utilization", can be defined as the ratio between this context-specific, observed reaction flux and the maximum reaction flux(Davidi and Milo, 2017). If this ratio is one, enzymes are being utilized at full capacity and activity is **machinery-limited**. However, if this ratio is less than one, one of the aforementioned factors is decreasing the reaction rate. If this is due to saturation effects, not all of the expressed enzyme is used(Xia et al., 2022) and activity is instead **nutrient-limited**. Unused,

free enzymes may point to hedging for rapid adaptation to future conditions which require increased flux through those reactions (Appendix A).

2.2.3 Communication: Coordinating Signaling and Secretion with Gene Expression—Signaling and secretion link a cell's extracellular environment with its intracellular activity, regulating the higher-order functions of multicellular systems. While signaling pathways sense and respond to extracellular signals, the secretory pathway produces communicatory molecules to send such information. These two molecular processes are not only complementary conceptually, but also biologically, coordinating each others' activity(Farhan and Rabouille, 2011; Shvartsman et al., 2002). Secreted proteins are the product of gene expression. Unlike machinery, these proteins do not directly contribute to biomass production or intracellular activity. Yet, human cells allocate a massive amount of resources to protein secretion: secreted proteins represent >25% of the proteome by mass(Kuo et al., 2021), despite the fact that these proteins do not contribute to intracellular tasks such as biomass production. This speaks to the importance of secretory tasks such as cell-cell communication(Francis and Palsson, 1997; Le Bihan et al., 2012; Wegrzyn et al., 2010), cytotoxicity(Lopez et al., 2012; Reefman et al., 2010), and remodeling of the extracellular matrix(Bonnans et al., 2014) to multicellular systems. Signal transduction pathways and their downstream transcription regulatory networks use extracellular cues, i.e. nutrients and communicatory molecules, to induce gene expression. Specifically, a receptor will sense the extracellular cue, downstream machinery processes the information encoded by that signal, and transcription factors induce the synthesis of target genes. As such, signaling pathways enable context-specific cellular decision-making(Hill et al., 2017; Klumpe et al., 2022; Larson et al., 2022; Yang Shen et al., 2022; Shvartsman et al., 2002).

Signaling pathways have multiple possible objectives, including **signal amplification**, **sensing precision** (i.e., noise mitigation)(Lestas et al., 2010), **information transfer**, **parameter robustness**, and **response time**(Alves et al., 2021). However, the signaling pathway activities underlying these objectives are constrained by energetic and machinery resource costs that the cell minimizes(Lan et al., 2012; Mehta and Schwab, 2012; T.-L. Wang et al., 2022). For example, Goldbeter–Koshland push–pull network sensing systems–signal transduction pathways ubiquitous across prokaryotes and eukaryotes(van Albada and ten Wolde, 2007)–prioritize sensing precision. Here, receptors, downstream signaling machinery, and energy each independently constrain the extent to which noise can be mitigated. For optimality, these three constraints evolved to be equally limiting(Govern and Ten Wolde, 2014). A lack of sensing precision can propagate downstream to cause stochastic gene expression (Elowitz et al., 2002) (Appendix B). Recent studies have indicated that, when sufficiently accounting for cell phenotype and context, this stochasticity is minimal(Battich et al., 2015; Foreman and Wollman, 2020). This is because individual mammalian cells can mitigate downstream noise of the final machinery products by "smoothing" across time. For example, subcompartmentalization shows that increased nuclear retention times decrease cytoplasmic mRNA noise(Battich et al., 2015) and reduced protein degradation rates, relative to mRNA degradation rates, decrease protein noise (Raj et al., 2006). Similarly, noise can also be mitigated by the signaling network topology(Austin et al., 2006; Zhang et al., 2007).

More broadly, the efficiency by which signaling pathways and downstream transcription regulatory networks achieve their objective depends on their network topology(Alon, 2007). Consequently, evolution has converged on a small number of prevalent topologies, termed network motifs, that determine the dynamics and robustness of network input-output relationships. Since there are multiple possible signaling objectives, it remains unclear how the interplay between these various objectives may affect resource allocation. For example, only two experimentally observed network motifs demonstrate fold-change detection across a wide range of organisms because they are uniquely **Pareto optimal** for response time, sensing precision, and signal amplification(Adler et al., 2017).

Network motifs are building blocks for global network structures. Convex analysis(Schilling et al., 2000) of signaling networks identifies a minimal set of pathways representative of the network state from its global topology. These "extreme pathways" reveals how cells divert metabolic and machinery resources across the network, encoding for **signaling crosstalk** and redundancy between pathway reactions to achieve robust input-output relationships(Papin and Palsson, 2004a, 2004b). Reducing crosstalk trades-off with increasing sensing precision(Barton and Sontag, 2013) due to the energetic costs of signaling modularity(Saez-Rodriguez et al., 2005). Thus, cells employ combinatorial strategies that instead leverage crosstalk to reduce resource costs. For example, by sharing the tumor necrosis factor (TNF) ligand, the nuclear factor kappa B (NF-κB) and c-Jun N-terminal protein kinase (JNK) pathways bypass noisy signaling to increase information transfer relative to either pathway acting in isolation.

Just as multiple signaling pathways can share a ligand to increase information transfer within an individual cell, multiple cells can share a signaling pathway (and thus, a ligand) to analogously improve the average response to a ligand.(Cheong et al., 2011) In contrast to an individual cell, sharing a ligand across cells does not have an upper bound on information transfer(Cheong et al., 2011), demonstrating the utility of multicellularity. Furthermore, individual cells can couple their responses to other cells, leveraging their inherent stochasticity in combination with the underlying signaling network topology, to control the extent of heterogeneity across the tissue(Smith and Grima, 2018). This demonstrates how multicellular systems can use communication to take advantage of noise at the single-cell level to yield emergent properties at the tissue-level. In fact, when coordinating in multicellular systems (Fig. 3b), a number of strategies reduce the resource costs associated with synthesis and secretion of communicatory molecules. For example, a single shared ligand can achieve diverse population-level behaviors such as bistability, e.g. all-or-nothing responses, and bimodality, e.g. cell fate decisions, by combining autocrine and paracrine communication(Youk and Lim, 2014). Finally, when considering both multiple signaling pathways and a cell population, promiscuous ligand-receptor combinations enable more robust activation of multiple cell types as compared to one-to-one binding(Su et al., 2022). Overall, mammalian cells have developed a number of resource optimization strategies to efficiently communicate, lowering the barriers to multicellularity.

2.3 Trade-offs Occur Due to Multiple Objectives

Cells balance multiple objectives(Alon, 2019). Allocating resources towards one objective induces a trade-off because the shared and limited pool of resources must be diverted away from the pathways that enable a competing objective. A simple case is in the expression of two different genes within a cell: under a fixed resource budget, due to resource loading of biosynthetic machinery, increased expression of one gene is achieved by decreasing expression of the other(Gyorgy et al., 2015). Additionally, at the tissue-scale, different systems in the brain are each specialized for one or more tasks and trade-off against each other(Alonso et al., 2013). These tissue-scale tasks are coordinated within the multicellular system(Rueffler et al., 2012) to appropriately distribute resources and enable context-specific task prioritization.

Under resource optimality assumptions, such trade-offs are mathematically represented by a Pareto front (Fig. 3a), or the set of all optima for which performance of one objective cannot be improved without decreasing performance of another objective. Pareto analysis reduces the resource-constrained phenotype space(Szekely et al., 2013), enabling more accurate identification of the biological mechanisms evolution converged upon. Using genome-scale models (GEMs) (Appendix B, Table 1) in Pareto analysis has demonstrated trade-offs between five objectives (e.g., synthesis of albumin, glutathione, and NADPH depending on nutrient availability) in hepatocytes(Nagrath et al., 2007) and between growth and protein secretion in CHO cells(Gutierrez et al., 2020). Pareto analysis has also been adopted to understand omics data, enabling the identification of the number and type of objectives present in the dataset, and the features that support each objective (Table 1). For example, applying this to human breast cancer tumors revealed four distinct objectives (de-differentiation and division, differentiation in healthy tissue, signaling, and growth) that changed according to the tumor type(Hart et al., 2015). In the proceeding sections, we discuss the various manners by which a cell may encounter more than one objective.

2.3.1 Context-specific Trade-offs Underlie Cellular Decision-Making—Trade-offs between multiple objectives require a cell to choose how to allocate its resources and prioritize certain activities. Context-dependent changes in phenotype and the underlying cell state can be understood by cellular decision-making: different contexts introduce different objectives and resource budgets to the cell, imposing trade-offs along the context dimension (Fig. 3a). Context-dependent changes to the biological objective are reflected in the underlying molecular processes that drive activity, such as global changes in translational efficiency during differentiation(Ingolia et al., 2011) and spatial changes in glycolytic fluxes during development(Bulusu et al., 2017).

Multiple objectives are not always present simultaneously, but may arise in sequence according to some context variable (e.g., as a cell migrates, ages, or encounters stress). For example, trade-offs between growth and non-growth associated maintenance (NGAM) over time can explain age-related declines in biological function (Appendix D). Additionally, the extent to which eukaryotic gene expression programs optimize for growth depends on nutrient availability, indicative of context-specific tuning of machinery for non-growth objectives(Keren et al., 2016). It is worth noting that mammalian cells, particularly in

homeostatic tissue, likely often prioritize for non-growth objectives; however, research in this area remains limited, partially because studies using physiological readouts beyond growth are uncommon (see Conclusion for details).

Proteome allocation demonstrates how global strategies of machinery expression are selected according to context-specific trade-offs. Proteome allocation assumes a context-independent, constant upper bound allocated to total protein abundance due to synthesis costs and spatial constraints(Elsemman et al., 2022; Hui et al., 2015; Mori et al., 2016; Nilsson et al., 2017; Xia et al., 2022; Yang et al., 2016). Due to this upper bound, increases in expression of one or a group of proteins that support a given function requires compensatory decreased expression of others. An insightful consequence of this proteome allocation perspective is in the use of respiratory or glycolytic pathways in energy metabolism (Appendix A). Proteome allocation trade-offs explain why cells employ the machinery cost minimization strategies previously discussed, as it enables them to not only efficiently perform a single task, but also to have a larger capacity to perform multiple tasks simultaneously and express some machinery in excess to hedge for future conditions. Highly abundant proteins perform "core" functions, such as gene expression and energy metabolism, that tend to be conserved across contexts. In contrast, context-specific proteins have lower abundance, suggesting proteome re-allocation across contexts minimizes machinery biosynthetic costs by unevenly distributing their abundance according to function(Beck et al., 2011).

2.3.2 Cells Hedge for Future Contexts—Cells adjust their pathway activity accordingly to adapt to the resource demands of each context. To rapidly adapt, cells employ hedging: rather than being fully optimized for one context, cells divert some of their resources in anticipation of new tasks.

For example, the *E. coli* proteome is not fully optimized for growth, re-allocating up to 95% of its proteome by mass fraction from growth functions such as energy production to those such as cell signaling and membrane transport in anticipation of stresses(Yang et al., 2016). Indeed, *E. coli* balances multiple objectives, including growth, minimizing total metabolic fluxes (Appendix B), and ATP yield. However, they do not lie exactly on the Pareto front to decrease the cost of adjustment between objectives(Schuetz et al., 2012). In *S. cerevisiae*, cells allocate some of their ribosomes for future growth, and under hyperosmotic stress undergo cell cycle arrest, sacrificing the speed of their adaptive response to maintain glycogen reserves in preparation for subsequent stresses(Bonny et al., 2020). Similarly, mammalian cells may allocate some of their proteome towards aerobic glycolysis to hedge for hypoxia (Appendix A).

The extent to which cells utilize hedging varies, as some cells specialize for specific contexts. For example, different microbial strains tend to be optimized for glycolytic or gluconeogenic growth, resulting in long lag times upon nutrient shifts in one direction of central carbon metabolism. Probing this further, trade-offs between lag time, growth rate, and futile cycling prevent optimality in both directions, driving these cells towards **specialization**(Schink et al., 2022). While these trade-offs shape the decision-making of

unicellular organisms, multicellular, mammalian organisms have evolved strategies to limit trade-offs and the need for hedging.

2.4 Multicellularity: From Cells to Organisms

Multicellularity emerged to efficiently manage and mitigate resource trade-offs (Fig. 2). Tissues are multicellular organizations composed of diverse individual cells. Since tissues receive a variety of cues, individual cells display context-dependent heterogeneity. This heterogeneity, which can be quantitatively characterized using single-cell measurements, results in distinct cell types or states. From a resource allocation perspective, these distinct cell types are optimally fulfilling distinct objectives according to the context in a manner that imposes demands on distinct resources(Jerby-Arnon and Regev, 2022). Context-specific objectives and trade-offs at the cellular scale induce multicellular coordination to optimize tissue-level functions(Almet et al., 2021; Toda et al., 2019) that ultimately impact the whole-organism (Appendix C).

2.4.1 Division of Labor Distributes Resource Burdens—Individual cells represent the fundamental unit of tissues. These cells occupy a spectrum of distinct states according to their contexts, and single-cell resolution measurements can comprehensively quantify this heterogeneity(Wagner et al., 2016). For example, single-cell RNA-sequencing has helped characterize the pathogen specificity of immune responses(Blecher-Gonen et al., 2019), treatment effects in autoimmune disease(Baghdassarian et al., 2023), cell developmental trajectories across time(Fischer et al., 2019; Yeo et al., 2021), and the spatial organization of cells within tissue(Ren et al., 2020).

From a resource allocation perspective, such diverse cell states represent functional specialization(Arendt, 2008) to support a **division of labor** strategy employed by multicellular organisms: rather than performing all tissue tasks, individual cells specialize to more efficiently perform a subset of these tasks. Since the context dictates the information and resources provided to a cell via extracellular cues, a cell will specialize to optimally perform particular objectives accordingly. In steady-state tissues, spatial context gradients are often paramount (Fig. 3b). Single-cell measurements characterize the context-dependent gene expression programs a cell pursues in support of its objectives. For example, single-cell analysis reveals five distinct enterocyte cell states that form longitudinally along the small intestine, each with distinct metabolic activity to support absorption of specific nutrients (e.g., fatty acids, carbohydrates, lipoproteins and amino acids, and cholesterol and steroids) (Zwick et al., 2023). Similarly, hepatocytes alter the expression patterns of ~50% of their genes in accordance with their spatial location. These patterns reflect coordination between all three resource classes–liver zones with higher oxygen availability also demonstrated machinery shifts towards oxidative phosphorylation, likely generating energy to support higher protein secretion(Halpern et al., 2017).

In parallel, Pareto analysis has been used to identify relevant tissue objectives that trade-off against each other, and how cell types are distributed across these objectives. For example, neural arbors arrange their network topology in a Pareto optimal manner to minimize wiring costs and conduction delay(Chandrasekhar and Navlakha, 2019). These

two objectives support efficient communication, indicating the importance of coordination between cells, a concept that will be elaborated on in the following section. In this study, 15 distinct cell types were distributed across this Pareto front, indicating varying degrees of specialization towards either objective. Golgi and stellate cells, for example, were specialized for minimizing conduction delay and wiring costs, respectively, whereas projection cells represented generalists equally prioritizing both tasks.

Finally, single-cell measurements have been combined with the aforementioned high-dimensional Pareto analysis method(Hart et al., 2015) In line with the neural arbor cell type analysis(Chandrasekhar and Navlakha, 2019), these studies broadly demonstrate that, subject to trade-offs, single-cells represent specialists optimized for a particular task or generalists that can perform multiple tasks (Fig. 3a). For example, analysis of human colon crypt progenitor cells identified four objectives: stemness, activation of cell-type specific genes, reduction of global gene expression, and halting of division. Notably, mature cell types are also specialized in a manner corresponding to their spatial location(Korem et al., 2015). Similarly, enterocytes are distributed across three objectives–cell adhesion and lipid transport, carbohydrate and amino-acid uptake, and anti-bacterial defense–in a manner correlated to their location in the intestinal villus(Adler et al., 2019).

Both the colon progenitors and terminally differentiated enterocytes form continuums in gene expression space, bounded by their respective objectives. Single-cell continuums can be explained by external spatial gradients, are indicative of varying degrees of specialization, and are necessary to optimize tissue function (i.e., maximize net performance across all objectives)(Adler et al., 2019). Thus, division of labor does not simply lead to a random assortment of heterogeneous cells, but rather confers optimality at the tissue-scale. While each individual cell is specialized to perform some subset of tissue tasks, division of labor distributes these tasks across multiple cell types in a manner yielding synergistic effects: the cells' combined functions amplify performance across a range of tissue-level tasks. For example, division of labor mitigates both the cost of switching between multiple objectives in a tissue(Goldsby et al., 2012) and the loss of tissue function when cells proliferate (instead of performing the objective they are specialized for) for homeostatic maintenance and turnover(Rodríguez-Caso, 2013). Furthermore, diversity in the extent of specialization (represented as continuums in single-cell gene expression space) enables robustness against perturbations(Rueffler et al., 2012). In the next section, we will discuss the coordination strategies cells employ to achieve these higher-order functions.

2.4.2 Coordination Enables Higher-Order Functions—As cells specialize, emergent tissue-level functions arise from coordination, wherein resources are distributed across systems(Alonso et al., 2013) and yield synergistic effects that enable phenotypes no individual cell type can(Rueffler et al., 2012). At the molecular scale, coordination can be seen as the joint molecular activity across distinct cell types (i.e., "multicellular programs") (Jerby-Arnon and Regev, 2022; Mitchel et al., 2023; Ramirez Flores et al., 2023). Systems modeling approaches can probe the connection between the molecular activity of individual cells and tissue-level functions by characterizing the relationships between a cell and its environment (e.g., extracellular cues and neighboring cells)(Adler et al., 2023a; Polychronidou et al., 2023). GEMs, for example, can model intercellular resource

allocation and metabolic crosstalk between cells(Martins Conde et al., 2016). Multicellular GEMs for brain astrocytes and neurons demonstrated that energy pathways are distributed across cell types to minimize protein costs(Gustafsson et al., 2022) and revealed metabolic phenotypes underlying Alzheimer's Disease(Lewis et al., 2010b). GEMs also elucidated how fibroblasts reprogram colorectal cancer cell metabolism by stimulating pathways such as glycolysis and glutaminolysis without altering growth (J. Wang et al., 2022).

Coordination and the collective behavior of cells depends on information transfer (see Section 2.2.3 for the role of resource allocation in sending and interpreting information), often via cell-cell communication. Within the single-cell Pareto optimality framework previously described(Korem et al., 2015), the type and range of cell-cell communication influences tissue spatial patterning to coordinate specialization, enabling cells to self-organize as efficient multicellular systems. Colon fibroblasts distributed across one of five objectives (ECM degradation, ECM production, integrin production, regulation of the immune response, and contractile functions) communicate via specific ligand-receptor pairs that correspond to their spatial location and specialization(Adler et al., 2023b; Halpern et al., 2017; Zwick et al., 2023). Due to communication costs, resource allocation also impacts how the information to organize multicellular systems is distributed (Fig. 3b). As discussed previously, signaling pathways optimize for specific objectives such as sensing precision(Govern and Ten Wolde, 2014). To manage spatial-gradient-induced noise during wound-healing, cells maximize sensing precision by coordinating within optimal local distances via paracrine growth factor communication(Handly et al., 2015). Indeed, Pareto optimal task-distribution in tissues can be separately influenced by spatial gradients and local communication(Adler et al., 2023b; Halpern et al., 2017; Zwick et al., 2023).

Ultimately, coordination leads to higher-order properties such as compositional homeostasis and organismal defense. Communication, for example, maintains steady-state cell type proportions in tissue by tuning cell proliferation and removal rates (Fig. 3c–d). Zhou *et al.* identified a two-cell macrophage-fibroblast circuit that uses growth factor exchange for compositional homeostasis. In this circuit, fibroblast proliferation is limited by resource constraints whereas macrophages are limited by negative feedback of the growth factor CSF1(Zhou et al., 2018). The specific growth factors used are context-dependent across nutrient-limiting conditions, and the distinct cell types are competing for different limiting resources(Zhou et al., 2022). However, while context affects individual parameters, such as cell growth rates, the circuit's stability is generalizable. Separately, in the rove beetle tergan gland, cell specialization resulted in the co-evolution of two specialized cell types that each produce small molecules which are innocuous in isolation, but form a defensive toxin when combined(Brückner et al., 2021). Coordination between cell types can also be advantageous for disease states. In cancer, for example, groups of circulating tumor cells demonstrate more than an order of magnitude increased metastatic potential compared to individual cells (Aceto et al., 2014). Extending the previous discussion of motility resource allocation(Zanotelli et al., 2019) to the multicellular dynamics of cancer metastasis, cells invade cooperatively to minimize energetic costs of migration. A "leader" cell disproportionately expends its resources to displace the matrix, making migration easier for "follower" cells. After it has depleted its energy budget, the leader cell is replaced by a follower cell that still has a high energy budget(Zhang et al., 2019). In a simplified model,

one study demonstrated that metastatic invasion occurs in the presence of a nutrient gradient, indicating the metastatic population is willing to pay the energetic costs of migration in search of a location with more nutrient resources(Liu et al., 2013).

2.4.3 Resource Competition Maintains Homeostasis

—While division of labor improves the efficiency by which cells allocate resources and allows for coordination, much like the intracellular pathways of an individual cell, cells in the same microenvironment compete for a shared pool of extracellular resources. In some cases, cells in the same microenvironment–particularly if they share the same identity–are not only using the same pool of resources but are also using those resources in the same manner because they have a shared objective. We saw this in the macrophage-fibroblast circuits, in which macrophages competed for growth factors whereas fibroblasts competed for space(Zhou et al., 2022). During development, competition actually serves as a coordinating mechanism to improve morphogenesis (i.e., growth, differentiation, and structure), with resource scarcity being the coordinating signal(Smiley and Levin, 2022). Thus, competition is an important homeostatic mechanism constraining any individual or population of cells' objective (e.g., growth) from dominating.

Canonically, cell competition is defined as the "active elimination of intrinsically viable cells that differ in some way from their neighbors"(Baker, 2020). Within this definition, resource competition is one such mechanism for elimination, with less fit "loser" cells unable to use resources as efficiently as "winner" cells to achieve their objective, thus optimizing overall tissue fitness(Matamoro-Vidal and Levayer, 2019). For example, under conditions of nutrient abundance, lower Myc expression causes cells to have a lower anabolic capacity, ribosomal abundance, protein synthesis rates, and proliferative capacity(Clavería et al., 2013; Ellis et al., 2019). These less-fit cells are eliminated via apoptotic signaling and asymmetric cell division. In epidermal expansion, during mouse embryogenesis, for example, this elimination ensures appropriate tissue architecture.

Similarly, oncogenic epithelial cells are eliminated by wild-type cells via apical extrusion. Metabolically, the less-fit cells are inefficient, shifting towards aerobic glycolysis and exhausting glucose without substantially increasing ATP(Kon et al., 2017). In contrast to homeostatic maintenance, metabolic competition in tumors, which have high resource demands, can lead to disease progression. For example, tumor cells reduce tumor infiltrating lymphocyte (TIL) effector function by competing for glucose. Lower glucose availability decreases TILs' oxidative phosphorylation flux and their biosynthetic capacity to secrete interferon gamma(Chang et al., 2015). The high lactic acid levels produced by tumors via aerobic glycolysis in low glucose conditions also decreases immune cell ATP levels and biosynthetic capacity, ultimately suppressing TIL infiltration and survival(Brand et al., 2016). However, the presence of other nutrient sources and cell types may mitigate the role of competition(Reinfeld et al., 2021). Recent work has leveraged the high resource demands of cancer cells by engineering adipocyte glucose and lipid metabolism to outcompete tumors(Nguyen et al., 2023; Seki et al., 2022).

3. Conclusions

Resource allocation provides a unique perspective into the mechanisms underlying mammalian biology across cell-, tissue-, and whole-organism- scales. As outlined in this Review, resource allocation impacts homeostasis, and context-dependent changes in allocation are accompanied by physiological changes, as seen in diseases such as obesity, Alzheimer's, aging, diabetes, and cancer (Table 2). Resource allocation is one of many useful approaches to gain mechanistic insights to multicellular systems; given the complexity of such systems, particularly with changing contexts, there are scenarios in which resource allocation will only partially explain observations or will not be a driving force for certain biological behavior. However, the provided evidence indicates that resource allocation can be a lens by which to better understand biological phenomena and thus should be an avenue of continued development for mammalian multicellular systems.

To comprehensively understand the aforementioned context-dependent changes and better define general principles that are predictive across contexts, molecular measurements and the discussed systems biology approaches must be extended. High-throughput, high-resolution molecular quantitation is necessary to enable systems biology analyses. When considering multicellularity, single-cell resolution is particularly important to gain a comprehensive understanding of tissue subpopulations and heterogeneity(Wagner et al., 2016). While single-cell RNA-sequencing is commonly used, single-cell measurements that can capture multiple biological layers and contexts will be necessary to inform and parameterize resource allocation models. Spatial transcriptomics(Tian et al., 2023), for example, can be used to capture how spatial context gradients drive gene expression(Jerby-Arnon and Regev, 2022), leading to, for example, division of labor(Adler et al., 2023b; Halpern et al., 2017; Zwick et al., 2023). Additionally, since subcellular compartmentalization alters network dynamics, cells optimally distribute their machinery (i.e., in various organelles) accordingly(Giunta et al., 2022); thus, spatial measurements should not just account for tissue-architecture, but also quantify molecular distributions at the subcellular resolution(Mah et al., 2023). Given the importance of production, degradation, and catalytic rates of machinery in network dynamics, the ability to characterize the temporal context is also important. While omics measurements have the drawback of being static, time-series single-cell omics datasets are becoming more common. These can be integrated with emerging models that can characterize the temporal dynamics of high-dimensional data(Fischer et al., 2019; Klein et al., 2023; Qiu et al., 2022; Salehi et al., 2021) or continuous time quantitation at single-cell resolution, e.g., through imaging(Headley et al., 2016; Pinkard et al., 2021). Furthermore, a major limitation in parameterizing resource allocation models is the lack of characterization of these various rate constants in high-throughput(Cambridge et al., 2011; Chang et al., 2021; Gregersen et al., 2014; Li et al., 2021; Markin et al., 2021; Nilsson et al., 2017). Deep learning provides an avenue forward to robustly estimate such parameters from molecular features(Kroll et al., 2023; Li et al., 2022). Deep learning and other algorithmic approaches may be combined with GEMs to leverage flux predictions and metabolic network topology to estimate enzyme kinetic parameters(Andreozzi et al., 2016; Choudhury et al., 2023; Gopalakrishnan et al., 2020; Heckmann et al., 2020, 2018). Finally, measuring multiple biological layers (Fig.

1C) is important to fully and explicitly account for the resource costs of biological activity and understand how resource allocation decisions propagate to phenotype. Single-cell multi-omics(Baysoy et al., 2023) will be useful for this purpose. Conducting joint molecular and physiological (e.g., cell morphology(Haghighi et al., 2022), size(Neurohr et al., 2019), density(Bryan et al., 2014) and growth rate(Cermak et al., 2016) measurements in the same single cell will also be crucial to connect molecular activity with phenotype.

As these types of measurements become more readily available, systems biology analyses (Appendix B, Table 1) can enable studies that provide a mechanistic connection between resource allocation and phenotype(Nagle et al., 2021). The discussed resource allocation models should be combined with emerging methods designed to appropriately handle this data and account for multicellularity. For example, a number of recent tools can infer multicellular programs from omics data that measure multiple contexts(Jerby-Arnon and Regev, 2022; Mitchel et al., 2023; Ramirez Flores et al., 2023), which can help identify key features underlying the joint molecular activity in multicellular tissues. GEMs can be adapted for single-cell omics to understand the diversity of tissue metabolic phenotypes(Hrovatin et al., 2022; Wagner et al., 2021), including small-molecule mediated intercellular interactions(Armingol et al., 2022b; Zheng et al., 2022). Currently, many resource allocation models are limited to prokaryotes due to the complexity of mammalian systems (e.g., multiple subcompartments with distinct localization(Giunta et al., 2022)[,(Mah et al., 2023),(Hinzpeter et al., 2019; Schmitt and An, 2017)], protein secretion, etc.), and many have focused on protein machinery. However, other macromolecules, such as noncoding RNA (e.g. lncRNAs, tRNA(Torrent et al., 2018), etc.), also constrain cell activity; without incorporating these molecular details, models may miss key regulatory components that affect phenotype. Finally, while resource allocation is apparent at the whole-organism scale (Appendix C), the underlying molecular mechanisms regulating this have not been extensively studied. Recently, whole-body models have begun to extend the GEM framework to address this gap(Thiele et al., 2020), but these can benefit from more detailed measurements, especially at the resolution of specific cell-types. Improving modeling approaches, when complemented by more comprehensive quantitation, will provide excellent opportunities to uncover principles of resource allocation in mammalian cells and will also be important to link extra- and intra-cellular activity to understand multicellularity.

Finally, an understanding of mammalian resource allocation can be informative for cell engineering. Genetic engineering has high utility for production of biofuels, engineering of efficient food crops, introducing perturbations to advance our understanding of basic biological processes, and in mammalian cells, design of protein- and cell-based therapeutics(Bashor et al., 2022; Way et al., 2014). However, resource loading causes the coupling of exogenous genetic components, in which the output of one gene depends on that of seemingly independent other genes due to shared resources(Di Blasi et al., 2021; Rondelez, 2012). While the use of host-independent, orthogonal components may eliminate coupling with endogenous genes, the issue of coupling still remains in exogenous multi-gene circuits. This coupling can result in unexpected behavior of the cell and its exogenous parts when resource loading is not accounted for. Consequently, resource allocation is important for optimal design of engineered circuits. In biomanufacturing, for example,

quantification of the energetic resource costs of endogenous proteins using the secretory GEM(Gutierrez et al., 2020) enabled targeted knock-out engineering of CHO clones to improve therapeutic protein productivity(Kol et al., 2020). Combining modeling with engineering can also quantify the extent of resource loading, thus identifying the specific limiting resources and most prominent genetic features causing the coupling(Di Blasi et al., 2023; Frei et al., 2020; Jones et al., 2020). Two separate studies used this approach to design incoherent feed-forward loop network topologies–introducing miRNAs(Frei et al., 2020) and endoribonucleases(Jones et al., 2020) to the circuit–that mitigate resource loading by decoupling the genetic components. Importantly, coupling can be explicitly leveraged in engineering designs(Rondelez, 2012). For example, one study used model predictions of resource loading to select exogenous parts with specific parameters that result in accurate stoichiometric production of a virus-like particle(Qin et al., 2023). As discussed (see section 2.1.2), stoichiometric production is an important resource allocation principle for mammalian cells. Overall, resource allocation can help guide cell engineering, decreasing time and resources spent on troubleshooting and improving manufacturing quality.
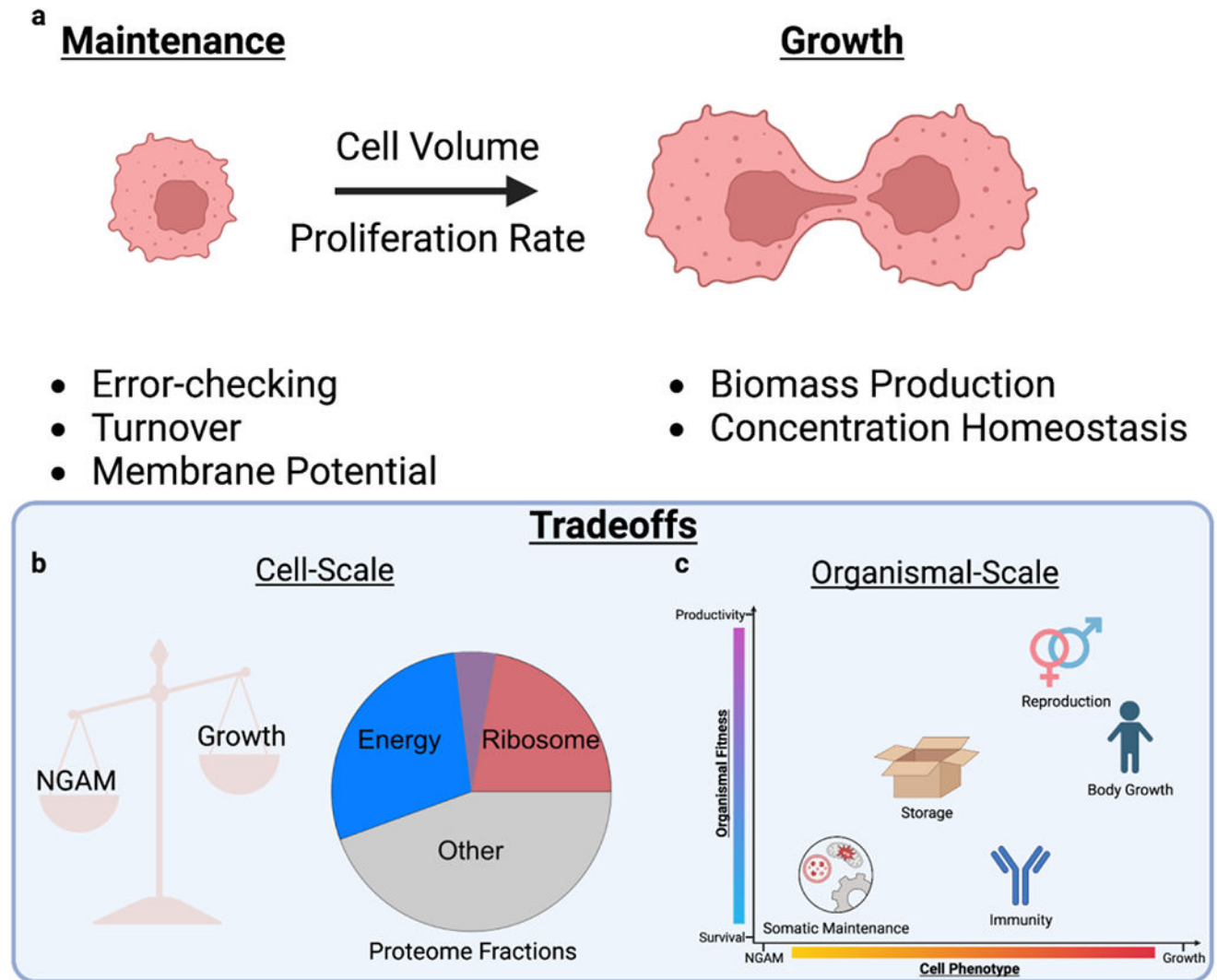
Funding

Appendix

4.

4. 4.1 Appendix A: Resource Constraints and Growth

While some cell types endure dynamic phenotypic changes (e.g., immune responses, development, and hepatocyte communication), many cells in tissue exist in a steady-state, with resources allocated to homeostatic maintenance. Thus, resource allocation is often simplified into a stratification between growth- and non-growth associated maintenance (NGAM) costs (Appendix A Fig. a–b). NGAM represents biological processes that do not directly contribute to growth, such as error-checking(Sartori and Pigolotti, 2015), maintenance of membrane potentials, and macromolecular maintenance given turnover. While some of these processes may change with growth, they have baseline NGAM activity quantitatively defined as resource costs at zero growth(Feist and Palsson, 2010; Thiele and Palsson, 2010). Underlying the balance of growth and NGAM are alterations in gene expression of cellular machinery and energy management that ultimately affect organismal phenotypes (Appendix D, Appendix A Fig. c).

Appendix A Figure: Maintenance and growth objectives in cells and organisms.
a | Cell maintenance and growth both require resource investments and incorporate distinct biological activities. **b** | Consequently, they trade-off with each other. Trade-offs are observed by the proteome fraction allocated to translational machinery for biomass production (red) and machinery for catalysis of bioenergy metabolism (blue). The purple shaded region represents varying cell proteome allocation towards translation or bioenergy with changing context. **c** | Life-history traits optimally trade-off against each other to maximize whole-organism fitness via productivity and survival (y-axis). While these trade-offs mirror those at the cell-scale, rather than being binary, they use a combination of cell growth and NGAM (x-axis). The yellow-red color bar represents the gradient across NGAM and growth at the cell-scale, whereas the blue-purple color bar represents the gradient across survival and productivity at the organismal-scale.

4.1.1   Growth Phenotypes Depend On Gene Expression

Gene expression indirectly (as machinery facilitating biosynthesis) and directly (as biosynthetic products) contributes to biomass production. The relationship between gene expression and growth maintains concentration homeostasis–which is necessary for appropriate cell function(Neurohr et al., 2019)–with cell volume expansion by dynamically adjusting synthesis rates through resource loading of transcriptional and translational machinery(Lin and Amir, 2018). Thus, in prokaryotes(Scott et al., 2010) and eukaryotes(Björkeroth et al., 2020; Metzl-Raz et al., 2017; Xia et al., 2022), the proteome fraction allocated to ribosomes increases linearly with increasing growth rate to support increased biosynthetic demand. Such linear relationships delineate the extent to which cells are nutrient- or machinery- limited in growth, with cells allocating a baseline unused portion of ribosomes to hedge for future increases in growth rate.

In rapidly proliferating prokaryotes, protein degradation is often assumed to be negligible because dilution rates due to cell division far outweigh degradation rates(Hausser et al., 2019). Yet, in slower-growing mammalian cells, degradation rates play a substantially more important role in dictating overall protein abundance(Jovanovic et al., 2015; J. J. Li et al., 2014). Macromolecular synthesis must not only contribute to biomass production and counteract biomass loss due to dilution, but also biomass loss due to degradation. Consequently, the linear relationship between ribosomal mass fraction and growth rate is altered at slow growth, shifting a larger than predicted fraction of proteome mass to active ribosomes to maintain biomass when faced with non-negligible protein degradation(Calabrese et al., 2022).

4.1.2   Energy Budgets are Balanced Between Growth and NGAM

In mammalian cells, linear relationships exist between individual genes' abundance with cell size(Miettinen et al., 2014) and between other phenotypes such as migration with growth rate(Kochanowski et al., 2021). Omics measurements of individual genes enable further exploration of proteome re-allocation between translational machinery and other functional protein sectors, such as energy metabolism (Appendix A Fig. b). Consistently, there is a shift in energy metabolism from respiratory to glycolytic activity with larger cell size and higher growth rate(Metzl-Raz et al., 2017; Miettinen et al., 2014; Xia et al., 2022).

By knocking out key enzymes facilitating aerobic glycolysis, rapidly proliferating mammalian cells shift back to OxPhos without reducing their growth rate(Hefzi and Lewis, 2017). Additionally, under both respiratory and glycolytic conditions, the effect of ribosomal proteins on growth rate is independent of the energy budget(Mendelsohn et al., 2018). This indicates that, unlike in microbes (Appendix D), proteome constraints alone cannot explain the shift to anaerobic glycolysis at high growth rate in mammalian cells. The metabolic shift may not provide enough of a fitness benefit, with mammalian OxPhos having higher protein efficiency (Appendix D) as compared to aerobic glycolysis(Yihui Shen et al., 2022). An alternative explanation may lie in proteome hedging, wherein cells express excess anaerobic machinery for future contexts, such as hypoxia at high growth(Argüello et al., 2020)[,(Fan et al., 2013)]. However, in this case, resource allocation might not be as applicable to mammals,

whose coordinated tissue systems mitigate trade-offs and typically do not anticipate high growth.

4. 4.2 Appendix B: Systems Biology Approaches to Understand Resource Allocation

The coupling of activity between different intracellular molecular processes, constrained by the cellular resource budget, dictates phenotype. Many systems biology approaches combine high-throughput measurements with computational algorithms to model the interplay between intracellular processes and understand phenotype.
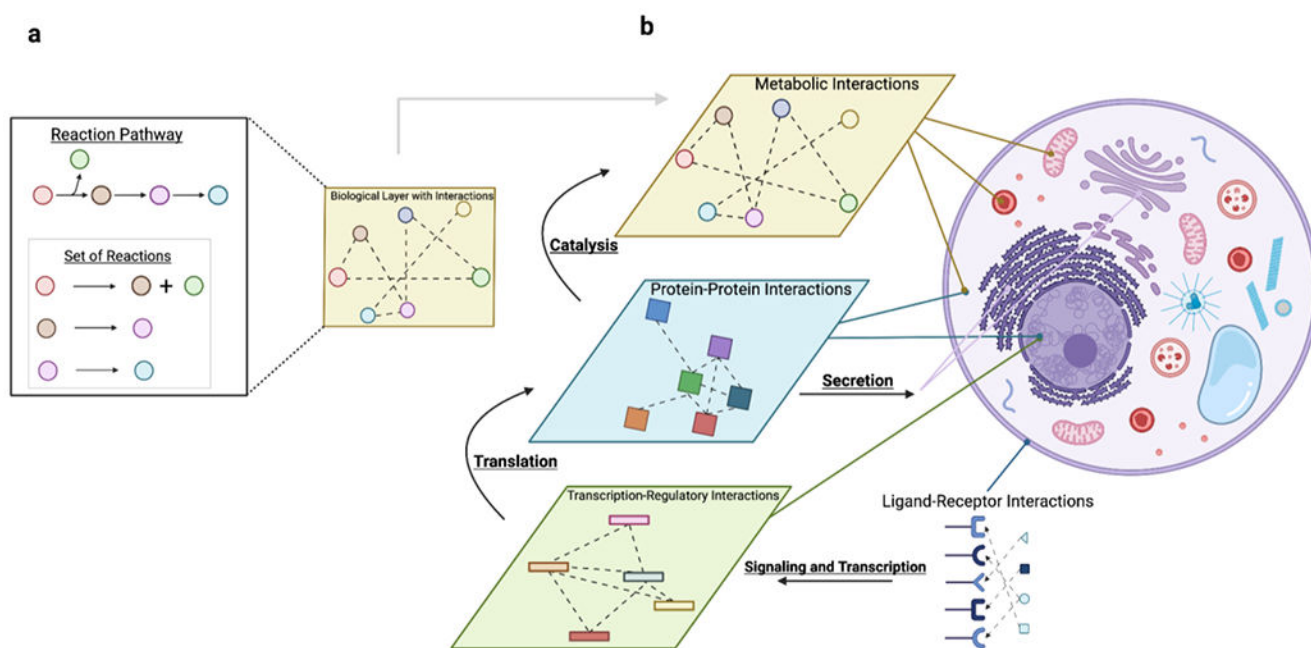
Phenomenological models, for example, are coarse-grained representations that identify quantitative relationships between resource constraints, cellular activity, and phenotype. Such models have described relationships between gene expression and growth(Scott et al., 2010), proteome allocation under resource limitation(Hui et al., 2015), and macromolecular concentration homeostasis(Lin and Amir, 2018). Describing such relationships in a few meaningful parameters that are robust across contexts, these models shed light on principles of resource allocation. However, they lack molecular details.

Thus, models that integrate resource availability with mechanisms are necessary. Kinetic ordinary differential equations (ODEs) are commonly used to model gene expression (Appendix B Fig. a). Such approaches have been extended to account for gene expression noise via a "two-state model" that can account for random, non-constitutive transcription(Munsky et al., 2012). However, these ODE models require extensive measurements of kinetic parameters and cannot account for resource availability. In contrast, genome-scale metabolic models (M-Models) map out all metabolic pathways of the cell, represent them mathematically using their stoichiometric coefficients(Lewis et al., 2012), and use flux balance analysis (FBA) to simulate the reaction fluxes(Lewis et al., 2012; Orth et al., 2010). These fluxes optimize a cellular objective that represents a phenotype of interest (often growth rate(Feist and Palsson, 2010)) while directly accounting for nutrient and bioenergy resource constraints. In mammalian cells, FBA has explored numerous questions, including polyamine metabolism in T-helper 17 cell pathogenicity(Wagner et al., 2021) and enzymes that affect migration, but not proliferation, of cancer cells(Yizhak et al., 2014).

M-Models do not comprehensively account for machinery resources. They can partially do so using methods to overlay gene expression measurements that prune the metabolic network(Opdam et al., 2017), but this only incorporates machinery in a binary manner. Other methods have constrained M-Models by more explicitly minimizing machinery costs. Parsimonious FBA, for example, minimizes the sum of fluxes throughout the network as a secondary objective. Here, the total flux is a proxy for the global "effort" or resource cost of biological activity(Holzhütter, 2004; Lewis et al., 2010a). Another method estimates the extent of total reaction flux that is backwards as a proxy for machinery costs, with higher backwards flux requiring a larger enzyme budget to drive the reaction forward(Noor et al., 2014). Finally, a number of strategies constrain reaction fluxes by machinery abundance

at varying resolution(Noor et al., 2016)·(Mori et al., 2016),(Domenzain et al., 2022; Sánchez et al., 2017). Machinery coupling is not limited to canonical catalytic enzymes, but can be extended to transport(Sahoo et al., 2014), gene expression(Schwanhäusser et al., 2011), and protein secretion(Gutierrez et al., 2020).

Such methods that incorporate individual enzymes into genome-scale models differentiate between nutrient- and machinery-limiting conditions. However, to explicitly account for the entire machinery budget and costs, genome-scale models of metabolism and expression (ME-Models) add gene synthesis reactions for each enzyme(Thiele et al., 2009) and couple them to metabolism (Appendix B Fig. b)(Lerman et al., 2012; O'Brien et al., 2013). In prokaryotes, ME-Models(Dahal et al., 2021) have shed light on proteome allocation strategies under oxidative(Yang et al., 2019), acidic(Du et al., 2019), and thermal(Chen et al., 2017) stress. In eukaryotes, the ME-Modeling framework accounts for compartment-specific proteome constraints, enabling analysis of metabolic shifts, machinery protein costs, and proteome reallocation(Elsemman et al., 2022). Resource Balance Analysis (RBA) models employ similar concepts to encode gene expression and metabolism while also accounting for spatial constraints("Cell design in bacteria as a convex optimization problem," 2011). While RBA is limited to prokaryotes, a theoretical roadmap for eukaryotes exists(Goelzer and Fromion, 2019). Finally, whole-cell models (WCMs) additionally characterize kinetics and encompass more cellular processes(Macklin et al., 2020). By modeling each intracellular system separately then connecting them via common inputs and outputs, WCMs can account for resources shared between multiple intracellular subsystems(Karr et al., 2012) and interconnectivity of molecular processes, e.g. the effect of glycolytic flux for producing dNTPs used in chromosomal replication(Thornburg et al., 2022).

Appendix B Figure: Modeling cellular activity from individual reactions to global networks.

a | A pathway with a set of connected molecules can be decomposed into its individual reactions. These reactions can be used for high-resolution modeling of a particular process, incorporating detailed kinetic parameters. Globally, all the reaction pathways form a network defining some molecular process such as metabolism. **b** | Processes can be coupled (black arrows) using first-principles to create more comprehensive genome-scale models such as ME-models. Signaling and secretion incorporate extracellular interactions, providing a basis for modeling multicellular systems.

For details on how these modeling approaches are implemented and practical use-cases, please see the following references: network dynamics(Alon, 2006), M-models(Palsson, 2015), and whole-cell models(Covert, 2017).

4. 4.3 Appendix C: Resource Allocation Affects the Whole-Organism

Much like coordination between cells in tissue, tissues interact to efficiently allocate resources across the whole-organism. Such strategies reveal how whole-organism physiology is affected by factors such as diet and exercise.

Mammals use complex endocrine signaling mechanisms to sense their internal nutrient state(French et al., 2011; Hardie et al., 2012; Lutter and Nestler, 2009; Wang et al., 1998), which affects their food choices and, ultimately, the composition(Simpson and Raubenheimer, 1993) and elemental stoichiometry(Sterner and Elser, 2017) of nutrients available to cells. Regulatory mechanisms(Khan et al., 2021; Solon-Biet et al., 2016; Yan et al., 2021) ensure that diets optimally balance nutrient ratios to maximize organismal performance. If individual foods do not meet these ratios, mammals consume mixed diets with complementary foods to target this optimum(Felton et al., 2009; Hewson-Hughes et al., 2016; Johnson et al., 2013; Rode and Robbins, 2000). Furthermore, when food availability is constrained and the ideal balance cannot be met, mammals may over- or under-consume some nutrients to prioritize target amounts of others(Jensen et al., 2014; Rothman et al., 2011). Humans, for example, prioritize protein intake over carbohydrates(Simpson et al., 2003). Multicellular organisms may also employ post-ingestion strategies to balance nutrient ratios, particularly under scarcity (Cavigliasso et al., 2020). Insects, for example, modulate secretion of digestive enzymes to re-balance nutrient ratios while also minimizing machinery costs(Clissold et al., 2010).

Diets are tightly regulated because nutrient imbalances have associated costs that constrain performance(Anderson et al., 2020). Mammals must handle excesses by voiding or storing(Azzout-Marniche et al., 2007) them and deficits by conserving them or mobilizing nutrient stores. Protein excesses lead to increased excretion(Bender, 2012) and macromolecular degradation(Harber et al., 2005) costs. Nutrient imbalances can also force cells to utilize less efficient metabolic pathways. For example, gluconeogenesis is used in high-protein, low-carbohydrate diets to form glucose from amino acid precursors. This has substantially higher energetic costs than using carbohydrates directly(Veldhorst et al., 2009). Metabolic changes from imbalanced diets are tied to systemic changes involving multiple tissues(Bisschop et al., 2003), such as starvation from deficits(Soeters et al., 2012) and obesity from excesses(Simpson and Raubenheimer, 2005). For example, amino acid

variability in human diets in association with obesity is higher than that of carbohydrates and fats(Dai et al., 2022).

After ingestion, the body optimally allocates resources across tissues with different metabolic rates and resource expenditures(Heymsfield et al., 2018; Wang et al., 2010). Competing demands between tissues inevitably lead to trade-offs that impact whole-organism performance(Lailvaux and Husak, 2014). The high-energy demands of the brain, for example, impose evolutionary decreases in net resource expenditure of other organs such as the gut(Aiello and Wheeler, 1995) and trade-off with human juvenile body growth(Kuzawa et al., 2014). Since the brain processes the regulatory signals, one theory proposes that the brain prioritizes its own glucose supply to maintain intracellular ATP homeostasis(Hitze et al., 2010; Peters, 2011; Peters et al., 2004). These allocation decisions have also explained trade-offs between life-history traits(van Noordwijk and de Jong, 1986) such as survival and reproduction (Appendix D).

Diet influences these trade-offs because certain nutrient balances are more optimal for certain traits(Cotter et al., 2011; Dai et al., 2022). For example, specific diets can affect performance of specific types of exercise(Lee et al., 2017) (e.g. aerobic endurance training(Ferguson-Stegall et al., 2011; Harber et al., 2010; Vandenbogaerde and Hopkins, 2011) vs. anaerobic high-intensity training(Sale et al., 2011; Wroble et al., 2019)). This makes sense since distinct nutrient stores and bioenergetic pathways are used for different exercise(Hargreaves and Spriet, 2020). Furthermore, diet interacts with exercise to yield synergistic effects on performance(Gomez-Pinilla, 2011; Magkos et al., 2020; Webster et al., 2016; Wu et al., 2008).

Skeletal muscle accounts for ~25% of the whole-body basal metabolic rate(Gallagher et al., 1998). At the cell-scale, this is due to the ATP-consuming processes that enable muscles to perform mechanical work(Barclay, 2015). The energetic costs depend on factors such as the type(Beltman et al., 2004; Tillin et al., 2012), frequency(Bergström and Hultman, 1988), and duration(Hogan et al., 1998) of contraction, with more rigorous exercises consuming more resources. These high resource demands cause physical activity to trade-off with other energy-demanding functions, such as reproduction(Lailvaux and Husak, 2017) and immunity(Kistner et al., 2022). For example, upon antigen exposure, mice must divert energy resources from tasks such as locomotor activity to immunity(Ganeshan et al., 2019). Furthermore, during nutrient scarcity, insulin-dependent GLUT4 glucose uptake by skeletal muscle and adipose tissue is suppressed to preserve resources for the brain(Hitze et al., 2010). To manage these trade-offs, mammals have evolved various strategies for efficient muscle use. This includes tight regulation of concentration homeostasis for maximal bioenergy metabolism(Glancy et al., 2013; Glancy and Balaban, 2021), cell-type specialization(Schiaffino and Reggiani, 2011) and tissue heterogeneity(Lai et al., 2021; Liu et al., 2012) optimized for distinct mechanical tasks, and use of energy-conserving motions(Miller and Hamill, 2015; Rues et al., 2008; Schindler et al., 2007; Umberger et al., 2003).

4. 4.4 Appendix D: Further Insights into Growth and Maintenance

4.4.1 Microbial Shifts in Energy Metabolism at High Growth Rate

In microbes, resource allocation has provided a possible explanation for the shift from respiratory to glycolytic activity with higher growth rate. First, machinery facilitating protein synthesis impose a large resource burden(Liebermeister et al., 2014); in human cells, for example, translational machinery comprise more than 15% of total proteome mass(Nagaraj et al., 2011). Given an upper limit on the total proteome mass, increases in the ribosome mass fraction with growth rate induces trade-offs with other protein sectors. Second, as growth rate increases, the energy budget must also increase(Bennett et al., 2020)(Mendelsohn et al., 2018), largely to accommodate increased ATP consumption for biosynthesis(Lynch and Marinov, 2015). Thus, the cell needs a strategy to accommodate increased proteome allocation towards translational machinery while still maintaining or increasing its energy budget. As such, cells will shift from high yield (ATP generated per unit glucose) but low protein efficiency (ATP generated per unit machinery mass) oxidative phosphorylation to low yield but high protein efficiency aerobic glycolysis as growth increases(Basan et al., 2015).

4.4.2 Energetic Trade-offs Beyond Proteome Allocation

Energetic trade-offs extend beyond proteome allocation, with nutrients used for anabolism incurring indirect costs–defined by their potential to be fully oxidized to yield energy–in addition to the direct energetic costs of biosynthesis(Mahmoudabadi et al., 2019). As such, cells must account for the opportunity cost of the fitness gain from energy production relative to biosynthesis. In line with this, mammalian cells demonstrate sensitivity(Son et al., 2015) and specificity(Hosios et al., 2016) in the nutrient type used for biomass generation. These opportunity costs also contribute to trade-offs between NGAM and growth(Chen and Nielsen, 2019). For example, maintaining protein levels at slow-growth consumes 20% of the mammalian energy budget (BioNumbers(Milo and Phillips, 2015) ID 113244).

4.4.3 Growth and NGAM Scale to Whole-Organisms

Life-history traits maximize organismal-scale fitness by contributing to survival and productivity (i.e., energy invested in activities other than survival)(Kuzawa, 2007). Traits classically include body growth prior to maturity, reproduction after maturity, and somatic maintenance; these traits optimally trade-off against each in a manner analogous to cell growth and NGAM. The connection between these scales lies in nutrient sensing and signaling (e.g., insulin-signaling(Lewin et al., 2017) and target of rapamycin pathways) that stimulate either cell growth or NGAM depending on resource availability, thus prioritizing certain traits over others(Adler and Bonduriansky, 2014). While cell growth largely contributes to body growth and reproduction, NGAM contributes strongly to somatic maintenance(Kuzawa, 2007),(Adler and Bonduriansky, 2014). However, these traits tend to lie on a gradient requiring both cell growth and NGAM (Appendix A Fig.c). Somatic maintenance, for example, uses cell growth to balance apoptosis of damaged cells during tissue turnover.

Additional functions such as immunity(Urlacher et al., 2018) and nutrient storage(Fischer et al., 2011) also contribute to organismal fitness, but with additional costs that induce further trade-offs. These trade-offs are dynamic over changing resource availability in an attempt to optimize lifetime fitness(Fischer et al., 2009); whereas immunity contributes to immediate survival, storage is a hedging strategy for future scarcity. For example, children that exhibit higher levels of immune activity demonstrate decreased body growth, but this trade-off is tempered if those individuals have more body fat(Urlacher et al., 2018). Over time, such trade-offs introduce various stresses to the body that must be dealt with(Poganik et al., 2023), leading to a decrease in cell- and organismal-fitness that possibly explain aging(Kirkwood, 2017). Finally, maintenance tasks can also trade-off between each other; for example dairy cow calcium homeostasis is Pareto optimal between effectiveness–or a rapid return to physiological blood concentrations after milk production–and economy–or avoiding excess release of calcium from body stores(Szekely et al., 2013).

4. 4.5 Appendix E: Modeling Machinery Activity and Abundance to Couple Protein with Metabolism

As an example of systems biology approaches, we model here enzyme-catalyzed reactions. The assumptions regarding their reaction kinetics are used to constrain models with machinery costs and couple gene expression to metabolism.

For conversion of substrate (S) to product (P) by a machinery enzyme (E), Michaelis-Menten kinetics is often assumed:

$$v = k_{cat}[E]\frac{[S]}{[S] + K_M}$$

(1)

Under in vitro, fully saturated conditions ($[S] > > K_M$),, the maximal reaction rate is achieved:

$$v_{max} = k_{cat}[E]$$

(2)

In equation (2), reaction rates depend on machinery abundance and activity. However, *in vivo* observed reaction rates often deviate from this maximum value due to saturating, thermodynamic, and regulatory effects:

$$v_{obs} = k_{cat}[E] \cdot \eta(C) = v_{max} \cdot \eta(C)$$

(3)

$\eta(C)$ is a context-dependent scaling parameter that accounts for the discrepancy between v_{max} and v_{obs} due to *in vivo* variables such as metabolite concentration, pH, and molecular crowding. $\eta(C)$ can be decomposed into saturating, thermodynamic, and regulatory components. Saturating and thermodynamic components can only decrease v_{obs} relative to

$v_{\max}$. However, regulatory effects such as allostery and post-translational modifications can cause $v_{\mathrm{obs}} > v_{\max}$

4.5.1 Saturation

Focusing on saturating effects, if substrate concentration is no longer sufficiently high such that K_M is not negligible, then enzymes are not fully saturated. In this case, we can represent total enzyme concentration as:

$$[E] = [E]_{\mathrm{used}} + [E]_{\mathrm{free}}$$

(A1)

From Michaelis-Menten derivations:

$$[E]_{\mathrm{used}} = [ES] = \frac{[E][S]}{[S] + K_M}$$

(A2)

We assume the scaling factor as proportional to the fraction of used enzyme:

$$\eta_{\mathrm{saturation}}(C) = \frac{[E]_{\mathrm{used}}}{[E]} = \frac{[S]}{[S] + K_M}$$

(A3)

Thus, $\frac{[S]}{[S] + K_M}$ is the enzyme saturation scaling factor. From equations (3) and (A3) (and also shown in the Michaelis-Menten derivation) Equation (1) can also be written as:

$$v_{\mathrm{obs}} = k_{\mathrm{cat}}[E]_{\mathrm{used}}$$

(A4)

Defining the capacity utilization of a reaction as the ratio between the observed and maximal reaction rate yields the following equality from equations (2) and (A4):

$$\frac{v_{\mathrm{obs}}}{v_{\max}} = \frac{[E]_{\mathrm{used}}}{[E]}$$

(A5)

Note that the capacity utilization and saturation scaling factor are equivalent and analogous concepts, and many of these equations are different conceptual representations of the same mathematical equivalencies. Broadly, equation (A5) indicates that with saturating effects, there is some fraction of unused enzyme that is decreasing the overall reaction rate.

4.5.2 Resource Loading

Due to resource loading, multiple substrates may be competing for a shared machinery resource. Resultant resource-limitation can be modeled in enzyme-catalyzed reactions by simply adding a resource term R that scales the reaction rate. Let's take the subscript i to represent the substrate of interest. Thus, equation (1) can be represented as follows:

$$v_i = k_{\text{cat},i}[E]\frac{[S_i]}{[S_i] + K_{M,i}}$$

(B1)

Separately, given an inhibitor represented by the subscript j, competitive inhibition in Michaelis-Menten is typically modeled as follows:

$$v_i = k_{\text{cat},i}[E]\frac{[S_i]}{K_{M,i}(1 + \frac{[S_j]}{K_{M,j}}) + [S_i]}$$

(B2)

For formatting, let's rewrite equation (B2) as follows:

$$v_i = k_{\text{cat},i}[E]\frac{[S_i]}{K_{M,i}(1 + \frac{[S_i]}{K_{M,i}} + \frac{[S_j]}{K_{M,j}})}$$

(B3)

Let's take all possible substrates of the machinery E to be represented by the subscript j. Then, we can expand on this competitive inhibition model to derive a reaction flux term that accounts for resource loading. First, let's define a term Y to represent all competing substrates:

$$Y = \sum_{j \neq i} \frac{[S_j]}{K_{M,j}}$$

(B4)

Then, using this definition in (B4) to extend (B3) to account for all competing substrates $j \neq i$, we can get:

$$v_i = k_{\text{cat},i}[E]\frac{[S_i]}{K_{M,i}(1 + \frac{[S_i]}{K_{M,i}} + Y)}$$

(B5)

Ultimately, substituting (B4) into (B5) gives us a reaction rate term that can account for resource competition:

$$v_i = k_{\text{cat},i}[E]\frac{[S_i]}{K_{M,i}(1 + \sum_j \frac{[S_j]}{K_{M,j}})}$$

(B6)

From equation (B6) and equation (3), we can define scaling due to resource competition as follows:

$$\eta_{\text{competition}}(C) = \frac{[S_i]}{K_{M,i}(1 + \sum_j \frac{[S_j]}{K_{M,j}})}$$

(B7)

Note that the saturation term (A3) can be related to resource competition effects (B7). We can derive a resource competition term R which relates $\eta_{\text{competition}}(C)$ to $\eta_{\text{saturation}}(C)$:

$$\eta_{\text{competition}}(C) = \eta_{\text{saturation}}(C) \cdot R$$

(B8)

To derive a term for R, we can substitute (B4) back into (B7) as follows:

$$\eta_{\text{competition}}(C) = \frac{[S_i]}{K_{M,i} + [S_i] + Y}$$

(B9)

This can be rearranged as follows:

$$\begin{aligned}
\eta_{\text{competition}}(C) &= \frac{[S_i]}{K_{M,i} + [S_i]} \cdot \frac{1}{1 + \frac{Y}{K_{M,i} + [S_i]}} \\
&= \frac{[S_i]}{K_{M,i} + [S_i]} \cdot \frac{1}{\frac{K_{M,i} + [S_i] + Y}{K_{M,i} + [S_i]}} \\
&= \frac{[S_i]}{K_{M,i} + [S_i]} \cdot \frac{K_{M,i} + [S_i]}{K_{M,i} + [S_i] + Y}
\end{aligned}$$

(B10)

Substituting (B4) back into the derivation for (B10) gives:

$$\eta_{\text{competition}}(C) = \frac{[S_i]}{K_{M,i} + [S_i]} \cdot \frac{K_{M,i} + [S_i]}{K_{M,i}(1 + \sum_j \frac{[S_j]}{K_{M,j}})}$$

(B11)

Finally, using equations (A3), (B8), and (B11) gives us:

$$R = \frac{K_{M,i} + [S_i]}{K_{M,i}(1 + \sum_j \frac{[S_j]}{K_{M,j}})}$$

(B12)

Thus, R accounts for the effect of the relevant substrate in the numerator, normalized to the effects of multiple competing substrates in the denominator. Together, equations (B8) and (B12) demonstrate that the reaction rate that accounts for resource competition in equation (B6) is simply a scaling of equation (1) in which saturation effects (derived in (A3)) include competitive inhibition from multiple substrates.

Furthermore, both (A3) and (B7) are a specific version of the context-dependent scaling parameter $\eta(C)$ introduced in equation (3), and both depend on substrate concentration. Substrate concentration may be estimated by joint molecular abundance and cell volume(Bryan et al., 2014) measurements. The relative abundance of all competitive substrates, for example, may be estimated across multiple samples representing distinct contexts with omics data. Notably, subcellular compartmentalization alters reaction dynamics by influencing the availability of machinery and the abundance of machinery substrates. Furthermore, the spatial distribution of machinery across these compartments to maximize reaction flux has been demonstrated to be a relevant resource allocation principle(Giunta et al., 2022). Thus, the subcellular localization of machinery must be measured in the future(Mah et al., 2023). Overall, context-dependent modeling depends on the resolution at which technologies are capable of measuring the cells' and machineries' microenvironments. For example, when considering a cell's communicatory partners, the local microenvironment of a receptor's interacting ligand partners can be mapped at 1nm resolution(Geri et al., 2020). Thus, technological improvements that increase the throughput and resolution of context-dependent molecular measurements will improve model accuracy, and inversely, models will need to be expanded to better account for the additional information provided by such measurements.

4.5.3 Thermodynamics

Next, we will focus on thermodynamic effects. For simplicity, we will consider an isothermal, isobaric reaction of a substrate converted into product, disregarding Michaelis-Menten kinetics (conclusions are the same):

$$S \underset{k_r}{\overset{k_f}{\rightleftharpoons}} P$$

The reaction kinetics can be written as:

$$v_{obs} = v_f - v_r = k_f[S] - k_r[P]$$

(C1)

The reaction thermodynamics can be written as:

$$\Delta G = -RT\ln(\frac{[S]K_{eq}}{[P]})$$

(C2)

The kinetics and thermodynamics are related to each other via the equilibrium constant K_{eq} from the following:

$$K_{eq} = \frac{k_f}{k_r}$$

(C3)

Thus, equations (C2) can be rewritten using equations (C1) and (C3) to link thermodynamics with kinetics as:

$$\Delta G = -RT\ln(\frac{v_f}{v_r})$$

(C4)

Equation (C4) holds for more complex reactions, including Michaelis-Menten kinetics and the Hill equation. From (C4), reactions far from equilibrium ($\Delta G < < 0$) tend not to have a high reverse flux. However, enzymes catalyzing reactions near equilibrium ($\Delta G \sim 0$) face a higher reverse flux. In this sense, thermodynamic forces (e.g., intermediate metabolite concentrations) can affect machinery costs, with reactions that have a higher reverse flux requiring a larger enzyme investment per unit of forward flux.

Relevant Sources: (Rondelez, 2012; Beard and Qian, 2007; Davidi et al., 2016; Dourado et al., 2021; Noor et al., 2016, 2014; Chou and Talalay, 1977).

8.1   Availability of data and materials

Not applicable.

Abbreviations

FBA	flux balance analysis
GEM	genome-scale model
M-Model	genome-scale metabolic model
ME-Model	genome scale model of metabolism and expression
NGAM	non-growth associated maintenance
ODE	ordinary differential equation
RBA	resource balance analysis

| WCM | whole-cell model |

Glossary

5.

Cellular context	A combination of the current intracellular state (e.g., genomic variants, cell type, and machinery concentrations and localization) and extracellular cues from the microenvironment (e.g., nutrients and communicatory molecules) that together inform cellular decision-making and change as a function of factors such as time, space, and disease.
Cell specialization	The extent to which a cell is optimized for the performance of a specific, single objective.
Division of labor	A resource allocation strategy in which multicellular systems distribute multiple objectives across cells with varying degrees of specialization.
Fitness	The efficiency by which a system uses its resource budget to achieve its objective; mathematically, this is the extent to which the system minimizes resource costs while simultaneously maximizing its objectives.
Hedging	Resource allocated in preparation for future objectives, particularly at the cost of a current objective.
Information Transfer	The extent to which the output depends on or is informed by the input (e.g., mutual information).
Machinery	The macromolecular products of anabolism and gene expression, often enzymes, that catalyze and enable cell functions.
Machinery-limiting	The flux through a reaction is limited by saturation of the machinery.
Nutrient-limiting	The flux through a reaction is limited by the availability of a metabolic substrate (nutrient or downstream intermediate).
Objective	The biological goal that a cell or system is trying to achieve (e.g., motility, proliferation, and differentiation) through the integration of its various biological activities.
Optimality	The maximization of an objective that is constrained by the resource budget.

Resource budget	The total quantity of a resource (i.e., nutrient, machinery, and bioenergy) that is available to the cell for use.
Resource cost	The total quantity of resources that are consumed or sequestered for biological activities contributing to the cell objective.
Resource loading	Competition in the cell for a shared and often limiting resource (e.g., competition between mRNA transcripts for ribosome).
Response Time	The time between when the pathway senses the input and when it generates the output.
Signal Amplification	The magnitude change in the output relative to the magnitude change in the input.
Signaling Crosstalk	the interaction of shared components between signaling pathways, particularly in the presence of multiple inputs and/or outputs, which requires resource sharing across the signaling network
Signaling Modularity	A set of signaling components that can convert inputs to outputs while limiting retroactivity (i.e., instances in which the inputs and the outputs are not unidirectional).
Sensing Precision	The ability of a signaling pathway to accurately convert a given input to the desired output with limited variance, also known as "noise mitigation".
Parameter Robustness	The change in the output response given a change to one of the system's parameters (e.g. binding affinities).
Pareto optimality	A state in which increasing performance of one objective can only occur by decreasing the performance of another objective due to resource constraints, leading to trade-offs.

9.   References

Aceto N, Bardia A, Miyamoto DT, Donaldson MC, Wittner BS, Spencer JA, Yu M, Pely A, Engstrom A, Zhu H, Brannigan BW, Kapur R, Stott SL, Shioda T, Ramaswamy S, Ting DT, Lin CP, Toner M, Haber DA, Maheswaran S, 2014. Circulating tumor cell clusters are oligoclonal precursors of breast cancer metastasis. Cell 158, 1110–1122. [PubMed: 25171411]

Adler M, Chavan AR, Medzhitov R, 2023a. Tissue Biology: In Search of a New Paradigm. Annu. Rev. Cell Dev. Biol 39, 67–89. [PubMed: 37607470]

Adler MI, Bonduriansky R, 2014. Why do the well-fed appear to die young? A new evolutionary hypothesis for the effect of dietary restriction on lifespan. Bioessays 36, 439–450. [PubMed: 24609969]

Adler M, Korem Kohanim Y, Tendler A, Mayo A, Alon U, 2019. Continuum of Gene-Expression Profiles Provides Spatial Division of Labor within a Differentiated Cell Type. Cell Syst 8, 43–52.e5. [PubMed: 30638811]

Adler M, Moriel N, Goeva A, Avraham-Davidi I, Mages S, Adams TS, Kaminski N, Macosko EZ, Regev A, Medzhitov R, Nitzan M, 2023b. Emergence of division of labor in tissues through cell interactions and spatial cues. Cell Rep. 42, 112412. [PubMed: 37086403]

Adler M, Szekely P, Mayo A, Alon U, 2017. Optimal Regulatory Circuit Topologies for Fold-Change Detection. Cell Syst 4, 171–181.e8. [PubMed: 28089543]

Aiello LC, Wheeler P, 1995. The Expensive-Tissue Hypothesis: The Brain and the Digestive System in Human and Primate Evolution. Current Anthropology 36, 199–221.

Al-Bassam MM, Kim J-N, Zaramela LS, Kellman BP, Zuniga C, Wozniak JM, Gonzalez DJ, Zengler K, 2018. Optimization of carbon and energy utilization through differential translational efficiency. Nat. Commun 9, 4474. [PubMed: 30367068]

Alle H, Roth A, Geiger JRP, 2009. Energy-efficient action potentials in hippocampal mossy fibers. Science 325, 1405–1408. [PubMed: 19745156]

Allen BL, Taatjes DJ, 2015. The Mediator complex: a central integrator of transcription. Nat. Rev. Mol. Cell Biol 16, 155–166. [PubMed: 25693131]

Almet AA, Cang Z, Jin S, Nie Q, 2021. The landscape of cell-cell communication through single-cell transcriptomics. Curr Opin Syst Biol 26, 12–23. [PubMed: 33969247]

Alonso R, Brocas I, Carrillo JD, 2013. Resource Allocation in the Brain. Rev. Econ. Stud 81, 501–534.

Alon U, 2019. Multi-Objective Optimality in Biology, in: An Introduction to Systems Biology. Chapman and Hall/CRC, Second edition. | Boca Raton, Fla. : CRC Press, [2019], pp. 249–272.

Alon U, 2007. Network motifs: theory and experimental approaches. Nat. Rev. Genet 8, 450–461. [PubMed: 17510665]

Alon U, 2006. An Introduction to Systems Biology: Design Principles of Biological Circuits. CRC Press.

Alves R, Salvadó B, Milo R, Vilaprinyo E, Sorribas A, 2021. Maximization of information transmission influences selection of native phosphorelay architectures. PeerJ 9, e11558. [PubMed: 34178454]

Anderson TR, Raubenheimer D, Hessen DO, Jensen K, Gentleman WC, Mayor DJ, 2020. Geometric Stoichiometry: Unifying Concepts of Animal Nutrition to Understand How Protein-Rich Diets Can Be "Too Much of a Good Thing." Front. Ecol. Evol 8. 10.3389/fevo.2020.00196

Andreozzi S, Miskovic L, Hatzimanikatis V, 2016. iSCHRUNK--In Silico Approach to Characterization and Reduction of Uncertainty in the Kinetic Models of Genome-scale Metabolic Networks. Metab. Eng 33, 158–168. [PubMed: 26474788]

Arendt D, 2008. The evolution of cell types in animals: emerging principles from molecular studies. Nat. Rev. Genet 9, 868–882. [PubMed: 18927580]

Argüello RJ, Combes AJ, Char R, Gigan J-P, Baaziz AI, Bousiquot E, Camosseto V, Samad B, Tsui J, Yan P, Boissonneau S, Figarella-Branger D, Gatti E, Tabouret E, Krummel MF, Pierre P, 2020. SCENITH: A Flow Cytometry-Based Method to Functionally Profile Energy Metabolism with Single-Cell Resolution. Cell Metab. 32, 1063–1075.e7. [PubMed: 33264598]

Armingol E, Baghdassarian HM, Martino C, Perez-Lopez A, Aamodt C, Knight R, Lewis NE, 2022a. Context-aware deconvolution of cell-cell communication with Tensor-cell2cell. Nat. Commun 13, 3665. [PubMed: 35760817]

Armingol E, Larsen RO, Cequeira M, Baghdassarian H, Lewis NE, 2022b. Unraveling the coordinated dynamics of protein- and metabolite-mediated cell-cell communication. bioRxiv. 10.1101/2022.11.02.514917

Armingol E, Officer A, Harismendy O, Lewis NE, 2021. Deciphering cell-cell interactions and communication from gene expression. Nat. Rev. Genet 22, 71–88. [PubMed: 33168968]

Attwell D, Laughlin SB, 2001. An energy budget for signaling in the grey matter of the brain. J. Cereb. Blood Flow Metab 21, 1133–1145. [PubMed: 11598490]

Austin DW, Allen MS, McCollum JM, Dar RD, Wilgus JR, Sayler GS, Samatova NF, Cox CD, Simpson ML, 2006. Gene network shaping of inherent noise spectra. Nature 439, 608–611. [PubMed: 16452980]

Azzout-Marniche D, Gaudichon C, Blouet C, Bos C, Mathé V, Huneau J-F, Tomé D, 2007. Liver glyconeogenesis: a pathway to cope with postprandial amino acid excess in high-protein fed rats? Am. J. Physiol. Regul. Integr. Comp. Physiol 292, R1400–7. [PubMed: 17158265]

Baghdassarian H, Blackstone SA, Clay OS, Philips R, Matthiasardottir B, Nehrebecky M, Hua VK, McVicar R, Liu Y, Tucker SM, Randazzo D, Deuitch N, Rosenzweig S, Mark A, Sasik R, Fisch KM, Pimpale Chavan P, Eren E, Watts NR, Ma CA, Gadina M, Schwartz DM, Sanyal A, Werner G, Murdock DR, Horita N, Chowdhury S, Dimmock D, Jepsen K, Remmers EF, Goldbach-Mansky R, Gahl WA, O'Shea JJ, Milner JD, Lewis NE, Chang J, Kastner DL, Torok K, Oda H, Putnam CD, Broderick L, 2023. Variant and Response to Ruxolitinib in an Autoinflammatory Syndrome. N. Engl. J. Med 388, 2241–2252. [PubMed: 37256972]

Baker NE, 2020. Emerging mechanisms of cell competition. Nat. Rev. Genet 21, 683–697. [PubMed: 32778819]

Barclay CJ, 2015. Energetics of contraction. Compr. Physiol 5, 961–995. [PubMed: 25880520]

Barton JP, Sontag ED, 2013. The energy costs of insulators in biochemical networks. Biophys. J 104, 1380–1390. [PubMed: 23528097]

Basan M, 2018. Resource allocation and metabolism: the search for governing principles. Curr. Opin. Microbiol 45, 77–83. [PubMed: 29544124]

Basan M, Hui S, Okano H, Zhang Z, Shen Y, Williamson JR, Hwa T, 2015. Overflow metabolism in Escherichia coli results from efficient proteome allocation. Nature 528, 99–104. [PubMed: 26632588]

Bashor CJ, Hilton IB, Bandukwala H, Smith DM, Veiseh O, 2022. Engineering the next generation of cell-based therapeutics. Nat. Rev. Drug Discov 21, 655–675. [PubMed: 35637318]

Battich N, Stoeger T, Pelkmans L, 2015. Control of Transcript Variability in Single Mammalian Cells. Cell 163, 1596–1610. [PubMed: 26687353]

Baysoy A, Bai Z, Satija R, Fan R, 2023. The technological landscape and applications of single-cell multi-omics. Nat. Rev. Mol. Cell Biol 24, 695–713. [PubMed: 37280296]

Beard DA, Qian H, 2007. Relationship between thermodynamic driving force and one-way fluxes in reversible processes. PLoS One 2, e144. [PubMed: 17206279]

Beck M, Schmidt A, Malmstroem J, Claassen M, Ori A, Szymborska A, Herzog F, Rinner O, Ellenberg J, Aebersold R, 2011. The quantitative proteome of a human cell line. Mol. Syst. Biol 7, 549. [PubMed: 22068332]

Beltman JGM, van der Vliet MR, Sargeant AJ, de Haan A, 2004. Metabolic cost of lengthening, isometric and shortening contractions in maximally stimulated rat skeletal muscle. Acta Physiol. Scand 182, 179–187. [PubMed: 15450114]

Bender DA, 2012. The metabolism of "surplus" amino acids. Br. J. Nutr 108 Suppl 2, S113–21. [PubMed: 23107522]

Ben-Moshe S, Itzkovitz S, 2019. Spatial heterogeneity in the mammalian liver. Nat. Rev. Gastroenterol. Hepatol 16, 395–410. [PubMed: 30936469]

Bennett NK, Nguyen MK, Darch MA, Nakaoka HJ, Cousineau D, Ten Hoeve J, Graeber TG, Schuelke M, Maltepe E, Kampmann M, Mendelsohn BA, Nakamura JL, Nakamura K, 2020. Defining the ATPome reveals cross-optimization of metabolic pathways. Nat. Commun 11, 4319. [PubMed: 32859923]

Bergström M, Hultman E, 1988. Energy cost and fatigue during intermittent electrical stimulation of human skeletal muscle. J. Appl. Physiol 65, 1500–1505. [PubMed: 3182513]

Bisschop PH, De Sain-Van Der Velden MGM, Stellaard F, Kuipers F, Meijer AJ, Sauerwein HP, Romijn JA, 2003. Dietary carbohydrate deprivation increases 24-hour nitrogen excretion without affecting postabsorptive hepatic or whole body protein metabolism in healthy men. J. Clin. Endocrinol. Metab 88, 3801–3805. [PubMed: 12915672]

Björkeroth J, Campbell K, Malina C, Yu R, Di Bartolomeo F, Nielsen J, 2020. Proteome reallocation from amino acid biosynthesis to ribosomes enables yeast to grow faster in rich media. Proc. Natl. Acad. Sci. U. S. A 117, 21804–21812. [PubMed: 32817546]

Blecher-Gonen R, Bost P, Hilligan KL, David E, Salame TM, Roussel E, Connor LM, Mayer JU, Bahar Halpern K, Tóth B, Itzkovitz S, Schwikowski B, Ronchese F, Amit I, 2019. Single-Cell Analysis of Diverse Pathogen Responses Defines a Molecular Roadmap for Generating Antigen-Specific Immunity. Cell Syst 8, 109–121.e6. [PubMed: 30772378]

Bonnans C, Chou J, Werb Z, 2014. Remodelling the extracellular matrix in development and disease. Nat. Rev. Mol. Cell Biol 15, 786–801. [PubMed: 25415508]

Bonny AR, Kochanowski K, Diether M, El-Samad H, 2020. Stress-Induced Transient Cell Cycle Arrest Coordinates Metabolic Resource Allocation to Balance Adaptive Tradeoffs. bioRxiv. 10.1101/2020.04.08.033035

Brand A, Singer K, Koehl GE, Kolitzus M, Schoenhammer G, Thiel A, Matos C, Bruss C, Klobuch S, Peter K, Kastenberger M, Bogdan C, Schleicher U, Mackensen A, Ullrich E, Fichtner-Feigl S, Kesselring R, Mack M, Ritter U, Schmid M, Blank C, Dettmer K, Oefner PJ, Hoffmann P, Walenta S, Geissler EK, Pouyssegur J, Villunger A, Steven A, Seliger B, Schreml S, Haferkamp S, Kohl E, Karrer S, Berneburg M, Herr W, Mueller-Klieser W, Renner K, Kreutz M, 2016. LDHAAssociated Lactic Acid Production Blunts Tumor Immunosurveillance by T and NK Cells. Cell Metab. 24, 657–671. [PubMed: 27641098]

Brückner A, Badroos JM, Learsch RW, Yousefelahiyeh M, Kitchen SA, Parker J, 2021. Evolutionary assembly of cooperating cell types in an animal chemical defense system. Cell 184, 6138–6156.e28. [PubMed: 34890552]

Bryan AK, Hecht VC, Shen W, Payer K, Grover WH, Manalis SR, 2014. Measuring single cell mass, volume, and density with dual suspended microchannel resonators. Lab Chip 14, 569–576. [PubMed: 24296901]

Buccitelli C, Selbach M, 2020. mRNAs, proteins and the emerging principles of gene expression control. Nat. Rev. Genet 21, 630–644. [PubMed: 32709985]

Bulusu V, Prior N, Snaebjornsson MT, Kuehne A, Sonnen KF, Kress J, Stein F, Schultz C, Sauer U, Aulehla A, 2017. Spatiotemporal Analysis of a Glycolytic Activity Gradient Linked to Mouse Embryo Mesoderm Development. Dev. Cell 40, 331–341.e4. [PubMed: 28245920]

Buttgereit F, Brand MD, 1995. A hierarchy of ATP-consuming processes in mammalian cells. Biochem. J 312 (Pt 1), 163–167. [PubMed: 7492307]

Calabrese L, Grilli J, Osella M, Kempes CP, Lagomarsino MC, Ciandrini L, 2022. Protein degradation sets the fraction of active ribosomes at vanishing growth. PLoS Comput. Biol 18, e1010059. [PubMed: 35500024]

Cambridge SB, Gnad F, Nguyen C, Bermejo JL, Krüger M, Mann M, 2011. Systems-wide proteomic analysis in mammalian cells reveals conserved, functional protein turnover. J. Proteome Res 10, 5275–5284. [PubMed: 22050367]

Cantó C, Jiang LQ, Deshmukh AS, Mataki C, Coste A, Lagouge M, Zierath JR, Auwerx J, 2010. Interdependence of AMPK and SIRT1 for metabolic adaptation to fasting and exercise in skeletal muscle. Cell Metab. 11, 213–219. [PubMed: 20197054]

Carey BW, Finley LWS, Cross JR, Allis CD, Thompson CB, 2015. Intracellular α-ketoglutarate maintains the pluripotency of embryonic stem cells. Nature 518, 413–416. [PubMed: 25487152]

Carr EL, Kelman A, Wu GS, Gopaul R, Senkevitch E, Aghvanyan A, Turay AM, Frauwirth KA, 2010. Glutamine uptake and metabolism are coordinately regulated by ERK/MAPK during T lymphocyte activation. J. Immunol 185, 1037–1044. [PubMed: 20554958]

Cavigliasso F, Dupuis C, Savary L, Spangenberg JE, Kawecki TJ, 2020. Experimental evolution of post-ingestive nutritional compensation in response to a nutrient-poor diet. Proc. Biol. Sci 287, 20202684. [PubMed: 33259760]

Cell design in bacteria as a convex optimization problem, 2011. . Automatica 47, 1210–1218.

Cermak N, Olcum S, Delgado FF, Wasserman SC, Payer KR, A Murakami M, Knudsen SM, Kimmerling RJ, Stevens MM, Kikuchi Y, Sandikci A, Ogawa M, Agache V, Baléras F, Weinstock DM, Manalis SR, 2016. High-throughput measurement of single-cell growth rates using serial microfluidic mass sensor arrays. Nat. Biotechnol 34, 1052–1059. [PubMed: 27598230]

Cham CM, Driessens G, O'Keefe JP, Gajewski TF, 2008. Glucose deprivation inhibits multiple key gene expression events and effector functions in CD8+ T cells. Eur. J. Immunol 38, 2438–2450. [PubMed: 18792400]

Cham CM, Gajewski TF, 2005. Glucose availability regulates IFN-gamma production and p70S6 kinase activation in CD8+ effector T cells. J. Immunol 174, 4670–4677. [PubMed: 15814691]

Chandrasekhar A, Navlakha S, 2019. Neural arbors are Pareto optimal. Proc. Biol. Sci 286, 20182727. [PubMed: 31039719]

Chaneton B, Hillmann P, Zheng L, Martin ACL, Maddocks ODK, Chokkathukalam A, Coyle JE, Jankevics A, Holding FP, Vousden KH, Frezza C, O'Reilly M, Gottlieb E, 2012. Serine is a natural ligand and allosteric activator of pyruvate kinase M2. Nature 491, 458–462. [PubMed: 23064226]

Chang A, Jeske L, Ulbrich S, Hofmann J, Koblitz J, Schomburg I, Neumann-Schaal M, Jahn D, Schomburg D, 2021. BRENDA, the ELIXIR core data resource in 2021: new developments and updates. Nucleic Acids Res. 49, D498–D508. [PubMed: 33211880]

Chang C-H, Qiu J, O'Sullivan D, Buck MD, Noguchi T, Curtis JD, Chen Q, Gindin M, Gubin MM, van der Windt GJW, Tonc E, Schreiber RD, Pearce EJ, Pearce EL, 2015. Metabolic Competition in the Tumor Microenvironment Is a Driver of Cancer Progression. Cell 162, 1229–1241. [PubMed: 26321679]

Chantranupong L, Wolfson RL, Sabatini DM, 2015. Nutrient-sensing mechanisms across evolution. Cell 161, 67–83. [PubMed: 25815986]

Chen K, Gao Y, Mih N, O'Brien EJ, Yang L, Palsson BO, 2017. Thermosensitivity of growth is determined by chaperone-mediated proteome reallocation. Proc. Natl. Acad. Sci. U. S. A 114, 11548–11553. [PubMed: 29073085]

Chen Y, McConnell BO, Gayatri Dhara V, Mukesh Naik H, Li C-T, Antoniewicz MR, Betenbaugh MJ, 2019. An unconventional uptake rate objective function approach enhances applicability of genome-scale models for mammalian cells. NPJ Syst. Biol. Appl 5, 25. [PubMed: 31341637]

Chen Y, Nielsen J, 2019. Energy metabolism controls phenotypes by protein efficiency and allocation. Proc. Natl. Acad. Sci. U. S. A 116, 17592–17597. [PubMed: 31405984]

Cheong R, Rhee A, Wang CJ, Nemenman I, Levchenko A, 2011. Information transduction capacity of noisy biochemical signaling networks. Science 334, 354–358. [PubMed: 21921160]

Choudhury S, Narayanan B, Moret M, Hatzimanikatis V, Miskovic L, 2023. Generative machine learning produces kinetic models that accurately characterize intracellular metabolic states. bioRxiv. 10.1101/2023.02.21.529387

Chou TC, Talalay P, 1977. A simple generalized equation for the analysis of multiple inhibitions of Michaelis-Menten kinetic systems. J. Biol. Chem 252, 6438–6442. [PubMed: 893418]

Clavería C, Giovinazzo G, Sierra R, Torres M, 2013. Myc-driven endogenous cell competition in the early mammalian embryo. Nature 500, 39–44. [PubMed: 23842495]

Clissold FJ, Tedder BJ, Conigrave AD, Simpson SJ, 2010. The gastrointestinal tract as a nutrient-balancing organ. Proc. Biol. Sci 277, 1751–1759. [PubMed: 20129973]

Cotter SC, Simpson SJ, Raubenheimer D, Wilson K, 2011. Macronutrient balance mediates trade- offs between immune function and life history traits. Functional Ecology. 10.1111/j.1365-2435.2010.01766.x

Covert MW, 2017. Fundamentals of Systems Biology: From Synthetic Circuits to Whole-cell Models. CRC Press.

Csárdi G, Franks A, Choi DS, Airoldi EM, Drummond DA, 2015. Accounting for experimental noise reveals that mRNA levels, amplified by post-transcriptional processes, largely determine steady-state protein levels in yeast. PLoS Genet. 11, e1005206. [PubMed: 25950722]

Dahal S, Zhao J, Yang L, 2021. Genome-scale Modeling of Metabolism and Macromolecular Expression and Their Applications. Biotechnol. Bioprocess Eng 25, 931–943.

Dai Z, Zheng W, Locasale JW, 2022. Amino acid variability, tradeoffs and optimality in human diet. Nat. Commun 13, 6683. [PubMed: 36335142]

da Silva Novaes A, Borges FT, Maquigussa E, Varela VA, Dias MVS, Boim MA, 2019. Influence of high glucose on mesangial cell-derived exosome composition, secretion and cell communication. Sci. Rep 9, 6270. [PubMed: 31000742]

Davidi D, Milo R, 2017. Lessons on enzyme kinetics from quantitative proteomics. Curr. Opin. Biotechnol 46, 81–89. [PubMed: 28288339]

Davidi D, Noor E, Liebermeister W, Bar-Even A, Flamholz A, Tummler K, Barenholz U, Goldenfeld M, Shlomi T, Milo R, 2016. Global characterization of in vivo enzyme catalytic rates and their correspondence to in vitro kcat measurements. Proc. Natl. Acad. Sci. U. S. A 113, 3401–3406. [PubMed: 26951675]

Dekel E, Alon U, 2005. Optimality and evolutionary tuning of the expression level of a protein. Nature 436, 588–592. [PubMed: 16049495]

Di Blasi R, Marbiah MM, Siciliano V, Polizzi K, Ceroni F, 2021. A call for caution in analysing mammalian co-transfection experiments and implications of resource competition in data misinterpretation. Nat. Commun 12, 2545. [PubMed: 33953169]

Di Blasi R, Pisani M, Tedeschi F, Marbiah MM, Polizzi K, Furini S, Siciliano V, Ceroni F, 2023. Resource-aware construct design in mammalian cells. Nat. Commun 14, 3576. [PubMed: 37328476]

Ding F, Elowitz MB, 2019. Constitutive splicing and economies of scale in gene expression. Nat. Struct. Mol. Biol 26, 424–432. [PubMed: 31133700]

Domenzain I, Sánchez B, Anton M, Kerkhoven EJ, Millán-Oropeza A, Henry C, Siewers V, Morrissey JP, Sonnenschein N, Nielsen J, 2022. Reconstruction of a catalogue of genome-scale metabolic models with enzymatic constraints using GECKO 2.0. Nat. Commun 13, 3766. [PubMed: 35773252]

Dourado H, Mori M, Hwa T, Lercher MJ, 2021. On the optimality of the enzyme-substrate relationship in bacteria. PLoS Biol. 19, e3001416. [PubMed: 34699521]

Du B, Yang L, Lloyd CJ, Fang X, Palsson BO, 2019. Genome-scale model of metabolism and gene expression provides a multi-scale description of acid stress responses in Escherichia coli. PLoS Comput. Biol 15, e1007525. [PubMed: 31809503]

Du F, Zhu X-H, Zhang Y, Friedman M, Zhang N, Ugurbil K, Chen W, 2008. Tightly coupled brain activity and cerebral ATP metabolic rate. Proc. Natl. Acad. Sci. U. S. A 105, 6409–6414. [PubMed: 18443293]

Edelman GM, Gally JA, 2001. Degeneracy and complexity in biological systems. Proc. Natl. Acad. Sci. U. S. A 98, 13763–13768. [PubMed: 11698650]

Edfors F, Danielsson F, Hallström BM, Käll L, Lundberg E, Pontén F, Forsström B, Uhlén M, 2016. Gene-specific correlation of RNA and protein levels in human cells and tissues. Mol. Syst. Biol 12, 883. [PubMed: 27951527]

Efeyan A, Comb WC, Sabatini DM, 2015. Nutrient-sensing mechanisms and pathways. Nature 517, 302–310. [PubMed: 25592535]

Ellis SJ, Gomez NC, Levorse J, Mertz AF, Ge Y, Fuchs E, 2019. Distinct modes of cell competition shape mammalian tissue morphogenesis. Nature 569, 497–502. [PubMed: 31092920]

Elowitz MB, Levine AJ, Siggia ED, Swain PS, 2002. Stochastic gene expression in a single cell. Science 297. 10.1126/science.1070919

Elsemman IE, Rodriguez Prado A, Grigaitis P, Garcia Albornoz M, Harman V, Holman SW, van Heerden J, Bruggeman FJ, Bisschops MMM, Sonnenschein N, Hubbard S, Beynon R, Daran-Lapujade P, Nielsen J, Teusink B, 2022. Whole-cell modeling in yeast predicts compartment-specific proteome constraints that drive metabolic strategies. Nat. Commun 13, 801. [PubMed: 35145105]

Fan J, Kamphorst JJ, Mathew R, Chung MK, White E, Shlomi T, Rabinowitz JD, 2013. Glutamine-driven oxidative phosphorylation is a major ATP source in transformed mammalian cells in both normoxia and hypoxia. Mol. Syst. Biol 9, 712. [PubMed: 24301801]

Farhan H, Rabouille C, 2011. Signalling to and from the secretory pathway. J. Cell Sci 124, 171–180. [PubMed: 21187344]

Feist AM, Palsson BO, 2010. The biomass objective function. Curr. Opin. Microbiol 13, 344–349. [PubMed: 20430689]

Felton AM, Felton A, Wood JT, Foley WJ, Raubenheimer D, Wallis IR, Lindenmayer DB, 2009. Nutritional Ecology of Ateles chamek in lowland Bolivia: How Macronutrient Balancing Influences Food Choices. Int. J. Primatol 30, 675–696.

Ferguson-Stegall L, McCleave E, Ding Z, Doerner PG Iii, Liu Y, Wang B, Healy M, Kleinert M, Dessard B, Lassiter DG, Kammer L, Ivy JL, 2011. Aerobic exercise training adaptations are increased by postexercise carbohydrate-protein supplementation. J. Nutr. Metab 2011, 623182. [PubMed: 21773022]

Fischer B, Dieckmann U, Taborsky B, 2011. When to store energy in a stochastic environment. Evolution 65, 1221–1232. [PubMed: 21108636]

Fischer B, Taborsky B, Dieckmann U, 2009. Unexpected patterns of plastic energy allocation in stochastic environments. Am. Nat 173, E108–20. [PubMed: 19196158]

Fischer DS, Fiedler AK, Kernfeld EM, Genga RMJ, Bastidas-Ponce A, Bakhti M, Lickert H, Hasenauer J, Maehr R, Theis FJ, 2019. Inferring population dynamics from single-cell RNA-sequencing time series data. Nat. Biotechnol 37, 461–468. [PubMed: 30936567]

Foreman R, Wollman R, 2020. Mammalian gene expression variability is explained by underlying cell state. Mol. Syst. Biol 16, e9146. [PubMed: 32043799]

Francis K, Palsson BO, 1997. Effective intercellular communication distances are determined by the relative time constants for cyto/chemokine secretion and diffusion. Proc. Natl. Acad. Sci. U. S. A 94, 12258–12262. [PubMed: 9356436]

Frei T, Cella F, Tedeschi F, Gutiérrez J, Stan G-B, Khammash M, Siciliano V, 2020. Characterization and mitigation of gene expression burden in mammalian cells. Nat. Commun 11, 4641. [PubMed: 32934213]

French SS, Dearing MD, Demas GE, 2011. Leptin as a physiological mediator of energetic trade-offs in ecoimmunology: implications for disease. Integr. Comp. Biol 51, 505–513. [PubMed: 21940777]

Funk L, Su K-C, Ly J, Feldman D, Singh A, Moodie B, Blainey PC, Cheeseman IM, 2022. The phenotypic landscape of essential human genes. Cell. 10.1016/j.cell.2022.10.017

Gallagher D, Belmonte D, Deurenberg P, Wang Z, Krasnow N, Pi-Sunyer FX, Heymsfield SB, 1998. Organ-tissue mass measurement allows modeling of REE and metabolically active tissue mass. Am. J. Physiol 275, E249–58. [PubMed: 9688626]

Ganeshan K, Nikkanen J, Man K, Leong YA, Sogawa Y, Maschek JA, Van Ry T, Chagwedera DN, Cox JE, Chawla A, 2019. Energetic Trade-Offs and Hypometabolic States Promote Disease Tolerance. Cell 177, 399–413.e12. [PubMed: 30853215]

Gazestani VH, Pramparo T, Nalabolu S, Kellman BP, Murray S, Lopez L, Pierce K, Courchesne E, Lewis NE, 2019. A perturbed gene network containing PI3K-AKT, RAS-ERK and WNT-β-catenin pathways in leukocytes is linked to ASD genetics and symptom severity. Nat. Neurosci 22, 1624–1634. [PubMed: 31551593]

Gerashchenko MV, Peterfi Z, Yim SH, Gladyshev VN, 2021. Translation elongation rate varies among organs and decreases with age. Nucleic Acids Res. 49, e9. [PubMed: 33264395]

Geri JB, Oakley JV, Reyes-Robles T, Wang T, McCarver SJ, White CH, Rodriguez-Rivera FP, Parker DL Jr, Hett EC, Fadeyi OO, Oslund RC, MacMillan DWC, 2020. Microenvironment mapping via Dexter energy transfer on immune cells. Science 367, 1091–1097. [PubMed: 32139536]

Ghosh S, Körte A, Serafini G, Yadav V, Rodenfels J, 2022. Developmental energetics: Energy expenditure, budgets and metabolism during animal embryogenesis. Semin. Cell Dev. Biol 10.1016/j.semcdb.2022.03.009

Gingold H, Pilpel Y, 2011. Determinants of translation efficiency and accuracy. Mol. Syst. Biol 7, 481. [PubMed: 21487400]

Giunta G, Tostevin F, T nase-Nicola S, Gerland U, 2022. Optimal spatial allocation of enzymes as an investment problem. Communications Physics 5, 1–12.

Glancy B, Balaban RS, 2021. Energy metabolism design of the striated muscle cell. Physiol. Rev 101, 1561–1607. [PubMed: 33733879]

Glancy B, Willis WT, Chess DJ, Balaban RS, 2013. Effect of calcium on the oxidative phosphorylation cascade in skeletal muscle mitochondria. Biochemistry 52, 2793–2809. [PubMed: 23547908]

Goelzer A, Fromion V, 2019. RBA for eukaryotic cells: foundations and theoretical developments. bioRxiv. 10.1101/750182

Goelzer A, Fromion V, 2017. Resource allocation in living organisms. Biochem. Soc. Trans 45, 945–952. [PubMed: 28687715]

Goldsby HJ, Dornhaus A, Kerr B, Ofria C, 2012. Task-switching costs promote the evolution of division of labor and shifts in individuality. Proc. Natl. Acad. Sci. U. S. A 109, 13686–13691. [PubMed: 22872867]

Gomez-Pinilla F, 2011. The combined effects of exercise and foods in preventing neurological and cognitive disorders. Prev. Med 52 Suppl 1, S75–80. [PubMed: 21281667]

Gopalakrishnan S, Dash S, Maranas C, 2020. K-FIT: An accelerated kinetic parameterization algorithm using steady-state fluxomic data. Metab. Eng 61, 197–205. [PubMed: 32173504]

Govern CC, Ten Wolde PR, 2014. Optimal resource allocation in cellular sensing systems. Proc. Natl. Acad. Sci. U. S. A 111, 17486–17491. [PubMed: 25422473]

Gregersen LH, Schueler M, Munschauer M, Mastrobuoni G, Chen W, Kempa S, Dieterich C, Landthaler M, 2014. MOV10 Is a 5' to 3′ RNA helicase contributing to UPF1 mRNA target degradation by translocation along 3′ UTRs. Mol. Cell 54, 573–585. [PubMed: 24726324]

Gustafsson J, Robinson JL, Zetterberg H, Nielsen J, 2022. Brain energy metabolism is optimized to minimize the cost of enzyme synthesis and transport. bioRxiv. 10.1101/2022.11.14.516523

Gutierrez JM, Feizi A, Li S, Kallehauge TB, Hefzi H, Grav LM, Ley D, Baycin Hizal D, Betenbaugh MJ, Voldborg B, Faustrup Kildegaard H, Min Lee G, Palsson BO, Nielsen J, Lewis NE, 2020. Genome-scale reconstructions of the mammalian secretory pathway predict metabolic costs and limitations of protein secretion. Nat. Commun 11, 68. [PubMed: 31896772]

Gyorgy A, Jiménez JI, Yazbek J, Huang H-H, Chung H, Weiss R, Del Vecchio D, 2015. Isocost Lines Describe the Cellular Economy of Genetic Circuits. Biophys. J 109, 639–646. [PubMed: 26244745]

Haghighi M, Caicedo JC, Cimini BA, Carpenter AE, Singh S, 2022. High-dimensional gene expression and morphology profiles of cells across 28,000 genetic and chemical perturbations. Nat. Methods 19, 1550–1557. [PubMed: 36344834]

Halpern KB, Shenhav R, Matcovitch-Natan O, Toth B, Lemze D, Golan M, Massasa EE, Baydatch S, Landen S, Moor AE, Brandis A, Giladi A, Avihail AS, David E, Amit I, Itzkovitz S, 2017. Single-cell spatial reconstruction reveals global division of labour in the mammalian liver. Nature 542, 352–356. [PubMed: 28166538]

Handly LN, Pilko A, Wollman R, 2015. Paracrine communication maximizes cellular response fidelity in wound signaling. Elife 4, e09652. [PubMed: 26448485]

Harber MP, Konopka AR, Jemiolo B, Trappe SW, Trappe TA, Reidy PT, 2010. Muscle protein synthesis and gene expression during recovery from aerobic exercise in the fasted and fed states. Am. J. Physiol. Regul. Integr. Comp. Physiol 299, R1254–62. [PubMed: 20720176]

Harber MP, Schenk S, Barkan AL, Horowitz JF, 2005. Effects of dietary carbohydrate restriction with high protein intake on protein metabolism and the somatotropic axis. J. Clin. Endocrinol. Metab 90, 5175–5181. [PubMed: 15972575]

Hardie DG, Ross FA, Hawley SA, 2012. AMPK: a nutrient and energy sensor that maintains energy homeostasis. Nat. Rev. Mol. Cell Biol 13, 251–262. [PubMed: 22436748]

Hargreaves M, Spriet LL, 2020. Skeletal muscle energy metabolism during exercise. Nat Metab 2, 817–828. [PubMed: 32747792]

Harper JW, Bennett EJ, 2016. Proteome complexity and the forces that drive proteome imbalance. Nature 537, 328–338. [PubMed: 27629639]

Hart Y, Sheftel H, Hausser J, Szekely P, Ben-Moshe NB, Korem Y, Tendler A, Mayo AE, Alon U, 2015. Inferring biological tasks using Pareto analysis of high-dimensional data. Nat. Methods 12, 233–5, 3 p following 235. [PubMed: 25622107]

Haschemi A, Kosma P, Gille L, Evans CR, Burant CF, Starkl P, Knapp B, Haas R, Schmid JA, Jandl C, Amir S, Lubec G, Park J, Esterbauer H, Bilban M, Brizuela L, Pospisilik JA, Otterbein LE, Wagner O, 2012. The sedoheptulose kinase CARKL directs macrophage polarization through control of glucose metabolism. Cell Metab. 15, 813–826. [PubMed: 22682222]

Hasenstaub A, Otte S, Callaway E, Sejnowski TJ, 2010. Metabolic cost as a unifying principle governing neuronal biophysics. Proc. Natl. Acad. Sci. U. S. A 107, 12329–12334. [PubMed: 20616090]

Hausser J, Mayo A, Keren L, Alon U, 2019. Central dogma rates and the trade-off between precision and economy in gene expression. Nat. Commun 10, 68. [PubMed: 30622246]

Headley MB, Bins A, Nip A, Roberts EW, Looney MR, Gerard A, Krummel MF, 2016. Visualization of immediate immune responses to pioneer metastatic cells in the lung. Nature 531, 513–517. [PubMed: 26982733]

Heckmann D, Campeau A, Lloyd CJ, Phaneuf PV, Hefner Y, Carrillo-Terrazas M, Feist AM, Gonzalez DJ, Palsson BO, 2020. Kinetic profiling of metabolic specialists demonstrates stability and consistency of in vivo enzyme turnover numbers. Proc. Natl. Acad. Sci. U. S. A 117, 23182–23190. [PubMed: 32873645]

Heckmann D, Lloyd CJ, Mih N, Ha Y, Zielinski DC, Haiman ZB, Desouki AA, Lercher MJ, Palsson BO, 2018. Machine learning applied to enzyme turnover numbers reveals protein structural correlates and improves metabolic models. Nat. Commun 9, 5252. [PubMed: 30531987]

Hefzi H, Lewis N, 2017. Mammalian cells devoid of lactate dehydrogenase activity. World Patent. 2017192437:A1.

Herculano-Houzel S, 2011. Scaling of brain metabolism with a fixed energy budget per neuron: implications for neuronal activity, plasticity and evolution. PLoS One 6, e17514. [PubMed: 21390261]

Hewson-Hughes AK, Colyer A, Simpson SJ, Raubenheimer D, 2016. Balancing macronutrient intake in a mammalian carnivore: disentangling the influences of flavour and nutrition. R Soc Open Sci 3, 160081. [PubMed: 27429768]

Heymsfield SB, Peterson CM, Bourgeois B, Thomas DM, Gallagher D, Strauss B, Müller MJ, Bosy-Westphal A, 2018. Human energy expenditure: advances in organtissue prediction models. Obes. Rev 19, 1177–1188. [PubMed: 30035381]

Hill SM, Nesser NK, Johnson-Camacho K, Jeffress M, Johnson A, Boniface C, Spencer SEF, Lu Y, Heiser LM, Lawrence Y, Pande NT, Korkola JE, Gray JW, Mills GB, Mukherjee S, Spellman PT, 2017. Context Specificity in Causal Signaling Networks Revealed by Phosphoprotein Profiling. Cell Syst 4, 73–83.e10. [PubMed: 28017544]

Hinzpeter F, Tostevin F, Gerland U, 2019. Regulation of reaction fluxes via enzyme sequestration and co-clustering. J. R. Soc. Interface 16, 20190444. [PubMed: 31362617]

Hitze B, Hubold C, van Dyken R, Schlichting K, Lehnert H, Entringer S, Peters A, 2010. How the selfish brain organizes its supply and demand. Front. Neuroenergetics 2, 7. [PubMed: 20616886]

Hofmeyr JS, Cornish-Bowden A, 2000. Regulating the cellular economy of supply and demand. FEBS Lett. 476, 47–51. [PubMed: 10878248]

Hogan MC, Ingham E, Kurdak SS, 1998. Contraction duration affects metabolic energy cost and fatigue in skeletal muscle. Am. J. Physiol 274, E397–402. [PubMed: 9530120]

Holzhütter H-G, 2004. The principle of flux minimization and its application to estimate stationary fluxes in metabolic networks. Eur. J. Biochem 271, 2905–2922. [PubMed: 15233787]

Hosios AM, Hecht VC, Danai LV, Johnson MO, Rathmell JC, Steinhauser ML, Manalis SR, Vander Heiden MG, 2016. Amino Acids Rather than Glucose Account for the Majority of Cell Mass in Proliferating Mammalian Cells. Dev. Cell 36, 540–549. [PubMed: 26954548]

Hrovatin K, Fischer DS, Theis FJ, 2022. Toward modeling metabolic state from single-cell transcriptomics. Mol Metab 57, 101396. [PubMed: 34785394]

Huang H, Zhou P, Wei J, Long L, Shi H, Dhungana Y, Chapman NM, Fu G, Saravia J, Raynor JL, Liu S, Palacios G, Wang Y-D, Qian C, Yu J, Chi H, 2021. In vivo CRISPR screening reveals nutrient signaling processes underpinning CD8+ T cell fate decisions. Cell 184, 1245–1261.e21. [PubMed: 33636132]

Hui S, Silverman JM, Chen SS, Erickson DW, Basan M, Wang J, Hwa T, Williamson JR, 2015. Quantitative proteomic analysis reveals a simple strategy of global resource allocation in bacteria. Mol. Syst. Biol 11, 784. [PubMed: 25678603]

Hukelmann JL, Anderson KE, Sinclair LV, Grzes KM, Murillo AB, Hawkins PT, Stephens LR, Lamond AI, Cantrell DA, 2016. The cytotoxic T cell proteome and its shaping by the kinase mTOR. Nat. Immunol 17, 104–112. [PubMed: 26551880]

Hu K, Yu Y, 2017. Metabolite availability as a window to view the early embryo microenvironment in vivo. Mol. Reprod. Dev 84, 1027–1038. [PubMed: 28722155]

Ingolia NT, Lareau LF, Weissman JS, 2011. Ribosome profiling of mouse embryonic stem cells reveals the complexity and dynamics of mammalian proteomes. Cell 147, 789–802. [PubMed: 22056041]

Itoh Y, Kawamata Y, Harada M, Kobayashi M, Fujii R, Fukusumi S, Ogi K, Hosoya M, Tanaka Y, Uejima H, Tanaka H, Maruyama M, Satoh R, Okubo S, Kizawa H, Komatsu H, Matsumura F, Noguchi Y, Shinohara T, Hinuma S, Fujisawa Y, Fujino M, 2003. Free fatty acids regulate insulin secretion from pancreatic beta cells through GPR40. Nature 422, 173–176. [PubMed: 12629551]

Jensen K, Simpson SJ, Nielsen VH, Hunt J, Raubenheimer D, Mayntz D, 2014. Nutrient-specific compensatory feeding in a mammalian carnivore, the mink, Neovison vison. Br. J. Nutr 112, 1226–1233. [PubMed: 25141190]

Jeong H, Tombor B, Albert R, Oltvai ZN, Barabási AL, 2000. The large-scale organization of metabolic networks. Nature 407, 651–654. [PubMed: 11034217]

Jerby-Arnon L, Regev A, 2022. DIALOGUE maps multicellular programs in tissue from single-cell or spatial transcriptomics data. Nat. Biotechnol 40, 1467–1477. [PubMed: 35513526]

Johnson CA, Raubenheimer D, Rothman JM, Clarke D, Swedell L, 2013. 30 days in the life: daily nutrient balancing in a wild chacma baboon. PLoS One 8, e70383. [PubMed: 23894645]

Jones RD, Qian Y, Siciliano V, DiAndreth B, Huh J, Weiss R, Del Vecchio D, 2020. An endoribonuclease-based feedforward controller for decoupling resource-limited genetic modules in mammalian cells. Nat. Commun 11, 5690. [PubMed: 33173034]

Jovanovic M, Rooney MS, Mertins P, Przybylski D, Chevrier N, Satija R, Rodriguez EH, Fields AP, Schwartz S, Raychowdhury R, Mumbach MR, Eisenhaure T, Rabani M, Gennert D, Lu D, Delorey T, Weissman JS, Carr SA, Hacohen N, Regev A, 2015. Immunogenetics. Dynamic profiling of the protein life cycle in response to pathogens. Science 347, 1259038. [PubMed: 25745177]

Kafri M, Metzl-Raz E, Jona G, Barkai N, 2016. The Cost of Protein Production. Cell Rep. 14, 22–31. [PubMed: 26725116]

Karr JR, Sanghvi JC, Macklin DN, Gutschow MV, Jacobs JM, Bolival B Jr, Assad-Garcia N, Glass JI, Covert MW, 2012. A whole-cell computational model predicts phenotype from genotype. Cell 150, 389–401. [PubMed: 22817898]

Keren L, Hausser J, Lotan-Pompan M, Vainberg Slutskin I, Alisar H, Kaminski S, Weinberger A, Alon U, Milo R, Segal E, 2016. Massively Parallel Interrogation of the Effects of Gene Expression Levels on Fitness. Cell 166, 1282–1294.e18. [PubMed: 27545349]

Khan MS, Spann RA, Münzberg H, Yu S, Albaugh VL, He Y, Berthoud H-R, Morrison CD, 2021. Protein Appetite at the Interface between Nutrient Sensing and Physiological Homeostasis. Nutrients 13. 10.3390/nu13114103

Khurana P, Burudpakdee C, Grupp SA, Beier UH, Barrett DM, Bassiri H, 2021. Distinct Bioenergetic Features of Human Invariant Natural Killer T Cells Enable Retained Functions in Nutrient-Deprived States. Front. Immunol 12, 700374. [PubMed: 34434191]

Kirkwood TBL, 2017. The Disposable Soma Theory, in: The Evolution of Senescence in the Tree of Life. Cambridge University Press, pp. 23–39.

Kistner TM, Pedersen BK, Lieberman DE, 2022. Interleukin 6 as an energy allocator in muscle tissue. Nat Metab 4, 170–179. [PubMed: 35210610]

Kiweler N, Delbrouck C, Pozdeev VI, Neises L, Soriano-Baguet L, Eiden K, Xian F, Benzarti M, Haase L, Koncina E, Schmoetten M, Jaeger C, Noman MZ, Vazquez A, Janji B, Dittmar G, Brenner D, Letellier E, Meiser J, 2022. Mitochondria preserve an autarkic one-carbon cycle to confer growth-independent cancer cell migration and metastasis. Nat. Commun 13, 2699. [PubMed: 35577770]

Klein D, Palla G, Lange M, Klein M, Piran Z, Gander M, Meng-Papaxanthos L, Sterr M, Bastidas-Ponce A, Tarquis-Medina M, Lickert H, Bakhti M, Nitzan M, Cuturi M, Theis FJ, 2023. Mapping cells through time and space with moscot. bioRxiv. 10.1101/2023.05.11.540374

Kleinridders A, Ferris HA, Reyzer ML, Rath M, Soto M, Manier ML, Spraggins J, Yang Z, Stanton RC, Caprioli RM, Kahn CR, 2018. Regional differences in brain glucose metabolism determined by imaging mass spectrometry. Mol Metab 12, 113–121. [PubMed: 29681509]

Klumpe HE, Langley MA, Linton JM, Su CJ, Antebi YE, Elowitz MB, 2022. The context-dependent, combinatorial logic of BMP signaling. Cell Syst.

Kochanowski K, Sander T, Link H, Chang J, Altschuler SJ, Wu LF, 2021. Systematic alteration of in vitro metabolic environments reveals empirical growth relationships in cancer cell phenotypes. Cell Rep. 34, 108647. [PubMed: 33472066]

Kol S, Ley D, Wulff T, Decker M, Arnsdorf J, Schoffelen S, Hansen AH, Jensen TL, Gutierrez JM, Chiang AWT, Masson HO, Palsson BO, Voldborg BG, Pedersen LE, Kildegaard HF, Lee GM,

Lewis NE, 2020. Multiplex secretome engineering enhances recombinant protein production and purity. Nat. Commun 11, 1908. [PubMed: 32313013]

Kon S, Ishibashi K, Katoh H, Kitamoto S, Shirai T, Tanaka S, Kajita M, Ishikawa S, Yamauchi H, Yako Y, Kamasaki T, Matsumoto T, Watanabe H, Egami R, Sasaki A, Nishikawa A, Kameda I, Maruyama T, Narumi R, Morita T, Sasaki Y, Enoki R, Honma S, Imamura H, Oshima M, Soga T, Miyazaki J-I, Duchen MR, Nam J-M, Onodera Y, Yoshioka S, Kikuta J, Ishii M, Imajo M, Nishida E, Fujioka Y, Ohba Y, Sato T, Fujita Y, 2017. Cell competition with normal epithelial cells promotes apical extrusion of transformed cells through metabolic changes. Nat. Cell Biol 19, 530–541. [PubMed: 28414314]

Korem Y, Szekely P, Hart Y, Sheftel H, Hausser J, Mayo A, Rothenberg ME, Kalisky T, Alon U, 2015. Geometry of the Gene Expression Space of Individual Cells. PLoS Comput. Biol 11, e1004224. [PubMed: 26161936]

Kroll A, Rousset Y, Hu X-P, Liebrand NA, Lercher MJ, 2023. Turnover number predictions for kinetically uncharacterized enzymes using machine and deep learning. Nat. Commun 14, 4139. [PubMed: 37438349]

Kuo C-C, Chiang AWT, Baghdassarian HM, Lewis NE, 2021. Dysregulation of the secretory pathway connects Alzheimer's disease genetics to aggregate formation. Cell Syst 12, 873–884.e4. [PubMed: 34171228]

Kuzawa CW, 2007. Developmental origins of life history: growth, productivity, and reproduction. Am. J. Hum. Biol 19, 654–661. [PubMed: 17639581]

Kuzawa CW, Chugani HT, Grossman LI, Lipovich L, Muzik O, Hof PR, Wildman DE, Sherwood CC, Leonard WR, Lange N, 2014. Metabolic costs and evolutionary implications of human brain development. Proc. Natl. Acad. Sci. U. S. A 111, 13010–13015. [PubMed: 25157149]

Lai AKM, Dick TJM, Biewener AA, Wakeling JM, 2021. Task-dependent recruitment across ankle extensor muscles and between mechanical demands is driven by the metabolic cost of muscle contraction. J. R. Soc. Interface 18, 20200765. [PubMed: 33402020]

Lailvaux SP, Husak JF, 2017. Predicting Life-History Trade-Offs with Whole-Organism Performance. Integr. Comp. Biol 57, 325–332. [PubMed: 28859417]

Lailvaux SP, Husak JF, 2014. The life history of whole-organism performance. Q. Rev. Biol 89, 285–318. [PubMed: 25510077]

Lane N, Martin W, 2010. The energetics of genome complexity. Nature 467, 929–934. [PubMed: 20962839]

Lan G, Sartori P, Neumann S, Sourjik V, Tu Y, 2012. The energy-speed-accuracy tradeoff in sensory adaptation. Nat. Phys 8, 422–428. [PubMed: 22737175]

Larson RC, Kann MC, Bailey SR, Haradhvala NJ, Llopis PM, Bouffard AA, Scarfó I, Leick MB, Grauwet K, Berger TR, Stewart K, Anekal PV, Jan M, Joung J, Schmidts A, Ouspenskaia T, Law T, Regev A, Getz G, Maus MV, 2022. CAR T cell killing requires the IFNγR pathway in solid but not liquid tumours. Nature 604, 563–570. [PubMed: 35418687]

Le Bihan M-C, Bigot A, Jensen SS, Dennis JL, Rogowska-Wrzesinska A, Lainé J, Gache V, Furling D, Jensen ON, Voit T, Mouly V, Coulton GR, Butler-Browne G, 2012. In-depth analysis of the secretome identifies three major independent secretory pathways in differentiating human myoblasts. J. Proteomics 77, 344–356. [PubMed: 23000592]

Lee EC, Fragala MS, Kavouras SA, Queen RM, Pryor JL, Casa DJ, 2017. Biomarkers in Sports and Exercise: Tracking Health, Performance, and Recovery in Athletes. J. Strength Cond. Res 31, 2920–2937. [PubMed: 28737585]

Lee JM, Gianchandani EP, Eddy JA, Papin JA, 2008. Dynamic analysis of integrated signaling, metabolic, and regulatory networks. PLoS Comput. Biol 4, e1000086. [PubMed: 18483615]

Lennie P, 2003. The cost of cortical computation. Curr. Biol 13, 493–497. [PubMed: 12646132]

Lerman JA, Hyduke DR, Latif H, Portnoy VA, Lewis NE, Orth JD, Schrimpe-Rutledge AC, Smith RD, Adkins JN, Zengler K, Palsson BO, 2012. In silico method for modelling metabolism and gene product expression at genome scale. Nat. Commun 3, 929. [PubMed: 22760628]

Lestas I, Vinnicombe G, Paulsson J, 2010. Fundamental limits on the suppression of molecular fluctuations. Nature 467, 174–178. [PubMed: 20829788]

Levy WB, Baxter RA, 1996. Energy efficient neural codes. Neural Comput 8, 531–543. [PubMed: 8868566]

Lewin N, Swanson EM, Williams BL, Holekamp KE, 2017. Juvenile concentrations of IGF - 1 predict life- history trade- offs in a wild mammal. Functional Ecology. 10.1111/1365-2435.12808

Lewis NE, Hixson KK, Conrad TM, Lerman JA, Charusanti P, Polpitiya AD, Adkins JN, Schramm G, Purvine SO, Lopez-Ferrer D, Weitz KK, Eils R, König R, Smith RD, Palsson BØ, 2010a. Omic data from evolved E. coli are consistent with computed optimal growth from genome-scale models. Mol. Syst. Biol 6, 390. [PubMed: 20664636]

Lewis NE, Nagarajan H, Palsson BO, 2012. Constraining the metabolic genotype-phenotype relationship using a phylogeny of in silico methods. Nat. Rev. Microbiol 10, 291–305. [PubMed: 22367118]

Lewis NE, Schramm G, Bordbar A, Schellenberger J, Andersen MP, Cheng JK, Patel N, Yee A, Lewis RA, Eils R, König R, Palsson BØ, 2010b. Large-scale in silico modeling of metabolic interactions between cell types in the human brain. Nat. Biotechnol 28, 1279–1285. [PubMed: 21102456]

Liebermeister W, Noor E, Flamholz A, Davidi D, Bernhardt J, Milo R, 2014. Visual account of protein investment in cellular functions. Proc. Natl. Acad. Sci. U. S. A 111, 8488–8493. [PubMed: 24889604]

Li F, Yuan L, Lu H, Li G, Chen Y, Engqvist MKM, Kerkhoven EJ, Nielsen J, 2022. Deep learning-based kcat prediction enables improved enzyme-constrained model reconstruction. Nature Catalysis 5, 662–672.

Li G-W, Burkhardt D, Gross C, Weissman JS, 2014. Quantifying absolute protein synthesis rates reveals principles underlying allocation of cellular resources. Cell 157, 624–635. [PubMed: 24766808]

Li J, Cai Z, Vaites LP, Shen N, Mitchell DC, Huttlin EL, Paulo JA, Harry BL, Gygi SP, 2021. Proteome-wide mapping of short-lived proteins in human cells. Mol. Cell 81, 4722–4735.e5. [PubMed: 34626566]

Li JJ, Bickel PJ, Biggin MD, 2014. System wide analyses have underestimated protein abundances and the importance of transcription in mammals. PeerJ 2, e270. [PubMed: 24688849]

Lin J, Amir A, 2018. Homeostasis of protein and mRNA concentrations in growing cells. Nat. Commun 9, 4496. [PubMed: 30374016]

Liu G, Mac Gabhann F, Popel AS, 2012. Effects of fiber type and size on the heterogeneity of oxygen distribution in exercising skeletal muscle. PLoS One 7, e44375. [PubMed: 23028531]

Liu L, Duclos G, Sun B, Lee J, Wu A, Kam Y, Sontag ED, Stone HA, Sturm JC, Gatenby RA, Austin RH, 2013. Minimization of thermodynamic costs in cancer cell invasion. Proc. Natl. Acad. Sci. U. S. A 110, 1686–1691. [PubMed: 23319630]

Liu Y, Beyer A, Aebersold R, 2016. On the Dependency of Cellular Protein Levels on mRNA Abundance. Cell 165, 535–550. [PubMed: 27104977]

Li Y, Yao L, Mori Y, Sun SX, 2019. On the energy efficiency of cell migration in diverse physical environments. Proc. Natl. Acad. Sci. U. S. A 116, 23894–23900. [PubMed: 31719206]

Long L, Wei J, Lim SA, Raynor JL, Shi H, Connelly JP, Wang H, Guy C, Xie B, Chapman NM, Fu G, Wang Y, Huang H, Su W, Saravia J, Risch I, Wang Y-D, Li Y, Niu M, Dhungana Y, Kc A, Zhou P, Vogel P, Yu J, Pruett-Miller SM, Peng J, Chi H, 2021. CRISPR screens unveil signal hubs for nutrient licensing of T cell immunity. Nature 600, 308–313. [PubMed: 34795452]

Lopez JA, Brennan AJ, Whisstock JC, Voskoboinik I, Trapani JA, 2012. Protecting a serial killer: pathways for perforin trafficking and self-defence ensure sequential target cell death. Trends Immunol. 33, 406–412. [PubMed: 22608996]

Lunt SY, Muralidhar V, Hosios AM, Israelsen WJ, Gui DY, Newhouse L, Ogrodzinski M, Hecht V, Xu K, Acevedo PNM, Hollern DP, Bellinger G, Dayton TL, Christen S, Elia I, Dinh AT, Stephanopoulos G, Manalis SR, Yaffe MB, Andrechek ER, Fendt S-M, Vander Heiden MG, 2015. Pyruvate kinase isoform expression alters nucleotide synthesis to impact cell proliferation. Mol. Cell 57, 95–107. [PubMed: 25482511]

Lutter M, Nestler EJ, 2009. Homeostatic and hedonic signals interact in the regulation of food intake. J. Nutr 139, 629–632. [PubMed: 19176746]

Lynch M, Marinov GK, 2015. The bioenergetic costs of a gene. Proc. Natl. Acad. Sci. U. S. A 112, 15690–15695. [PubMed: 26575626]

Macklin DN, Ahn-Horst TA, Choi H, Ruggero NA, Carrera J, Mason JC, Sun G, Agmon E, DeFelice MM, Maayan I, Lane K, Spangler RK, Gillies TE, Paull ML, Akhter S, Bray SR, Weaver DS, Keseler IM, Karp PD, Morrison JH, Covert MW, 2020. Simultaneous cross-evaluation of heterogeneous datasets via mechanistic simulation. Science 369. 10.1126/science.aav3751

Ma EH, Verway MJ, Johnson RM, Roy DG, Steadman M, Hayes S, Williams KS, Sheldon RD, Samborska B, Kosinski PA, Kim H, Griss T, Faubert B, Condotta SA, Krawczyk CM, DeBerardinis RJ, Stewart KM, Richer MJ, Chubukov V, Roddy TP, Jones RG, 2019. Metabolic Profiling Using Stable Isotope Tracing Reveals Distinct Patterns of Glucose Utilization by Physiologically Activated CD8 T Cells. Immunity 51, 856–870.e5. [PubMed: 31747582]

Magkos F, Hjorth MF, Astrup A, 2020. Diet and exercise in the prevention and treatment of type 2 diabetes mellitus. Nat. Rev. Endocrinol 16, 545–555. [PubMed: 32690918]

Mah CK, Ahmed N, Lopez N, Lam D, Monell A, Kern C, Han Y, Prasad G, Cesnik AJ, Lundberg E, Zhu Q, Carter H, Yeo GW, 2023. Bento: A toolkit for subcellular analysis of spatial transcriptomics data. bioRxiv. 10.1101/2022.06.10.495510

Mahmoudabadi G, Phillips R, Lynch M, Milo R, 2019. Defining the Energetic Costs of Cellular Structures. bioRxiv. 10.1101/666040

Marchingo JM, Cantrell DA, 2022. Protein synthesis, degradation, and energy metabolism in T cell immunity. Cell. Mol. Immunol 19, 303–315. [PubMed: 34983947]

Markin CJ, Mokhtari DA, Sunden F, Appel MJ, Akiva E, Longwell SA, Sabatti C, Herschlag D, Fordyce PM, 2021. Revealing enzyme functional architecture via high-throughput microfluidic enzyme kinetics. Science 373. 10.1126/science.abf8761

Martins Conde P. do R., Sauter T, Pfau T, 2016. Constraint Based Modeling Going Multicellular. Front Mol Biosci 3, 3. [PubMed: 26904548]

Matamoro-Vidal A, Levayer R, 2019. Multiple Influences of Mechanical Forces on Cell Competition. Curr. Biol 29, R762–R774. [PubMed: 31386857]

Mehta P, Schwab DJ, 2012. Energetic costs of cellular computation. Proc. Natl. Acad. Sci. U. S. A 109, 17978–17982. [PubMed: 23045633]

Mendelsohn BA, Bennett NK, Darch MA, Yu K, Nguyen MK, Pucciarelli D, Nelson M, Horlbeck MA, Gilbert LA, Hyun W, Kampmann M, Nakamura JL, Nakamura K, 2018. A high-throughput screen of real-time ATP levels in individual cells reveals mechanisms of energy failure. PLoS Biol. 16, e2004624. [PubMed: 30148842]

Metzl-Raz E, Kafri M, Yaakov G, Soifer I, Gurvich Y, Barkai N, 2017. Principles of cellular resource allocation revealed by condition-dependent proteome profiling. Elife 6. 10.7554/eLife.28034

Miettinen TP, Pessa HKJ, Caldez MJ, Fuhrer T, Diril MK, Sauer U, Kaldis P, Björklund M, 2014. Identification of transcriptional and metabolic programs related to mammalian cell size. Curr. Biol 24, 598–608. [PubMed: 24613310]

Miller RH, Hamill J, 2015. Optimal footfall patterns for cost minimization in running. J. Biomech 48, 2858–2864. [PubMed: 25952545]

Milo R, Phillips R, 2015. Cell biology by the numbers. Garland Science, London, England. 10.1201/9780429258770

Mitchel J, Grace Gordon M, Perez RK, Biederstedt E, Bueno R, Ye CJ, Kharchenko PV, 2023. Tensor decomposition reveals coordinated multicellular patterns of transcriptional variation that distinguish and stratify disease individuals. bioRxiv. 10.1101/2022.02.16.480703

Mori M, Hwa T, Martin OC, De Martino A, Marinari E, 2016. Constrained Allocation Flux Balance Analysis. PLoS Comput. Biol 12, e1004913. [PubMed: 27355325]

Mosier JA, Wu Y, Reinhart-King CA, 2021. Recent advances in understanding the role of metabolic heterogeneities in cell migration. Fac Rev 10, 8. [PubMed: 33659926]

Munding EM, Shiue L, Katzman S, Donohue JP, Ares M Jr, 2013. Competition between pre-mRNAs for the splicing machinery drives global regulation of splicing. Mol. Cell 51, 338–348. [PubMed: 23891561]

Munsky B, Neuert G, van Oudenaarden A, 2012. Using gene expression noise to understand gene regulation. Science 336, 183–187. [PubMed: 22499939]

Nagaraj N, Wisniewski JR, Geiger T, Cox J, Kircher M, Kelso J, Pääbo S, Mann M, 2011. Deep proteome and transcriptome mapping of a human cancer cell line. Mol. Syst. Biol 7, 548. [PubMed: 22068331]

Nagle MP, Tam GS, Maltz E, Hemminger Z, Wollman R, 2021. Bridging scales: From cell biology to physiology using in situ single-cell technologies. Cell Syst 12, 388–400. [PubMed: 34015260]

Nagrath D, Avila-Elchiver M, Berthiaume F, Tilles AW, Messac A, Yarmush ML, 2007. Integrated energy and flux balance based multiobjective framework for large-scale metabolic networks. Ann. Biomed. Eng 35, 863–885. [PubMed: 17393337]

Neurohr GE, Terry RL, Lengefeld J, Bonney M, Brittingham GP, Moretto F, Miettinen TP, Vaites LP, Soares LM, Paulo JA, Harper JW, Buratowski S, Manalis S, van Werven FJ, Holt LJ, Amon A, 2019. Excessive Cell Growth Causes Cytoplasm Dilution And Contributes to Senescence. Cell 176, 1083–1097.e18. [PubMed: 30739799]

Nguyen HP, Sheng R, Murray E, Ito Y, Bruck M, Biellak C, An K, Lynce F, Dillon DA, Magbanua MJM, Huppert LA, Hammerlindl H, Esserman L, Rosenbluth JM, Ahituv N, 2023. Implantation of engineered adipocytes that outcompete tumors for resources suppresses cancer progression. bioRxiv. 10.1101/2023.03.28.534564

Nilsson A, Nielsen J, Palsson BO, 2017. Metabolic Models of Protein Allocation Call for the Kinetome. Cell Syst 5, 538–541. [PubMed: 29284126]

Noor E, Bar-Even A, Flamholz A, Reznik E, Liebermeister W, Milo R, 2014. Pathway thermodynamics highlights kinetic obstacles in central metabolism. PLoS Comput. Biol 10, e1003483. [PubMed: 24586134]

Noor E, Flamholz A, Bar-Even A, Davidi D, Milo R, Liebermeister W, 2016. The Protein Cost of Metabolic Fluxes: Prediction from Enzymatic Rate Laws and Cost Minimization. PLoS Comput. Biol 12, e1005167. [PubMed: 27812109]

O'Brien EJ, Lerman JA, Chang RL, Hyduke DR, Palsson BØ, 2013. Genome-scale models of metabolism and gene expression extend and refine growth phenotype prediction. Mol. Syst. Biol 9, 693. [PubMed: 24084808]

Opdam S, Richelle A, Kellman B, Li S, Zielinski DC, Lewis NE, 2017. A Systematic Evaluation of Methods for Tailoring Genome-Scale Metabolic Models. Cell Syst 4, 318–329.e6. [PubMed: 28215528]

Ori A, Iskar M, Buczak K, Kastritis P, Parca L, Andrés-Pons A, Singer S, Bork P, Beck M, 2016. Spatiotemporal variation of mammalian protein complex stoichiometries. Genome Biol. 17, 47. [PubMed: 26975353]

Orth JD, Thiele I, Palsson BØ, 2010. What is flux balance analysis? Nat. Biotechnol. 28, 245–248. [PubMed: 20212490]

Palm W, Thompson CB, 2017. Nutrient acquisition strategies of mammalian cells. Nature 546, 234–242. [PubMed: 28593971]

Palsson BØ, 2015. Systems Biology: Constraint-based Reconstruction and Analysis.

Pantaleon M, Scott J, Kaye PL, 2008. Nutrient sensing by the early mouse embryo: hexosamine biosynthesis and glucose signaling during preimplantation development. Biol. Reprod 78, 595–600. [PubMed: 18046015]

Papin JA, Palsson BO, 2004a. Topological analysis of mass-balanced signaling networks: a framework to obtain network properties including crosstalk. J. Theor. Biol 227, 283–297. [PubMed: 14990392]

Papin JA, Palsson BO, 2004b. The JAK-STAT signaling network in the human B-cell: an extreme signaling pathway analysis. Biophys. J 87, 37–46. [PubMed: 15240442]

Parenteau J, Maignon L, Berthoumieux M, Catala M, Gagnon V, Abou Elela S, 2019. Introns are mediators of cell response to starvation. Nature 565, 612–617. [PubMed: 30651641]

Peters A, 2011. The selfish brain: Competition for energy resources. Am. J. Hum. Biol 23, 29–34. [PubMed: 21080380]

Peters A, Schweiger U, Pellerin L, Hubold C, Oltmanns KM, Conrad M, Schultes B, Born J, Fehm HL, 2004. The selfish brain: competition for energy resources. Neurosci. Biobehav. Rev 28, 143–180. [PubMed: 15172762]

Peth A, Nathan JA, Goldberg AL, 2013. The ATP costs and time required to degrade ubiquitinated proteins by the 26 S proteasome. J. Biol. Chem 288, 29215–29222. [PubMed: 23965995]

Pinkard H, Baghdassarian H, Mujal A, Roberts E, Hu KH, Friedman DH, Malenica I, Shagam T, Fries A, Corbin K, Krummel MF, Waller L, 2021. Learned adaptive multiphoton illumination microscopy for large-scale immune response imaging. Nat. Commun 12, 1916. [PubMed: 33772022]

Poganik JR, Zhang B, Baht GS, Tyshkovskiy A, Deik A, Kerepesi C, Yim SH, Lu AT, Haghani A, Gong T, Hedman AM, Andolf E, Pershagen G, Almqvist C, Clish CB, Horvath S, White JP, Gladyshev VN, 2023. Biological age is increased by stress and restored upon recovery. Cell Metab. 10.1016/j.cmet.2023.03.015

Polychronidou M, Hou J, Babu MM, Liberali P, Amit I, Deplancke B, Lahav G, Itzkovitz S, Mann M, Saez-Rodriguez J, Theis F, Eils R, 2023. Single-cell biology: what does the future hold? Mol. Syst. Biol 19, e11799. [PubMed: 37318792]

Popovic D, Koch B, Kueblbeck M, Ellenberg J, Pelkmans L, 2018. Multivariate Control of Transcript to Protein Variability in Single Mammalian Cells. Cell Syst 7, 398–411.e6. [PubMed: 30342881]

Pulido C, Ryan TA, 2021. Synaptic vesicle pools are a major hidden resting metabolic burden of nerve terminals. Sci Adv 7, eabi9027. [PubMed: 34860552]

Qin C, Xiang Y, Liu J, Zhang R, Liu Z, Li T, Sun Z, Ouyang X, Zong Y, Zhang HM, Ouyang Q, Qian L, Lou C, 2023. Precise programming of multigene expression stoichiometry in mammalian cells by a modular and programmable transcriptional system. Nat. Commun 14, 1500. [PubMed: 36932109]

Qiu X, Zhu DY, Yao J, Jing Z, Zuo L, Wang M, Min K.H. (joseph), Pan H, Wang S, Liao S, Lai Y, Hao S, Lu YR, Hill M, Martin-Rufino JD, Weng C, Riera-Escandell AM, Chen M, Wu L, Zhang Y, Wei X, Li M, Huang X, Xiang R, Yang Z, Liu C, Xia T, Liang Y, Xu J, Hu Q, Hu Y, Zhu H, Li Y, Chen A, Esteban MA, Gu Y, Lauffenburger DA, Xu X, Liu L, Weissman JS, Liu S, Bai Y, 2022. Spateo: multidimensional spatiotemporal modeling of single-cell spatial transcriptomics. bioRxiv. 10.1101/2022.12.07.519417

Rabani M, Levin JZ, Fan L, Adiconis X, Raychowdhury R, Garber M, Gnirke A, Nusbaum C, Hacohen N, Friedman N, Amit I, Regev A, 2011. Metabolic labeling of RNA uncovers principles of RNA production and degradation dynamics in mammalian cells. Nat. Biotechnol 29, 436–442. [PubMed: 21516085]

Raj A, Peskin CS, Tranchina D, Vargas DY, Tyagi S, 2006. Stochastic mRNA Synthesis in Mammalian Cells. PLoS Biol. 4, e309. [PubMed: 17048983]

Ramirez Flores RO, Lanzer JD, Dimitrov D, Velten B, Saez-Rodriguez J, 2023. Multicellular factor analysis of single-cell data for a tissue-centric understanding of disease. bioRxiv. 10.1101/2023.02.23.529642

Rathmell JC, Vander Heiden MG, Harris MH, Frauwirth KA, Thompson CB, 2000. In the absence of extrinsic signals, nutrient utilization by lymphocytes is insufficient to maintain either cell size or viability. Mol. Cell 6, 683–692. [PubMed: 11030347]

Reefman E, Kay JG, Wood SM, Offenhäuser C, Brown DL, Roy S, Stanley AC, Low PC, Manderson AP, Stow JL, 2010. Cytokine secretion is distinct from secretion of cytotoxic granules in NK cells. J. Immunol 184, 4852–4862. [PubMed: 20368273]

Reinfeld BI, Madden MZ, Wolf MM, Chytil A, Bader JE, Patterson AR, Sugiura A, Cohen AS, Ali A, Do BT, Muir A, Lewis CA, Hongo RA, Young KL, Brown RE, Todd VM, Huffstater T, Abraham A, O'Neil RT, Wilson MH, Xin F, Tantawy MN, Merryman WD, Johnson RW, Williams CS, Mason EF, Mason FM, Beckermann KE, Vander Heiden MG, Manning HC, Rathmell JC, Rathmell WK, 2021. Cell-programmed nutrient partitioning in the tumour microenvironment. Nature 593, 282–288. [PubMed: 33828302]

Ren X, Zhong G, Zhang Q, Zhang L, Sun Y, Zhang Z, 2020. Reconstruction of cell spatial organization from single-cell RNA sequencing data based on ligand-receptor mediated self-assembly. Cell Res. 30, 763–778. [PubMed: 32541867]

Reuveni S, Ehrenberg M, Paulsson J, 2017. Ribosomes are optimized for autocatalytic production. Nature 547, 293–297. [PubMed: 28726822]

Rode KD, Robbins CT, 2000. Why bears consume mixed diets during fruit abundance. Canadian Journal of Zoology 78, 1640–1645.

Rodríguez-Caso C, 2013. Can cell mortality determine division of labor in tissue organization? J. Theor. Biol 332, 161–170. [PubMed: 23665209]

Rolfe DF, Brown GC, 1997. Cellular energy utilization and molecular origin of standard metabolic rate in mammals. Physiol. Rev 77, 731–758. [PubMed: 9234964]

Rondelez Y, 2012. Competition for catalytic resources alters biological network dynamics. Phys. Rev. Lett 108, 018102. [PubMed: 22304295]

Rooyackers OE, Adey DB, Ades PA, Nair KS, 1996. Effect of age on in vivo rates of mitochondrial protein synthesis in human skeletal muscle. Proc. Natl. Acad. Sci. U. S. A 93, 15364–15369. [PubMed: 8986817]

Rothman JM, Raubenheimer D, Chapman CA, 2011. Nutritional geometry: gorillas prioritize non-protein energy while consuming surplus protein. Biol. Lett 7, 847–849. [PubMed: 21632622]

Rueffler C, Hermisson J, Wagner GP, 2012. Evolution of functional specialization and division of labor. Proc. Natl. Acad. Sci. U. S. A 109, E326–35. [PubMed: 22308336]

Rues S, Lenz J, Türp JC, Schweizerhof K, Schindler HJ, 2008. Forces and motor control mechanisms during biting in a realistically balanced experimental occlusion. Arch. Oral Biol 53, 1119–1128. [PubMed: 18675391]

Saez-Rodriguez J, Kremling A, Gilles ED, 2005. Dissecting the puzzle of life: modularization of signal transduction networks. Comput. Chem. Eng 29, 619–629.

Sahoo S, Aurich MK, Jonsson JJ, Thiele I, 2014. Membrane transporters in a human genome-scale metabolic knowledgebase and their implications for disease. Front. Physiol 5, 91. [PubMed: 24653705]

Sale C, Saunders B, Hudson S, Wise JA, Harris RC, Sunderland CD, 2011. Effect of β-alanine plus sodium bicarbonate on high-intensity cycling capacity. Med. Sci. Sports Exerc 43, 1972–1978. [PubMed: 21407127]

Salehi S, Kabeer F, Ceglia N, Andronescu M, Williams MJ, Campbell KR, Masud T, Wang B, Biele J, Brimhall J, Gee D, Lee H, Ting J, Zhang AW, Tran H, O'Flanagan C, Dorri F, Rusk N, de Algara TR, Lee SR, Cheng BYC, Eirew P, Kono T, Pham J, Grewal D, Lai D, Moore R, Mungall AJ, Marra MA, IMAXT Consortium, McPherson A, Bouchard-Côté A, Aparicio S, Shah SP, 2021. Clonal fitness inferred from time-series modelling of single-cell cancer genomes. Nature 595, 585–590. [PubMed: 34163070]

Sánchez BJ, Zhang C, Nilsson A, Lahtvee P-J, Kerkhoven EJ, Nielsen J, 2017. Improving the phenotype predictions of a yeast genome-scale metabolic model by incorporating enzymatic constraints. Mol. Syst. Biol 13, 935. [PubMed: 28779005]

Sartori P, Pigolotti S, 2015. Thermodynamics of error correction. Phys. Rev. X 5. 10.1103/physrevx.5.041039

Schell JC, Wisidagama DR, Bensard C, Zhao H, Wei P, Tanner J, Flores A, Mohlman J, Sorensen LK, Earl CS, Olson KA, Miao R, Waller TC, Delker D, Kanth P, Jiang L, DeBerardinis RJ, Bronner MP, Li DY, Cox JE, Christofk HR, Lowry WE, Thummel CS, Rutter J, 2017. Control of intestinal stem cell function and proliferation by mitochondrial pyruvate metabolism. Nat. Cell Biol 19, 1027–1036. [PubMed: 28812582]

Schiaffino S, Reggiani C, 2011. Fiber types in mammalian skeletal muscles. Physiol. Rev 91, 1447–1531. [PubMed: 22013216]

Schilling CH, Letscher D, Palsson BO, 2000. Theory for the systemic definition of metabolic pathways and their use in interpreting metabolic function from a pathway-oriented perspective. J. Theor. Biol 203, 229–248. [PubMed: 10716907]

Schindler HJ, Rues S, Türp JC, Schweizerhof K, Lenz J, 2007. Jaw clenching: muscle and joint forces, optimization strategies. J. Dent. Res 86, 843–847. [PubMed: 17720852]

Schink SJ, Christodoulou D, Mukherjee A, Athaide E, Brunner V, Fuhrer T, Bradshaw GA, Sauer U, Basan M, 2022. Glycolysis/gluconeogenesis specialization in microbes is driven by biochemical constraints of flux sensing. Mol. Syst. Biol 18, e10704. [PubMed: 34994048]

Schmidt CA, Fisher-Wellman KH, Neufer PD, 2021. From OCR and ECAR to energy: Perspectives on the design and interpretation of bioenergetics studies. J. Biol. Chem 297, 101140. [PubMed: 34461088]

Schmitt DL, An S, 2017. Spatial Organization of Metabolic Enzyme Complexes in Cells. Biochemistry 56, 3184–3196. [PubMed: 28580779]

Schuetz R, Zamboni N, Zampieri M, Heinemann M, Sauer U, 2012. Multidimensional optimality of microbial metabolism. Science 336, 601–604. [PubMed: 22556256]

Schuster S, Schuster R, Heinrich R, 1991. Minimization of intermediate concentrations as a suggested optimality principle for biochemical networks. II. Time hierarchy, enzymatic rate laws, and erythrocyte metabolism. J. Math. Biol 29, 443–455. [PubMed: 1875162]

Schwanhäusser B, Busse D, Li N, Dittmar G, Schuchhardt J, Wolf J, Chen W, Selbach M, 2011. Global quantification of mammalian gene expression control. Nature 473, 337–342. [PubMed: 21593866]

Scott M, Gunderson CW, Mateescu EM, Zhang Z, Hwa T, 2010. Interdependence of cell growth and gene expression: origins and consequences. Science 330, 1099–1102. [PubMed: 21097934]

Seki T, Yang Y, Sun X, Lim S, Xie S, Guo Z, Xiong W, Kuroda M, Sakaue H, Hosaka K, Jing X, Yoshihara M, Qu L, Li X, Chen Y, Cao Y, 2022. Brown-fatmediated tumour suppression by cold-altered global metabolism. Nature 608, 421–428. [PubMed: 35922508]

Shakiba N, Jones RD, Weiss R, Del Vecchio D, 2021. Context-aware synthetic biology by controller design: Engineering the mammalian cell. Cell Syst 12, 561–592. [PubMed: 34139166]

Shen Y, Dinh HV, Cruz E, Call CM, Baron H, Ryseck R-P, Pratas J, Subramanian A, Fatma Z, Weilandt D, Dwaraknath S, Xiao T, Hendry JI, Tran V, Yang L, Yoshikuni Y, Zhao H, Maranas CD, Wühr M, Rabinowitz JD, 2022. Proteome capacity constraints favor respiratory ATP generation. bioRxiv. 10.1101/2022.08.10.503479

Shen Y, Zhou M, Cai D, Filho DA, Fernandes G, Cai Y, de Sousa AF, Tian M, Kim N, Lee J, Necula D, Zhou C, Li S, Salinas S, Liu A, Kang X, Kamata M, Lavi A, Huang S, Silva T, Do Heo W, Silva AJ, 2022. CCR5 closes the temporal window for memory linking. Nature 606, 146–152. [PubMed: 35614219]

Shoval O, Sheftel H, Shinar G, Hart Y, Ramote O, Mayo A, Dekel E, Kavanagh K, Alon U, 2012. Evolutionary trade-offs, Pareto optimality, and the geometry of phenotype space. Science 336, 1157–1160. [PubMed: 22539553]

Shvartsman SY, Hagan MP, Yacoub A, Dent P, Wiley HS, Lauffenburger DA, 2002. Autocrine loops with positive feedback enable context-dependent cell signaling. Am. J. Physiol. Cell Physiol. 282, C545–59. [PubMed: 11832340]

Simpson SJ, Batley R, Raubenheimer D, 2003. Geometric analysis of macronutrient intake in humans: the power of protein? Appetite 41, 123–140. [PubMed: 14550310]

Simpson SJ, Raubenheimer D, 2005. Obesity: the protein leverage hypothesis. Obes. Rev 6, 133–142. [PubMed: 15836464]

Simpson SJ, Raubenheimer D, 1993. A multi-level analysis of feeding behaviour: the geometry of nutritional decisions. Phil. Trans. R. Soc. Lond. B 342, 381–402.

Singh R, Cuervo AM, 2011. Autophagy in the cellular energetic balance. Cell Metab. 13, 495–504. [PubMed: 21531332]

Smiley P, Levin M, 2022. Competition for finite resources as coordination mechanism for morphogenesis: An evolutionary algorithm study of digital embryogeny. Biosystems. 221, 104762. [PubMed: 36064151]

Smillie CS, Biton M, Ordovas-Montanes J, Sullivan KM, Burgin G, Graham DB, Herbst RH, Rogel N, Slyper M, Waldman J, Sud M, Andrews E, Velonias G, Haber AL, Jagadeesh K, Vickovic S, Yao J, Stevens C, Dionne D, Nguyen LT, Villani A-C, Hofree M, Creasey EA, Huang H, Rozenblatt-Rosen O, Garber JJ, Khalili H, Desch AN, Daly MJ, Ananthakrishnan AN, Shalek AK, Xavier RJ, Regev A, 2019. Intra- and Inter-cellular Rewiring of the Human Colon during Ulcerative Colitis. Cell 178, 714–730.e22. [PubMed: 31348891]

Smith S, Grima R, 2018. Single-cell variability in multicellular organisms. Nat. Commun 9, 345. [PubMed: 29367605]

Soeters MR, Soeters PB, Schooneman MG, Houten SM, Romijn JA, 2012. Adaptive reciprocity of lipid and glucose metabolism in human short-term starvation. Am. J. Physiol. Endocrinol. Metab 303, E1397–407. [PubMed: 23074240]

Soflaee MH, Kesavan R, Sahu U, Tasdogan A, Villa E, Djabari Z, Cai F, Tran DH, Vu HS, Ali ES, Rion H, O'Hara BP, Kelekar S, Hallett JH, Martin M, Mathews TP, Gao P, Asara JM, Manning BD, Ben-Sahra I, Hoxhaj G, 2022. Purine nucleotide depletion prompts cell migration by stimulating the serine synthesis pathway. Nat. Commun 13, 2698. [PubMed: 35577785]

Solon-Biet SM, Cogger VC, Pulpitel T, Heblinski M, Wahl D, McMahon AC, Warren A, Durrant-Whyte J, Walters KA, Krycer JR, Ponton F, Gokarn R, Wali JA, Ruohonen K, Conigrave AD, James DE, Raubenheimer D, Morrison CD, Le Couteur DG, Simpson SJ, 2016. Defining the Nutritional and Metabolic Context of FGF21 Using the Geometric Framework. Cell Metab. 24, 555–565. [PubMed: 27693377]

Son S, Stevens MM, Chao HX, Thoreen C, Hosios AM, Schweitzer LD, Weng Y, Wood K, Sabatini D, Vander Heiden MG, Manalis S, 2015. Cooperative nutrient accumulation sustains growth of mammalian cells. Sci. Rep 5, 17401. [PubMed: 26620632]

Stefl S, Nishi H, Petukh M, Panchenko AR, Alexov E, 2013. Molecular mechanisms of disease-causing missense mutations. J. Mol. Biol 425, 3919–3936. [PubMed: 23871686]

Sterner RW, Elser JJ, 2017. Ecological Stoichiometry. Princeton University Press.

Su CJ, Murugan A, Linton JM, Yeluri A, Bois J, Klumpe H, Langley MA, Antebi YE, Elowitz MB, 2022. Ligand-receptor promiscuity enables cellular addressing. Cell Syst 13, 408–425.e12. [PubMed: 35421362]

Szekely P, Sheftel H, Mayo A, Alon U, 2013. Evolutionary tradeoffs between economy and effectiveness in biological homeostasis systems. PLoS Comput. Biol 9, e1003163. [PubMed: 23950698]

Taggart JC, Li G-W, 2018. Production of Protein-Complex Components Is Stoichiometric and Lacks General Feedback Regulation in Eukaryotes. Cell Syst 7, 580–589.e4. [PubMed: 30553725]

Tepper N, Noor E, Amador-Noguez D, Haraldsdóttir HS, Milo R, Rabinowitz J, Liebermeister W, Shlomi T, 2013. Steady-state metabolite concentrations reflect a balance between maximizing enzyme efficiency and minimizing total metabolite load. PLoS One 8, e75370. [PubMed: 24086517]

Thiele I, Jamshidi N, Fleming RMT, Palsson BØ, 2009. Genome-scale reconstruction of Escherichia coli's transcriptional and translational machinery: a knowledge base, its mathematical formulation, and its functional characterization. PLoS Comput. Biol 5, e1000312. [PubMed: 19282977]

Thiele I, Palsson BØ, 2010. A protocol for generating a high-quality genome-scale metabolic reconstruction. Nat. Protoc 5, 93–121. [PubMed: 20057383]

Thiele I, Sahoo S, Heinken A, Hertel J, Heirendt L, Aurich MK, Fleming RM, 2020. Personalized whole-body models integrate metabolism, physiology, and the gut microbiome. Mol. Syst. Biol 16, e8982. [PubMed: 32463598]

Thornburg ZR, Bianchi DM, Brier TA, Gilbert BR, Earnest TM, Melo MCR, Safronova N, Sáenz JP, Cook AT, Wise KS, Hutchison CA 3rd, Smith HO, Glass JI, Luthey-Schulten Z, 2022. Fundamental behaviors emerge from simulations of a living minimal cell. Cell 185, 345–360.e28. [PubMed: 35063075]

Tian L, Chen F, Macosko EZ, 2023. The expanding vistas of spatial transcriptomics. Nat. Biotechnol 41, 773–782. [PubMed: 36192637]

Tillin NA, Pain MTG, Folland JP, 2012. Contraction type influences the human ability to use the available torque capacity of skeletal muscle during explosive efforts. Proc. Biol. Sci 279, 2106–2115. [PubMed: 22258636]

Toda S, Frankel NW, Lim WA, 2019. Engineering cell-cell communication networks: programming multicellular behaviors. Curr. Opin. Chem. Biol 52, 31–38. [PubMed: 31150899]

Torrent M, Chalancon G, de Groot NS, Wuster A, Madan Babu M, 2018. Cells alter their tRNA abundance to selectively regulate protein synthesis during stress conditions. Sci. Signal 11. 10.1126/scisignal.aat6409

Tuller T, Carmi A, Vestsigian K, Navon S, Dorfan Y, Zaborske J, Pan T, Dahan O, Furman I, Pilpel Y, 2010. An evolutionarily conserved mechanism for controlling the efficiency of protein translation. Cell 141, 344–354. [PubMed: 20403328]

Umberger BR, Gerritsen KGM, Martin PE, 2003. A model of human muscle energy expenditure. Comput. Methods Biomech. Biomed. Engin 6, 99–111. [PubMed: 12745424]

Urlacher SS, Ellison PT, Sugiyama LS, Pontzer H, Eick G, Liebert MA, Cepon-Robins TJ, Gildner TE, Snodgrass JJ, 2018. Tradeoffs between immune function and childhood growth among Amazonian forager-horticulturalists. Proc. Natl. Acad. Sci. U. S. A 115, E3914–E3921. [PubMed: 29632170]

van Albada SB, ten Wolde PR, 2007. Enzyme localization can drastically affect signal amplification in signal transduction pathways. PLoS Comput. Biol 3, 1925–1934. [PubMed: 17937496]

Vandenbogaerde TJ, Hopkins WG, 2011. Effects of acute carbohydrate supplementation on endurance performance: a meta-analysis. Sports Med. 41, 773–792. [PubMed: 21846165]

van Helvert S, Storm C, Friedl P, 2018. Mechanoreciprocity in cell migration. Nat. Cell Biol 20, 8–20. [PubMed: 29269951]

Vannini N, Girotra M, Naveiras O, Nikitin G, Campos V, Giger S, Roch A, Auwerx J, Lutolf MP, 2016. Specification of haematopoietic stem cell fate via modulation of mitochondrial activity. Nat. Commun 7, 13125. [PubMed: 27731316]

van Noordwijk AJ, de Jong G, 1986. Acquisition and Allocation of Resources: Their Influence on Variation in Life History Tactics. The American Naturalist 128, 137–142.

Veldhorst MAB, Westerterp-Plantenga MS, Westerterp KR, 2009. Gluconeogenesis and energy expenditure after a high-protein, carbohydrate-free diet. Am. J. Clin. Nutr 90, 519–526. [PubMed: 19640952]

Vogel C, Marcotte EM, 2012. Insights into the regulation of protein abundance from proteomic and transcriptomic analyses. Nat. Rev. Genet 13, 227–232. [PubMed: 22411467]

Wagner A, Regev A, Yosef N, 2016. Revealing the vectors of cellular identity with single-cell genomics. Nat. Biotechnol 34, 1145–1160. [PubMed: 27824854]

Wagner A, Wang C, Fessler J, DeTomaso D, Avila-Pacheco J, Kaminski J, Zaghouani S, Christian E, Thakore P, Schellhaass B, Akama-Garren E, Pierce K, Singh V, Ron-Harel N, Douglas VP, Bod L, Schnell A, Puleston D, Sobel RA, Haigis M, Pearce EL, Soleimani M, Clish C, Regev A, Kuchroo VK, Yosef N, 2021. Metabolic modeling of single Th17 cells reveals regulators of autoimmunity. Cell 184, 4168–4185.e21. [PubMed: 34216539]

Wang D, Eraslan B, Wieland T, Hallström B, Hopf T, Zolg DP, Zecha J, Asplund A, Li L-H, Meng C, Frejno M, Schmidt T, Schnatbaum K, Wilhelm M, Ponten F, Uhlen M, Gagneur J, Hahne H, Kuster B, 2019. A deep proteome and transcriptome abundance atlas of 29 healthy human tissues. Mol. Syst. Biol 15, e8503. [PubMed: 30777892]

Wang J, Delfarah A, Gelbach PE, Fong E, Macklin P, Mumenthaler SM, Graham NA, Finley SD, 2022. Elucidating tumor-stromal metabolic crosstalk in colorectal cancer through integration of constraint-based models and LC-MS metabolomics. Metab. Eng 69, 175–187. [PubMed: 34838998]

Wang J, Liu R, Hawkins M, Barzilai N, Rossetti L, 1998. A nutrient-sensing pathway regulates leptin gene expression in muscle and fat. Nature 393, 684–688. [PubMed: 9641678]

Wang T-L, Kuznets-Speck B, Broderick J, Hinczewski M, 2022. The price of a bit: energetic costs and the evolution of cellular signaling. bioRxiv. 10.1101/2020.10.06.327700

Wang Z, Ying Z, Bosy-Westphal A, Zhang J, Schautz B, Later W, Heymsfield SB, Müller MJ, 2010. Specific metabolic rates of major organs and tissues across adulthood: evaluation by mechanistic model of resting energy expenditure. Am. J. Clin. Nutr 92, 1369–1377. [PubMed: 20962155]

Way JC, Collins JJ, Keasling JD, Silver PA, 2014. Integrating biological redesign: where synthetic biology came from and where it needs to go. Cell 157, 151–161. [PubMed: 24679533]

Webster CC, Noakes TD, Chacko SK, Swart J, Kohn TA, Smith JAH, 2016. Gluconeogenesis during endurance exercise in cyclists habituated to a long-term low carbohydrate high-fat diet. J. Physiol 594, 4389–4405. [PubMed: 26918583]

Wegrzyn JL, Bark SJ, Funkelstein L, Mosier C, Yap A, Kazemi-Esfarjani P, La Spada AR, Sigurdson C, O'Connor DT, Hook V, 2010. Proteomics of dense core secretory vesicles reveal distinct
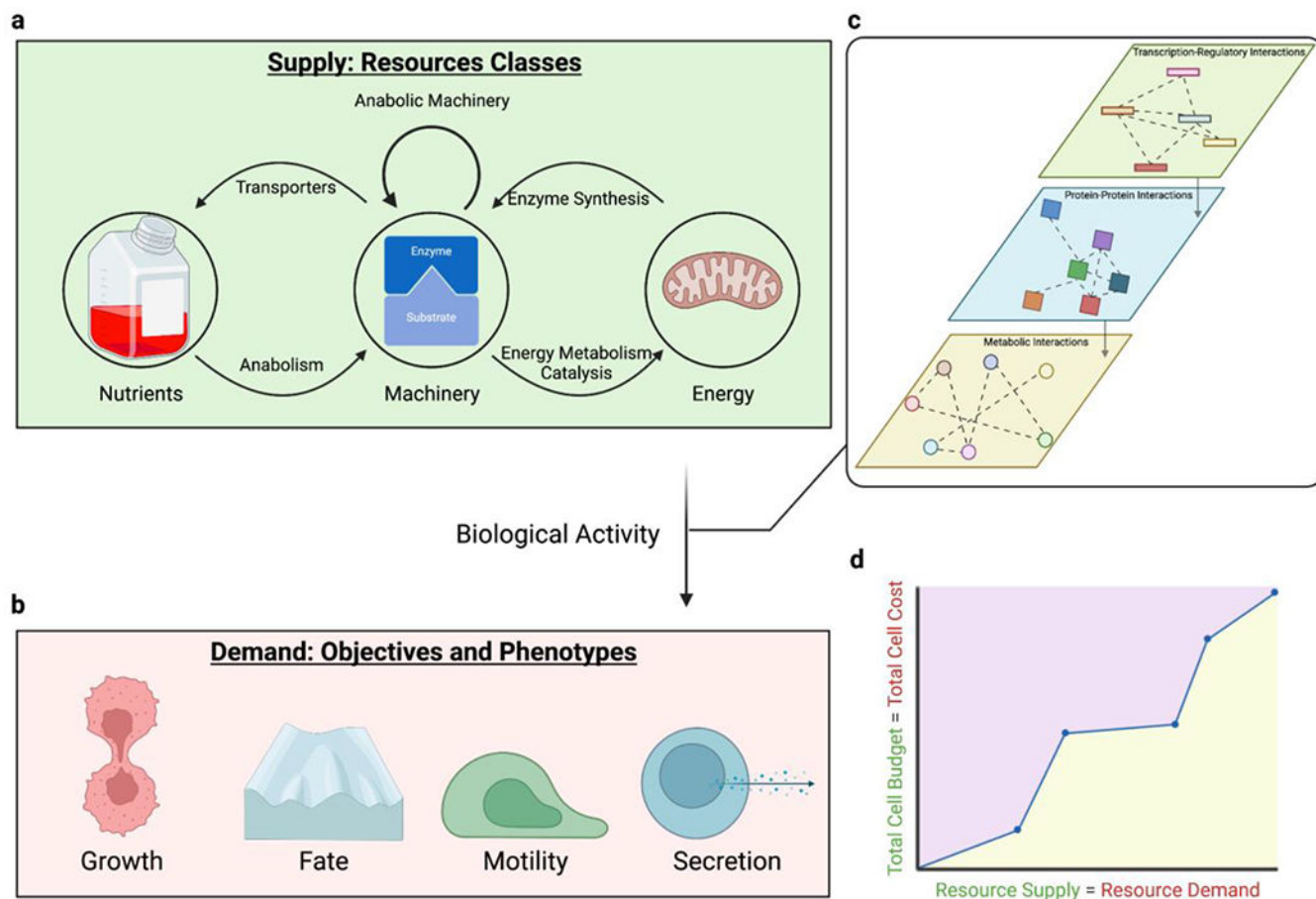
protein categories for secretion of neuroeffectors for cell-cell communication. J. Proteome Res 9, 5002–5024. [PubMed: 20695487]

Wilhelm M, Schlegl J, Hahne H, Gholami AM, Lieberenz M, Savitski MM, Ziegler E, Butzmann L, Gessulat S, Marx H, Mathieson T, Lemeer S, Schnatbaum K, Reimer U, Wenschuh H, Mollenhauer M, Slotta-Huspenina J, Boese J-H, Bantscheff M, Gerstmair A, Faerber F, Kuster B, 2014. Mass-spectrometry-based draft of the human proteome. Nature 509, 582–587. [PubMed: 24870543]

Wroble KA, Trott MN, Schweitzer GG, Rahman RS, Kelly PV, Weiss EP, 2019. Lowcarbohydrate, ketogenic diet impairs anaerobic exercise performance in exercise-trained women and men: a randomized-sequence crossover trial. J. Sports Med. Phys. Fitness 59, 600–607. [PubMed: 29619799]

Wu A, Ying Z, Gomez-Pinilla F, 2008. Docosahexaenoic acid dietary supplementation enhances the effects of exercise on synaptic plasticity and cognition. Neuroscience 155, 751–759. [PubMed: 18620024]

Xia J, Sánchez BJ, Chen Y, Campbell K, Kasvandik S, Nielsen J, 2022. Proteome allocations change linearly with the specific growth rate of Saccharomyces cerevisiae under glucose limitation. Nat. Commun 13, 2819. [PubMed: 35595797]

Yang L, Mih N, Anand A, Park JH, Tan J, Yurkovich JT, Monk JM, Lloyd CJ, Sandberg TE, Seo SW, Kim D, Sastry AV, Phaneuf P, Gao Y, Broddrick JT, Chen K, Heckmann D, Szubin R, Hefner Y, Feist AM, Palsson BO, 2019. Cellular responses to reactive oxygen species are predicted from molecular mechanisms. Proc. Natl. Acad. Sci. U. S. A 116, 14368–14373. [PubMed: 31270234]

Yang L, Yurkovich JT, Lloyd CJ, Ebrahim A, Saunders MA, Palsson BO, 2016. Principles of proteome allocation are revealed using proteomic data and genome-scale models. Sci. Rep 6, 36734. [PubMed: 27857205]

Yang X, Heinemann M, Howard J, Huber G, Iyer-Biswas S, Le Treut G, Lynch M, Montooth KL, Needleman DJ, Pigolotti S, Rodenfels J, Ronceray P, Shankar S, Tavassoly I, Thutupalli S, Titov DV, Wang J, Foster PJ, 2021. Physical bioenergetics: Energy fluxes, budgets, and constraints in cells. Proc. Natl. Acad. Sci. U. S. A 118. 10.1073/pnas.2026786118

Yan Y, Zhang L, Zhu T, Deng S, Ma B, Lv H, Shan X, Cheng H, Jiang K, Zhang T, Meng B, Mei B, Li W-G, Li F, 2021. Reconsolidation of a post-ingestive nutrient memory requires mTOR in the central amygdala. Mol. Psychiatry 26, 2820–2836. [PubMed: 32873898]

Yeo GHT, Saksena SD, Gifford DK, 2021. Generative modeling of single-cell time series with PRESCIENT enables prediction of cell trajectories with interventions. Nat. Commun 12, 3222. [PubMed: 34050150]

Yewdell JW, 2001. Not such a dismal science: the economics of protein synthesis, folding, degradation and antigen processing. Trends Cell Biol. 11, 294–297. [PubMed: 11413040]

Yizhak K, Le Dévédec SE, Rogkoti VM, Baenke F, de Boer VC, Frezza C, Schulze A, van de Water B, Ruppin E, 2014. A computational study of the Warburg effect identifies metabolic targets inhibiting cancer migration. Mol. Syst. Biol 10, 744. [PubMed: 25086087]

Youk H, Lim WA, 2014. Secreting and sensing the same molecule allows cells to achieve versatile social behaviors. Science 343, 1242782. [PubMed: 24503857]

Zanotelli MR, Rahman-Zaman A, VanderBurgh JA, Taufalele PV, Jain A, Erickson D, Bordeleau F, Reinhart-King CA, 2019. Energetic costs regulated by cell mechanics and confinement are predictive of migration path during decision-making. Nat. Commun 10, 4185. [PubMed: 31519914]

Zhang J, Goliwas KF, Wang W, Taufalele PV, Bordeleau F, Reinhart-King CA, 2019. Energetic regulation of coordinated leader-follower dynamics during collective invasion of breast cancer cells. Proc. Natl. Acad. Sci. U. S. A 116, 7867–7872. [PubMed: 30923113]

Zhang X-P, Cheng Z, Liu F, Wang W, 2007. Linking fast and slow positive feedback loops creates an optimal bistable switch in cell signaling. Phys. Rev. E Stat. Nonlin. Soft Matter Phys 76, 031924. [PubMed: 17930288]

Zheng R, Zhang Y, Tsuji T, Gao X, Wagner A, Yosef N, Chen H, Zhang L, Tseng Y-H, Chen K, 2022. MEBOCOST: Metabolite-mediated Cell Communication Modeling by Single Cell Transcriptome. bioRxiv. 10.1101/2022.05.30.494067
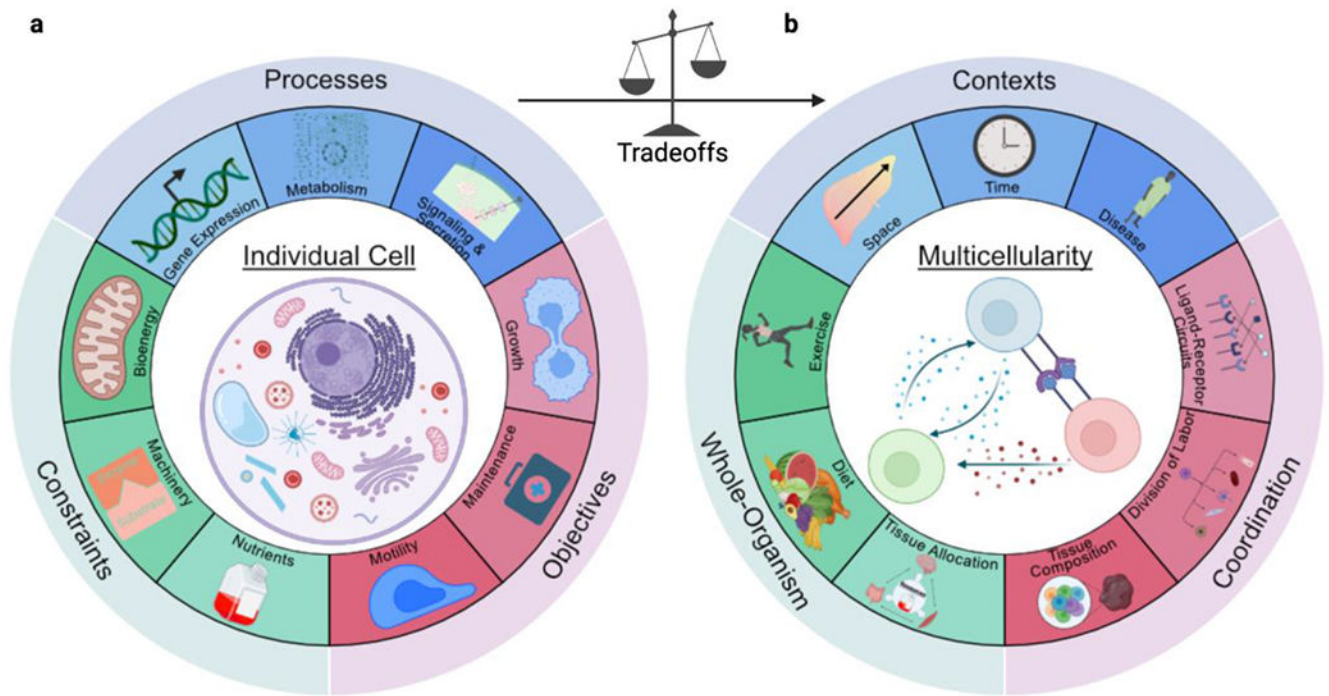
Zhou X, Franklin RA, Adler M, Carter TS, Condiff E, Adams TS, Pope SD, Philip NH, Meizlish ML, Kaminski N, Medzhitov R, 2022. Microenvironmental Sensing by Fibroblasts Controls Macrophage Population Size. bioRxiv. 10.1101/2022.01.18.476683

Zhou X, Franklin RA, Adler M, Jacox JB, Bailis W, Shyer JA, Flavell RA, Mayo A, Alon U, Medzhitov R, 2018. Circuit Design Features of a Stable Two-Cell System. Cell 172, 744–757.e17. [PubMed: 29398113]

Zhu J, Thompson CB, 2019. Metabolic regulation of cell growth and proliferation. Nat. Rev. Mol. Cell Biol 20, 436–450. [PubMed: 30976106]

Zisman A, Peroni OD, Abel ED, Michael MD, Mauvais-Jarvis F, Lowell BB, Wojtaszewski JF, Hirshman MF, Virkamaki A, Goodyear LJ, Kahn CR, Kahn BB, 2000. Targeted disruption of the glucose transporter 4 selectively in muscle causes insulin resistance and glucose intolerance. Nat. Med 6, 924–928. [PubMed: 10932232]

Zwick RK, Kasparek P, Palikuqi B, Viragova S, Weichselbaum L, McGinnis CS, McKinley KL, Rathnayake A, Vaka D, Nguyen V, Trentesaux C, Reyes E, Gupta AR, Gartner ZJ, Locksley RM, Gardner JM, Itzkovitz S, Boffelli D, Klein OD, 2023. Epithelial zonation along the mouse and human small intestine defines five discrete metabolic domains. bioRxiv. 10.1101/2023.09.20.558726
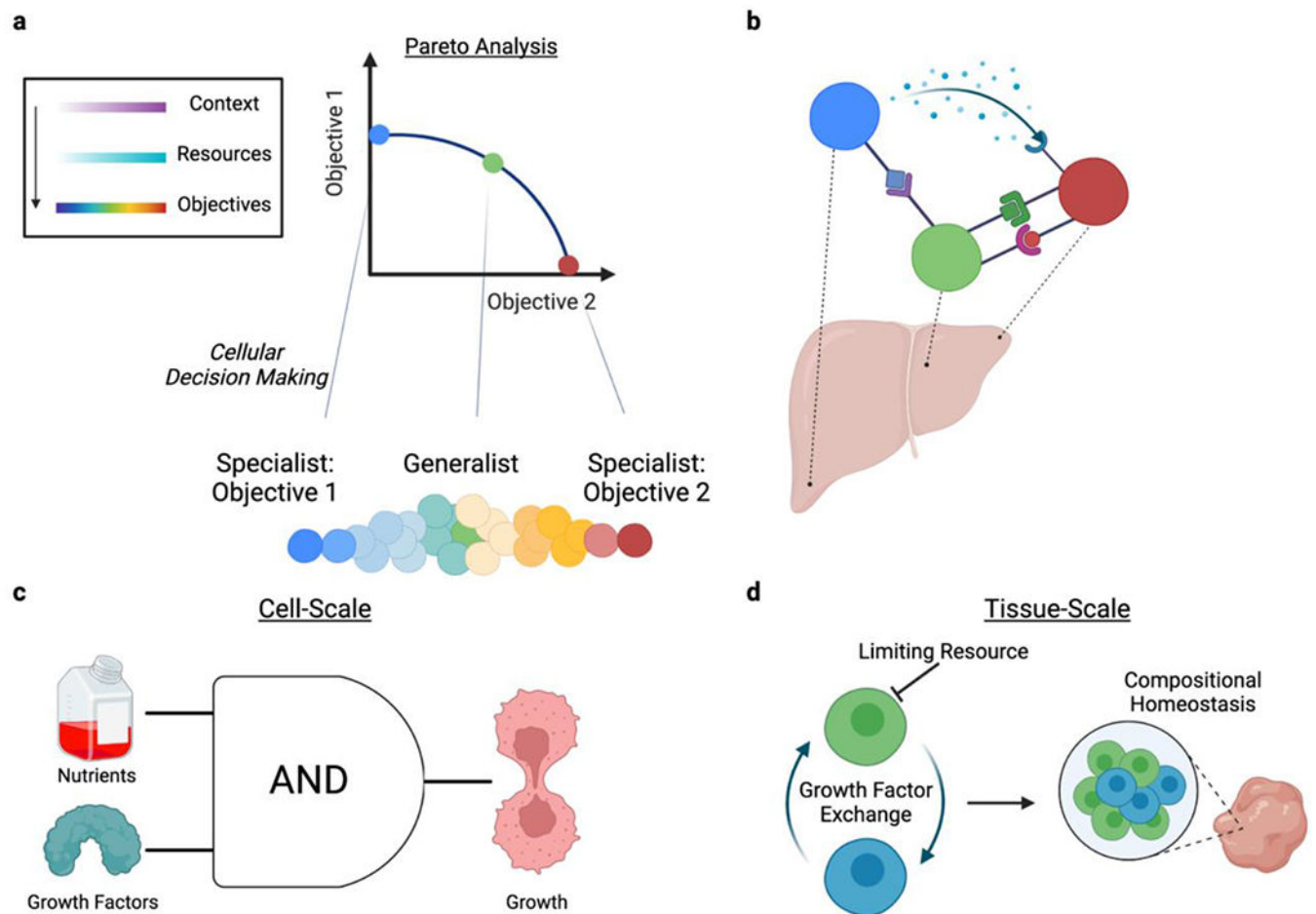
Fig. 1: Generation and use of a balanced cellular resource budget.

a | The total cellular budget is determined by the supply of nutrients, machinery, and energy resources. There is extensive crosstalk between these three resource classes, each depending on the others to generate its supply. **b** | Once the budget is generated, it is used to conduct diverse biological activities that contribute to the cell objectives and result in observed phenotypes. The amount of resources used to meet these functional demands represents the cost of executing biological function. **c** | Intracellular processes (e.g., transcriptional activity, protein activity, and metabolism) interact to drive the activities which connect resources to objectives. **d** | In an efficiently allocated system, the cellular budget generated will equal the resource demanded (blue line). Generating an excess budget (purple shaded region) results in higher resource costs than necessary, whereas not generating enough budget (yellow shaded region) means that not all the demands can be met. Overall, the total cellular budget constrains biological activity, and in turn, observable phenotypes.

Fig. 2: Key factors determining mammalian resource allocation strategies.

a | The individual cell must account for its resource constraints when trying to optimize various objectives. Mechanistically, constraints are tied to objectives by intracellular processes that determine the global activities of the cell. **b** | Constraints lead to trade-offs between multiple objectives, resulting in the evolution of multicellular organisms for more efficient allocation strategies. Coordination between cells enables specialization, communication, and tissue-scale steady-states that function robustly across multiple contexts. These concepts extend to the whole-organism scale, demonstrating that resource allocation can provide broad insights into biological function.

Fig. 3: Extending resource allocation to multicellularity.

a | The cellular context determines the available resources and cell objectives. Resource constraints limit the number of objectives a cell can achieve and the efficiency by which it performs each objective; thus, individual cells that face multiple objectives must manage trade-offs. Pareto analysis provides a quantitative view of trade-offs wherein competing objectives are plotted. Along the Pareto front, a cell cannot improve its performance in one objective without worsening its performance in another. Within multicellular systems, this leads to cell specialization for specific objectives along a context gradient. **b** | In a tissue, cell specialization can occur across, for example, spatial context gradients (see ref(Adler et al., 2019)). With division of labor, each cell performs a particular set of tasks, but the higher-order biological function results from the synergistic effects of the population. Tissue-level behavior is achieved by coordination between cells via mechanisms such as cell-cell communication, in which distinct signals are sent in a cell-type- and context-dependent manner. **c** | Individual cells receive communicatory signals such as growth-factors that, in combination with local nutrient availability, regulate growth phenotypes. The "AND" logic-gate highlights that mammalian cells tend to couple sensing of nutrient availability with communicatory protein signals such as growth factors when interpreting extracellular cues, such that neither factor alone determines the cell response. **d** | In a tissue, multi-

cell circuits involving growth factor exchange, in combination with resource constraints, maintain steady-state proportions of cell types (see (Zhou et al., 2018)).

Table 1

Methods to Probe Resource Allocation.

Molecular Process	Approach	Method	Biological Finding	Organism	Reference
Signal Transduction	Mass Action ODEs	Tests each of five possible objectives as a function of signaling resources estimated by mass action models that incorporate machinery abundance and activity.	Phosphorelay pathways tend to prioritize information transfer as their primary objective.	*B. subtilis, S. cerevisiae*	(Alves et al., 2021)
Signal Transduction	Mass Action ODEs	Estimates signal sensing error as a function of 1) receptor abundance, binding, and integration time, 2) downstream signaling machinery abundance and binding, and 3) ATP turnover. Further summarizes this function as a set of parameters that conceptually represent the resource classes of interest.	Goldbeter–Koshland push–pull network sensing systems maximize sensing precision. Each of receptors, signaling machinery, and energy resources are equally limiting on sensing precision to achieve efficient resource allocation.	*E. coli* (network type studied is ubiquitous across prokaryotes and eukaryotes)	(Govern and Ten Wolde, 2014)
Signal Transduction	Genome-Scale Modeling	Extreme Pathway Analysis uses convex analysis to identify a minimal set of "extreme pathways". Conceptually, these are pathways whose activities, according to the network stoichiometry and model constraints, each represent a functional state of the network.	Proof-of-concept application of the genome-scale metabolic modeling framework to assess signaling pathway activity, crosstalk, and redundancy in the context of a network with distinct combinations of ligand inputs and transcription factor activity outputs.	Prototypic example	(Papin and Palsson, 2004a)
Signal Transduction	Genome-Scale Modeling	Mathematically, these pathways are the edges of the steady-state convex solution space, with distributions that are independent and whose non-negative linear combinations represent all possible solutions to the objective.	Demonstrated certain properties of the human B-cell JAK-STAT signaling network, such as minimal crosstalk between pathways and high redundancy in STAT1-STAT3 heterodimerization	*H. sapiens*	(Papin and Palsson, 2004b)
Signal Transduction	Genome-Scale Modeling	Combines three molecular processes (signaling, transcriptional regulatory networks, and metabolism) which are connected by their respective inputs/outputs as well as metabolic intermediates. Developes integrated dynamic FBA (idFBA) to simulate reaction fluxes and resolve issues that arise due to mixed time-scales between reactions. idFBA treats reactions on fast time-scales as quasi steady-state, applying FBA at discrete time points; it treats slow reactions as instantaneous (steady-state) after some time-delay, incorporating it into the stoichiometric matrix.	Proof-of-concept integration of metabolism with signaling and transcription regulatory networks within the genome-scale modeling framework.	*S. cerevisiae*	(Lee et al., 2008)
Gene Expression	Mass Action ODEs	Estimate gene synthesis rates using ordinary differential equations modeling production (transcription/translation) and degradation of mRNA and protein and inputting experimentally measured	Translation rates have a large overall contribution to protein abundance. Combinations of mRNA and protein turnover rates (high vs low) are enriched for specific cell processes	*M. musculus*	(Schwanhäusser et al., 2011)

Molecular Process	Approach	Method	Biological Finding	Organism	Reference
			largely associated with metabolism and cell maintenance.		
Gene Expression	Mass Action ODEs	turnover rates (using metabolic pulse labeling) and abundance.	The extent each of mRNA abundance, translation rates, and protein degradation rates contributes to protein abundance changes with context (e.g., steady-state, LPS stimulation).	*M. musculus*	(Jovanovic et al., 2015)
Gene Expression	Mass Action ODEs	Use gene synthesis ODEs to identify a simplified, two-dimensional Crick space for the investigation of the observed range of gene synthesis rates. Used these synthesis rates to derive meaningful quantitative relationships between transcription and translation rates at the boundary of the Crick space, expressions for the fitness cost of transcription, and the relationship between fitness costs and stochasticity within the Crick space.	There is a lack of genes with high transcription rates and low translation rates due to a precision (stochasticity) - economy (resource costs) tradeoff in gene expression.	*E. coli, S. cerevisiae, M. musculus, H. sapiens*	(Hausser et al., 2019)
Gene Expression	Coarse-Graining/ Phenomenological Modeling	Builds on gene synthesis ODEs by further accounting for resource loading of RNA polymerases in transcription and ribosomes in translation rather than assuming constant synthesis rates. Resource loading is accounted for by modeling the total available machinery as well as fraction of said machinery that should be allocated to a particular gene. The model can be adjusted to have the machinery or substrates be limiting. Coarse-graining is in relation to modeling synthesis as a function of the mass fraction allocated to a gene rather than gene-specific features.	By dynamically adjusting synthesis rates through accounting of resource loading, the model reproduces observations that under machinery-limiting conditions, protein and mRNA numbers grow proportionally to cell volume, maintaining concentration homeostasis under exponential cell growth	generalizable	(Lin and Amir, 2018)
Gene Expression	Coarse-Graining/ Phenomenological Modeling	Measures growth rate and biomass composition across nutrient- and translational machinery- limiting conditions, fit parameters to the linear relationships between these variables, and used these variables to quantitatively reveal context-dependent resource allocation across coarse-grained proteome fractions (e. g., ribosomal fraction).	Under translation-limiting conditions, cells will re-allocate resources away from other proteome sectors and to ribosomal proteins in order to better support bioamss production.	*E. coli*	(Scott et al., 2010)
Gene Expression	Coarse-Graining/ Phenomenological Modeling	Grouped proteins into coarse-grained sectors by clustering proteomics measured across differing resource-limiting conditions (anabolic, catabolic, and translational). Treated these sectors as "coarse-grained enzymes" and modeled how fluxes move through these	In general, the fraction of proteome sectors associated with a specific limitation increases with increasing limitation, indicating proteome re-allocation to the machinery enabling the processes	*E. coli*	(Hui et al., 2015)

Molecular Process	Approach	Method	Biological Finding	Organism	Reference
		enzymes to understand how they change with respect to each other (proteome re-allocation) as a function of growth rate in a context-dependent manner.	effected by the limiting condition.		
Metabolism	Genome-Scale Modeling	Flux balance analysis (FBA) estimates optimal steady-state metabolomic fluxes from stoichiometric representations of metabolic networks and an objective function (one of the encoded reactions) using linear programming. The referenced reviews provides an overview of metabolic models (M-Models), FBA, and other methods to analyze M-models. Parsimonious FBA (pFBA) is a two-step linear programming approach.	*Review Paper: Genome-scale modeling is a mathematical formulation of resource allocation that can also reveal mechanistic insights. Encoded pathway activity is constrained by nutrient, energy, and machinery resource availability and fluxomics is predicted on the basis of cells diverting those resources to optimize for a specified objective or multiple objectives.	prokaryotes, eukaryotes	(Lewis et al., 2012; Orth et al., 2010)
Protein-Constrained Metabolism	Genome-Scale Modeling	The first step uses FBA to optimize the primary objective function. The second step sets a secondary objective of minimizing the sum of reaction fluxes, holding the optimal level of the primary objective constant. Conceptually, this secondary objective represents minimizing the total resource costs of metabolic activity while still optimizing the first objective.	GEM simulations are consistent with experimental data when predicting which machinery the cell uses to achieve growth.	*E. coli*	(Lewis et al., 2010a)
Protein-Constrained Metabolism	Genome-Scale Modeling	Constrained allocation flux balance analysis (CAFBA) accounts for machinery costs by constraining coarse-grained proteome sectors each metabolic reaction is associated with.	Proof-of-concept recapitulation of various findings, including the linear relationships between growth rate and ribosomal abundance as well as demonstration of overflow metabolism at high growth rates.	*E. coli*	(Mori et al., 2016)
Protein-Constrained Metabolism	Genome-Scale Modeling	Enzyme cost minimization (ECM) implements an approach to estimate the enzyme abundance required to sustain a given reaction flux based on the optimality principle that machinery costs are minimized. The enzyme cost is proportional to the net flux generated per unit enzyme. To consider in vivo condition-specific effects, the cost function is not only dependent on the catalytic rate constant, but also on factors that may prevent the enzyme from operating at maximal kinetic efficiency (which may be estimated from metabolite levels). This includes substrate concentrations that do not saturate the enzyme and reaction thermodynamics (i.e., reverse fluxes) which constrain the feasible space of metabolite concentrations from the equilibrium binding constants.	Proof-of-concept demonstration that machinery cost minimization can accurately predict enzyme abundance associated with central carbon metabolism. Decomposing the factors that prevent enzymes from operating at maximal capacity in vivo into saturation, reversibility, and regulatory-based parameters enables determining which factors contribute to the accuracy of the prediction.	*E. coli*	(Noor et al., 2016)

Molecular Process	Approach	Method	Biological Finding	Organism	Reference
		Finally, the function is scaled by a "burden" parameter that accounts for maintenance costs (e.g., molecular mass, misfolding, post-translational modifications, etc.).			
Protein-Constrained Metabolism	Genome-Scale Modeling	Max-min Driving Force (MDF) calculates the thermodynamic efficacy, or the ratio between the net flux and the total flux, of a given reaction as a function of pH, metabolite concentration, and the Gibbs free energy change. This metric is related to the kinetics of a reaction via the mass-action ratio and conceptually serves as a proxy for protein cost (i.e., a lower driving force requires a higher abundance of enzyme or higher catalytic rate per unit of forward flux). Using the optimality principle of enzyme cost minimization, MDF then uses linear programming to solve for the objective of maximizing the driving force throughout the metabolic network.	Analyzes central carbon metabolism to identify MDF bottlenecks and how pathways have evolved to resolve these bottlenecks via enzyme abundances, enzyme activity, and intermediate metabolite concentrations. Further uses MDF as an explanation for organisms choosing yield-inefficient pathways.	*E. coli*	(Noor et al., 2014)
Protein-Constrained Metabolism	Genome-Scale Modeling	GECKO directly constrains reaction fluxes with machinery resources by incorporating a simple enzyme production reaction (bounded by proteomics abundance) for catalysis of the respective metabolic reaction (coupled by a coefficient proportional to catalytic rate of enzyme), limiting reaction fluxes to a maximum according to first-principles	Ability to distinguish between nutrient- and machinery-limiting conditions and a reduced solution space (lower flux variability). Proof-of-concept demonstration of various findings with improved performance/ accuracy over tradiation M-models, including the Crabtree effect and physiologically accurate growth rates.	*S. cerevisiae, H. sapiens, multiple other organisms*	(Domenzain et al., 2022; Sánchez et al., 2017)
Gene Expression	Genome-Scale Modeling	Reconstructed an expression network in an analgous manner to M-Model networks. Synthesis reactions are the analogue of metabolic reactions, macromolecules that are being synthesized are the analogue of metabolites, and gene expression machinery (e.g., RNA polymerase and ribosomes) are the analogue of metabolic enzymes, resulting in a genome-scale stoichiometric matrix of gene expression (*E*-matrix).	Proof-of-concept recapitulation of various findings including the relationship between ribosome abundance and growth rate and rRNA operon redundancy based on nutrient uptake rates.	*E. coli*	(Thiele et al., 2009)
Gene Expression & Metabolism	Genome-Scale Modeling	ME-Models combine gene expression and metabolism into a coherent genome-scale model by explicitly encoding the gene expression reactions for each enzyme, then deriving "coupling constraints", or first principle quantitative relationships that link the enzyme products of expression reactions with the metabolic reactions they catalyze.	In silico differentially expressed genes across different carbon sources yields hypothesis generation for the de-orphaning of L-arabinose transport.	*T. maritima*	(Lerman et al., 2012)

Molecular Process	Approach	Method	Biological Finding	Organism	Reference
Gene Expression & Metabolism	Genome-Scale Modeling	Because coupling constraints are a function of growth, non-linear programs must be applied to find an optimal solution. Coupling gene expression with machinery allows for an explicit accounting of the machinery costs of metabolic activity and allows for variable RNA and protein content within the biomass composition.	*E. coli* utilize low-yield carbon metabolism to divert machinery resources to the catalysis of enzymes not operating at their maximal capacity.	*E. coli*	(O'Brien et al., 2013)
Gene Expression & Metabolism	Genome-Scale Modeling	Review of extensions and further applications of ME-Models.	*Review Paper	prokaryotes, human red blood cells	(Dahal et al., 2021)
Gene Expression & Metabolism	Genome-Scale Modeling	ME-Model framework extended to eukaryotes with additional considerations of subcompartments (e.g., transport and compartment-specific proteome constraints), proteome sector constraints, and molecular crowding.	Proof-of-concept results recapitulating various findings or experimental data; a result specific to ME-Models is the ability to assess the effect of excess or unecessary protein production on growth rate.	*S. cerevisiae*	(Elsemman et al., 2022)
Gene Expression & Metabolism	Genome-Scale Modeling	Resource Balance Analysis (RBA) connects gene expression to metabolism at the genome-scale using similar approaches as the ME-Model framework while also accounting for spatial constraints.	*Review Paper	prokaryote, theory in eukaryotes	(Goelzer and Fromion, 2017)
Metabolism & Secretory Pathway	Genome-Scale Modeling	Combines protein secretion and metabolism into a coherent genome-scale model by representing the secretory pathway in an analogous manner to metabolic networks inl M-Models. Secreted proteins are the analogue of metabolites and secretory machinery are the analogue of metabolic enzymes.	There is a negative correlation between secreted protein abundance and the energetic cost of producing that protein, and there exists tradeoffs between cell growth and protein secretion.	*C. griseus, M. musculus, H. sapiens*	(Gutierrez et al., 2020)
Secretory Pathway	Network Propagation	Applies a random-walk network propagation on a protein-protein interaction network between secretory pathway machinery and secreted proteins. Converts resultant transition probabilities to a "machinery support score" that indicates the extent to which machinery abundance aligns with production of a given secreted protein according to the network topology.	Changes to amyloid precursor protein (APP) abundance in Alzheimer's Disease, which cannot be explained at the transcriptional level, can be explained by how well APP is supported by secretory machinery abundance.	*H. sapiens*	(Kuo et al., 2021)
All Intracellular Systems	Whole-Cell Modeling	Creates a separate module for each of 28 intracellular systems and applies a relevant modeling approach to each module. Next, integrates these modules into a single, coherent model by linking their common inputs and outputs, treating each module as independent at short time-scales, and dividing	The duration of replication initiation has high variability due to stochastic DnaA expression, but this variability is mitigated across the entire cell cycle due to decreased dNTP availability for polymerization over the course of the cell cycle.	*M. genitalium*	(Karr et al., 2012)

Molecular Process	Approach	Method	Biological Finding	Organism	Reference
		the shared resources across the modules at each time point.			
All Intracellular Systems	Whole-Cell Modeling	Accounts for 3D cell structure and comprehensively incorporates kinetic parameters across cell subsystems.	The total energy budget in the minimal cell at each time point is estimated to be similar to the total energy cost at that time point, indicating efficient energy resource allocation.	Synthetic minimal cell (JCVI-syn3A)	(Thornburg et al., 2022)
Multicellularity: Division of Labor	Tradeoffs/Pareto Analysis	Identified three relevant objective functions by aligning M-model predicted fluxomics with experimentally measured fluxomics. Computes the Pareto surface generated by the three objectives.	Experimentally measured fluxomics are near but not exactly on the Pareto front in order to minimizing the cost of switching between objectives.	*E. coli*	(Schuetz et al., 2012)
Multicellularity: Division of Labor	Tradeoffs/Pareto Analysis	Pareto task inference (ParTI) estimates a low-dimensional polytope (n vertices fit using principal convex hull analysis) that encompasses omics datasets and represents Pareto optimal fronts in gene expression space. Such polytopes can be found in systems that perform multiple objectives and are Pareto optimal because, for any point outside the polytope, there exists a point inside it that can perform equally well or better at all tasks. The polytopes' vertices represent "archetypes" or gene expression profiles optimized for a particular objective. As samples move in gene expression space from one vertex to another, they undergo tradeoffs in their ability to perform each objective.	Generally, identified the biological objective of each archetype using enrichment analysis of the gene expression profiles of cells that clustered at the polytope vertices.	*M. musculus, H. sapiens*	(Hart et al., 2015)
Multicellularity: Division of Labor	Tradeoffs/Pareto Analysis		Generally, the continuum of gene expression profiles (in contrast to distinct clusters) found in some samples from single-cell sequencing technologies may be explained by varying extents of cell specialization, or the distance of a cell from the polytope vertex in gene expression space, within a Pareto optimal front. Less specialized cells perform multiple tasks whereas more specialized cells are optimized for a specific task.	*M. musculus, H. sapiens*	(Korem et al., 2015)
Multicellularity: Division of Labor	Tradeoffs/Pareto Analysis	Uses ParTI to further estimate tissue-level performance of each objective as well as overall tissue performance as a function of single-cell gene expression profiles. To quantify tissue-level function, individual cells' objective performance, based on their distance from polytope vertices, is aggregated across all cells and objectives.	By characterizing tissue-level performance as a mathematical function in gene expression space, this study is able to 1) calculate the optimal gene expression profile of individual cells, 2) characterize the expected behavior of cells to skew towards specialization and 3) incorporate spatial context gradients to accurately predict a continuum of expression profiles. This continuum is representative of a tissue-scale "division of labor" strategy in which individual cells tune their gene expression to perform one or more objectives based on their context, with the population-level outcome being optimized performance across all objectives.	*M. musculus*	(Adler et al., 2019)

Molecular Process	Approach	Method	Biological Finding	Organism	Reference
Multicellularity: Cell Coordination	Genome-Scale Modeling	First, creates a context-specific M-model of brain tissue. Next, cell type specific M-models are built based on gene expression profiles. The models are also curated for consistency with known cell type specific metabolic functions. Finally, based on the expression of metabolite transporters, cell type specific models are joined by metabolites that can be transferred between models.	Model simulations focus on metabolic crosstalk between astrocytes and different neuron cell types and were used for three analyses to identify key genes and reactions, enriched metabolic pathways, and mechanisms of perturbation (e.g., drug treatment) associated with cell-type and context-specific responses of metabolism.	*H. sapiens*	(Lewis et al., 2010b)
Multicellularity: Cell Coordination	Genome-Scale Modeling	Review of existing multi-cellular and multi-tissue M-models. Generally, a context-specific M-model of each cell type or tissue type is built and these models are connected to each other via a shared subcompartment and transport of shared metabolites. Just as standard M-models of a cell have compartments (e.g., nucleus, cytoplasm, mitochondria, etc.), individual cells or tissue types form the compartments of a single, large multi-cellular model.	*Review Paper	generalizable	(do Martins Conde et al., 2016)
Multicellularity: Cell Coordination	Genome-Scale Modeling	Rather than explicitly creating a multicellular M-model, this study experimentally measures metabolomics data of one cell type in the presence or absence of another cell type. It then uses this metabolomics data to constrain the M-models and compares the simulated fluxomics.	Used the M-models to investigate the metabolic effects of cancer-associated fiborblasts on colorectal cancer, observing activation or inhibition of a number of central carbon pathways such as glycolysis, glutaminolysis, and the TCA cycle.	*H. sapiens*	(Wang et al., 2022a)
Multicellularity: Cell Coordination	Cell Circuits and Communication	Models two cell types (macrophages and fibroblasts) as a network that can exchange growth factors. The amount of each cell type was dependent on growth factor exchange, cell proliferation and death rates, and a limiting environmental resource upon which cell growth depends (space). Assesses the stability, or ratio of cell type quantities over time, of different network topologies.	Macrophage-fibroblast circuits achieve stability (compositional homeostasis) by exchange of growth factors PDGF and CSF1 and, necessarily, spatial constraints on the carrying capacity of fibroblasts. Generally, two-cell circuits can ahieve stability if one cell is environmentally limited in its carrying capacity and growth factor exchange occurs to regulate proliferation.	*M. musculus*	(Zhou et al., 2018)
Multicellularity: Cell Coordination	Cell Circuits and Communication	Models the binding of a ligand to receptors, each associated with signaling pathways. Repeats this for multiple ligands and receptors and quantifies the cumulative signaling pathways' activity from the binding strength. Assesses the capability of these networks to activate cell types across a range of binding parameters and possible ligand-receptor combinations.	Relative to non-promiscuous interactions, promiscuous ligand-receptor binding enables few ligands to communicate specific signals to a wider range of cell types. This is achieved by utilizing specific combinations of multiple ligand-receptor pairs and is indicative of a strategy to minimize	*M. musculus*	(Su et al., 2022)

Molecular Process	Approach	Method	Biological Finding	Organism	Reference
			the resources required to synthesize communicatory macromolecules.		

Table 2:

Resource Allocation In Disease

Disease	Resource Allocation Concept	Reference
Aging	Context-dependent machinery synthesis rates	(Gerashchenko et al., 2021; Rooyackers et al., 1996)
Aging	Organismal-scale trade-offs	(Kirkwood, 2017)
Alzheimer's Disease	Machinery constraints	(Kuo et al., 2021)
Alzheimer's Disease	Multicellular GEMs	(Lewis et al., 2010b)
Autoimmunity	GEMs	(Wagner et al., 2021)
Cancer	Resource constraints on cell migration	(Kiweler et al., 2022; Soflaee et al., 2022; Yizhak et al., 2014)
Cancer	Multi-objective optimality	(Hart et al., 2015)
Cancer	Multicellular nutrient constraints and GEMs	(J. Wang et al., 2022)
Cancer	Multicellular bioenergy constraints	(Liu et al., 2013; Zhang et al., 2019)
Cancer	Multicellular resource competition	(Brand et al., 2016; Chang et al., 2015; Nguyen et al., 2023; Reinfeld et al., 2021; Seki et al., 2022)
Diabetes	Nutrient and machinery constraints	(Zisman et al., 2000)
Obesity	Nutrient imbalances	(Dai et al., 2022; Simpson and Raubenheimer, 2005)